


Spring 2024

Pulsed Electric Fields Sensitize Methicillin-Resistant *Staphylococcus Aureus* to Antibacterial Therapies and Stimulate Host Immune Responses

Alexandra E. Chittams-Miles
Old Dominion, alex.chittams@gmail.com

Follow this and additional works at: https://digitalcommons.odu.edu/gradschool_biomedicalsciences_etds

 Part of the [Biology Commons](#), [Biomedical Engineering and Bioengineering Commons](#), [Cell Biology Commons](#), [Immunology and Infectious Disease Commons](#), and the [Microbiology Commons](#)

Recommended Citation

Chittams-Miles, Alexandra E.. "Pulsed Electric Fields Sensitize Methicillin-Resistant *Staphylococcus Aureus* to Antibacterial Therapies and Stimulate Host Immune Responses" (2024). Doctor of Philosophy (PhD), Dissertation, , Old Dominion University, DOI: 10.25777/fd0q-4985
https://digitalcommons.odu.edu/gradschool_biomedicalsciences_etds/16

This Dissertation is brought to you for free and open access by the Graduate School Interdisciplinary Programs at ODU Digital Commons. It has been accepted for inclusion in Biomedical Sciences Theses & Dissertations by an authorized administrator of ODU Digital Commons. For more information, please contact digitalcommons@odu.edu.

**PULSED ELECTRIC FIELDS SENSITIZE METHICILLIN-RESISTANT
STAPHYLOCOCCUS AUREUS TO ANTIBACTERIAL THERAPIES AND
STIMULATE HOST IMMUNE RESPONSES**

by

Alexandra E. Chittams-Miles
B.S. December 2016, University of South Alabama
M.S. May 2019, American University

A Dissertation Submitted to the Faculty of
Old Dominion University in Partial Fulfillment of the
Requirements for the Degree of

DOCTOR OF PHILOSOPHY

BIOMEDICAL SCIENCES

OLD DOMINION UNIVERSITY

May 2024

Approved by:

Claudia Muratori (Director)

P. Thomas Vernier (Member)

Olga Pakhomova (Member)

Piotr Kraj (Member)

Robert Bruno (Member)

ABSTRACT

PULSED ELECTRIC FIELDS SENSITIZE METHICILLIN-RESISTANT STAPHYLOCOCCUS AUREUS TO ANTIBACTERIAL THERAPIES AND STIMULATE HOST IMMUNE RESPONSES

Alexandra E. Chittams-Miles
Old Dominion University, 2024
Director: Dr. Claudia Muratori

This research explores the impact of nanosecond pulsed electric fields (nsPEF) on two fronts: their immune stimulatory effects and their potential as a novel strategy to enhance the sensitivity of Methicillin-resistant *Staphylococcus aureus* (MRSA) to clinically relevant antibiotics. While pulsed electric fields have been reported to have an immune stimulatory effect, the mechanisms responsible for these effects have yet to be determined.

Our investigation addresses the rising concern of MRSA derived skin and soft tissue infections (SSTIs). Consistent with other publications, we found that nsPEF alone cause modest inactivation of planktonic MRSA. We then investigated the effects of nsPEF in combination with commonly used antibiotics for the treatment of SSTI: vancomycin, doxycycline and daptomycin. Notably, the combination of nsPEF with daptomycin demonstrates a significant increase in bacterial inactivation compared to each monotherapy, irrespective of the treatment order. Conversely, when combining nsPEF with doxycycline or vancomycin, the treatment order emerges as crucial factor influencing the level of inactivation. Cells treated with nsPEF prior to antibiotic exposure show an increase in MRSA sensitivity to these drugs, while the opposite order does not improve the efficacy of the combined treatment. Furthermore, co-treatment of nsPEF and vancomycin effectively treats MRSA growing in biofilms, structures known for their increased resistance to antimicrobials.

In parallel we investigated whether cellular perturbation by nsPEF triggered the NLRP3 inflammasome. Inflammasomes are intracellular innate immune platforms activated by damage- and pathogen- associated stress. Their activation is responsible for the processing and release of proinflammatory cytokines of the IL-1 family, constituting one of the first line of defense against pathogens including *S. aureus*. We present evidence that nsPEF trigger the formation of the NLRP3 inflammasome, through visualization of the inflammasome-adaptor protein (ASC), the activation caspase-1 and the release of IL-1 β in primary and immortal macrophages. Most interestingly, our study suggests that nsPEF can trigger the activation of multiple inflammasomes in response to the stimuli generated during and after pulse treatment.

In summary, these findings support the central idea guiding our current research: that nsPEF have a dual effect. Specifically, they enhance the susceptibility of bacteria to antibiotics while concurrently boosting the host immune responses against MRSA.

All other materials Copyright ©, 2024, Alexandra E. Chittams-Miles, All Rights Reserved.

This dissertation is dedicated to my children, Olivia and Augustus and my wonderful husband, Nicholas Miles. Nicholas, thank you for supporting me emotionally, financially and physically through this journey. Thank you for being an editor and presentation sounding board even though this isn't your wheelhouse.

ACKNOWLEDGEMENTS

There are many people who have contributed to the successful completion of this dissertation. To my committee members, Dr. P. Tom Vernier, Dr. Olga Pakhomova, Dr. Robert Bruno, and Dr. Piotr Kraj, thank you for your continuous support and confidence in my growth as a scientist.

To my dissertation chair and mentor, Dr. Claudia Muratori, thank you for taking a chance on me and accepting me into your lab. Most importantly, thank you for your everlasting patience throughout my constant “quick questions” and “I have good news and bad news”. Thank you for allowing me to grow as a scientist and giving me the opportunity to try new things and go new places.

To everyone in the Muratori lab over the years, especially Julia, Andrew, and Flavia, thank you for teaching me and having faith in me even when I didn’t have faith in myself. I appreciate all of you as fellow scientists but more importantly as my friends.

To my friends in the Pakhomov lab: Emily, Vitalii, Geidre, and Mantas, thank you for being my friends and helping me whenever the need arose. You have all made my time at the center so special.

And finally, to my therapist, thanks for keeping me sane.

NOMENCLATURE

ATP	Adenosine Triphosphate
BMDM	Bone Marrow Derived Macrophages
ECT	Electrochemotherapy
GET	Gene Electrotransfer
GSDMD	Gasdermin-D
IRE	Irreversible Electroporation
LPS	Lipopolysaccharide
MRSA	Methicillin-Resistant <i>Staphylococcus aureus</i>
NLR	Nod-like Receptor
nsPEF	Nanosecond Pulsed Electric Fields
PEF	Pulsed Electric Fields
PRR	Pattern Recognition Receptor
ROS	Reactive Oxygen Species
SSTI	Skin and Soft Tissue Infection

TABLE OF CONTENTS

Chapter	Page
LIST OF TABLES	viii
LIST OF FIGURES	ix
I. INTRODUCTION	1
II. NANOSECOND PULSED ELECTRIC FIELDS INCREASE ANTIBIOTIC SUSCEPTIBILITY IN METHICILLIN-RESISTANT STAPHYLOCOCCUS AUREUS.	9
INTRODUCTION	9
MATERIALS AND METHODS	13
RESULTS	17
DISCUSSION	30
III. INFLAMMASOME ACTIVATION AND IL-1B RELEASE TRIGGERED BY NANOSECOND PULSED ELECTRIC FIELDS IN MURINE INNATE IMMUNE CELLS AND SKIN.	34
INTRODUCTION	34
MATERIALS AND METHODS	37
RESULTS	42
DISCUSSION	54
IV. CONCLUSIONS AND FUTURE DIRECTIONS	59
REFERENCES	65
APPENDICES	80
APPENDIX A: SUPPLEMENTARY FIGURE 1	81
VITA	82

LIST OF TABLES

Table	Page
I. Temperatures measured immediately after the delivery of the indicated number of 600 ns pulses (30 kV/cm, 1Hz).	19

LIST OF FIGURES

Figure	Page
Figure 1. <i>S. aureus</i> growth in LB broth.....	12
Figure 2. Effect of nsPEF on planktonic <i>S. aureus</i> viability.. ..	18
Figure 3. Schematic of experimental methods.. ..	20
Figure 4. Pretreatment with daptomycin increases nsPEF cytotoxic effect.. ..	21
Figure 5. Daptomycin and nsPEF mutually enhance each other regardless of the order of application.. ..	22
Figure 6. Pre-treatment with doxycycline does not increase nsPEF efficacy but nsPEF sensitizes MRSA to doxycycline.....	24
Figure 7. Effect of nsPEF and extended incubation with doxycycline (A, B) and vancomycin (C, D)	28
Figure 8. Effect of nsPEF on antibiotic susceptibility of biofilm-derived cells.....	29
Figure 9. nsPEF trigger IL-1 β release in J774A.1 (A), BMDM (B).....	43
Figure 10. The nsPEF dose affects IL-1 β release (A, B) but does not impact TNF- α release (C).	46
Figure 11. nsPEF trigger ASC specks formation (A) and caspase-1 activation (B) but not GSDMD cleavage (C).....	47
Figure 12. 100 μ s pulses are weaker activators of the inflammasome.	48
Figure 13. MCC950 blocks IL-1 β release and rescued cells treated with nsPEF.	50
Figure 14. Relevance of NLRP3 expression for nsPEF-induced IL-1 β release.....	52
Figure 15. 200 ns pulses activate the inflammasome in mouse skin.. ..	53

INTRODUCTION

Skin and Soft Tissue Infections (SSTIs) are commonly occurring infections that have become more prevalent over time (3-5). There are many types of SSTIs ranging from purulent infected abscesses to non-purulent, and necrotizing infections (3). Purulent SSTIs are frequently attributed to the Gram-positive bacteria *Staphylococcus aureus* (*S. aureus*), however *S. aureus* have also been observed in necrotizing and non-purulent SSTI (3, 5). Common risk factors for SSTIs includes immune compromise, age, I.V. drug use and extended hospital stays (3).

Over time *S. aureus* has developed resistance to multiple classes of antibiotics, most notably leading to the development of methicillin-resistant *Staphylococcus aureus* (MRSA) (5). The emergence of MRSA has increased 50% since 2008 with nearly half of cultured bacterial clinical isolates being methicillin-resistant (3). MRSA infections are endemic in hospitals worldwide. In addition, community-associated MRSA (CA-MRSA) can cause infections in otherwise healthy individuals and is responsible for a significant percentage of *S. aureus* SSTIs in the United States (>50%) (6-8).

SSTIs treatment vary based of severity. The standard of care for uncomplicated SSTIs is to simply drain the abscess without antibiotic treatment, however if drainage is unsuccessful, or if patients have increased risk factors, antibiotics are recommended with hospitalization being suggested for only the most severe cases (3). Severe SSTIs require early aggressive surgical debridement accompanied by antibiotic interventions (7, 9). There are many antibiotics that are used in the treatment of SSTIs however, vancomycin is identified as the first-line treatment option.

When antibiotics are administered the duration of treatment ranges from 7 to 14 days, however this can be extended for up to 4 weeks dependent upon location of the infection (3). Regardless of these suggested durations, there are no current guidelines for treatment of SSTIs (10).

Approximately 15 to 30% of initial treatments for SSTIs fail due to increasing tolerance to antibiotic treatments (3). SSTIs can reestablish and become chronic if the infection is not completely removed. This especially occurs when biofilms are formed (11). When the skin barrier is breached, *S. aureus*, typically a normal member of the skin microbiota, infiltrates and binds to the host matrix creating a biofilm (12). Formation of the biofilm allows for the development of microbial tolerance to antibiotic treatment (13). The extracellular polymeric substance of the biofilm, or EPS, surrounds the microbe and restricts the diffusion of antimicrobial therapies into the biofilm decreasing the efficacy (14, 15). This decrease in efficacy can cause an increase of antibiotic concentrations needed for treatment by up to 1000 times (16). The EPS also restricts immune cell infiltration into the biofilm structure and creates an immune-suppressive environment that protect *S. aureus* from the host immunosurveillance (11, 14, 17). In wounds where biofilms proliferate, the infection can become chronic and the healing response is delayed (11). Chronic wounds derived from *S. aureus* are especially of concern for patients with increased risk factors like diabetes (11, 12).

S. aureus has developed resistance to many classes of antibiotics, including β -lactams, glycopeptides, tetracyclines and oxazolidinones (18, 19). The development of antibiotic resistance has made treatment more complex. While resistance is developing, the research and development of new antibiotics have decreased significantly (20). Therefore, it is imperative to develop new strategies to treat *S. aureus* SSTIs.

Ongoing research has investigated the potential development of an anti-*S. aureus* vaccine; however, all attempts have failed to create a lasting immune response in clinical trials. This has been attributed to the numerous virulence factors and the immune evasion mechanisms of *S. aureus* (21, 22).

Recently, the potential use of physical methods as an aid to antibiotics in the battle against bacterial pathogens has received greater attention: photodynamic therapy (23, 24), thermotherapy (25), and weak electric currents (26-30) are all being tested as treatment modalities against pathogenic microorganisms. However, each of these proposed treatment methods have limitations including high levels of heating (31) or production of reactive oxygen species (ROS), both of which can damage the tissues in and around the target area (32). Ultrasound therapy also looked promising, especially when paired with antibiotic treatments; however, damage to surrounding tissues were observed when treatments were administered at higher intensities (33-35). To date, none of these approaches have developed into approved treatment methods to combat bacterial pathogens.

Pulsed electric fields (PEF) have been successfully used in clinical settings ranging from tumor treatment to cardiac ablation (36, 37). PEF application results in the formation of aqueous pores in the cell membrane, a phenomenon that is called ‘electroporation’ (37, 38). Electroporation can be classified into two modalities, reversible or irreversible. Reversible electroporation creates temporary pores in the cell plasma membrane that eventually reseals, and the cells remain viable (37). This type of electroporation is used in gene electrotransfer and electrochemotherapy (37). Conversely, irreversible electroporation, which has been used for tumor and cardiac ablation, creates pores in the cell plasma membrane that do not reseal and leads to ion efflux, ATP release and eventually cell death (37, 39-41).

PEF have been used as a method of bacterial inactivation for over 60 years (42). This promising treatment method has been applied to the inactivation of bacteria in liquid, food (43) and wastewater (44, 45). Though many believe irreversible electroporation is the primary driver of bacterial inactivation, Pillet and colleagues have recently determined that PEF treatment can impact bacterial structures such as the cell wall as well (46). Notably, due to the physical nature of the main underlying mechanism - formation of aqueous pores in the plasma membrane - bacteria cannot easily develop resistance against it. Moreover, the EPS of biofilms should not impact the efficacy of PEF. Additionally, the few studies investigating biofilm inactivation by electroporation reported encouraging results (47, 48)

PEF treatment modalities make use of high-intensity electric fields in the millisecond to microsecond duration range. Pulses of this duration are routinely used for tumor and tissue ablation, gene electrotransfer as well as for drug delivery and bacterial decontamination (40, 41, 49, 50).

The advancement of pulse generators has enabled the generation of nanosecond duration PEF (nsPEF), introducing several additional benefits. Pulses of this duration generates a non-thermal, high voltage pulse which prevents chemical injuries to surrounding tissues while also efficiently permeabilizing cells (51). nsPEF also minimizes neuromuscular stimulation, where PEF treatments of longer durations stimulate neuromuscular excitation resulting in involuntary muscle contractions and significant patient discomfort (52-57). Moreover, nsPEF have been observed to permeabilize both the plasma membrane and the membranes of intracellular organelles and cause a variety of cytophysiological effects such as pore formation, blebbing, water uptake, and ion flux (41, 49, 51, 58-60).

Though PEF have been studied extensively in mammalian cells, there are still many unknowns about the effects of PEF on bacterial cells. Multiple studies have shown that PEF can selectively inactivate microbes though the reasons for this phenomenon are currently unknown (39). Much of the research exploring the effects of PEF on bacterial cells are in relation to food processing and wastewater treatment. The first study investigating the use of PEF for bacterial inactivation was completed in 1898 to purify river water (16). Later studies have explored making use of PEF in milk pasteurization and juice sterilization (16). One study showed that when PEF is combined with a commonly utilized antibacterial toxin peptides that a synergistic inactivation effect can be observed, particularly on bacteria that were previously unimpacted by single toxin peptide treatment (61). Altogether these studies show potential in PEF application for bacterial inactivation especially in combination with antimicrobial therapies. While these new implications are promising, the potential effects of PEF on the bacterial cell wall are relatively unexplored, however, a recent study indicated that PEF targets the cell wall in two possible ways, this effect could be due to direct targeting of the cell wall or indirectly by the permeabilization of the plasma membrane (46).

Recently, studies have explored the effects of PEF treatments when combined with other treatments options such as antibiotics or thermal therapies. These studies investigated the use of μ s and ns duration PEF and found that when combined with additional treatments there is a mild synergistic effect (62, 63). Though the study investigating the effects of nsPEF treatment in combination with antibiotics showed promising initial results, the study did not include antibiotics currently approved to treat *S. aureus* derived SSTIs (63). Regardless, these studies show that PEF could be of benefit particularly when single treatments are observed to be insufficient for bacterial inactivation.

Results from our research reported in Chapter 2 demonstrate the significant impact of nsPEF on the efficacy of antibiotics approved for SSTIs (2). When applied to planktonic MRSA, nsPEF treatment exhibited a dose-dependent reduction in viability (Fig. 2). Notably, co-treatment with SSTI-approved antibiotics—daptomycin (Figs. 4 and 5), doxycycline (Figs. 6 and 7), and vancomycin (Fig. 7)—resulted in enhanced antimicrobial effects. Previous studies were limited to testing bacterial susceptibility to antibiotics only after nsPEF were delivered (63-65), while we directly compared the efficacy of multiple antibiotics administered either before or after the pulse treatment. Our results show that treatment duration and order (nsPEF-antibiotics, antibiotics-nsPEF) are essential in determining the most effective result, findings which will guide experimental design for future *in vivo* studies of the interaction between nsPEF and antibiotics to treat SSTIs.

In an *in vivo* setting, another significant advantage of nsPEF lies in their potential to stimulate the host immune system against *S. aureus*. Numerous groups have documented the immunostimulatory effects of nsPEF (66-69) but our distinctive contribution is in revealing the fundamental mechanisms driving this phenomenon. These previously published studies have shown that PEF can have an immune stimulatory effect on both healthy and tumor cells (67, 70-72). nsPEF in particular has been seen to stimulate anti-tumor immune responses in the tumor microenvironment (TME) which is frequently characterized as immune suppressed (70, 71).

Membrane permeabilization by nsPEF causes colloid-osmotic cell swelling (73) and ion flux, including K^+ efflux (74) and influx of Ca^{2+} (75-78). Additional effects of nsPEF cause an increase of ROS production and the triggering of ER stress (66, 79, 80). Notably, many of these responses are known to activate the inflammasome (81-83), a multiprotein complex expressed in innate immune cells that acts as a molecular sensor within cells and initiates inflammatory

responses. This led us to explore whether the damage caused by nsPEF is sensed intracellularly by the inflammasome, thereby alerting the innate immune system.

Inflammasome oligomerization requires the assembly of a sensor protein, among which the NLRP-3 is the most studied, an adaptor protein (ASC), and an inflammatory caspase (Caspase-1) (84). When the multi-protein complex oligomerizes, caspase-1 is activated to cleave its targets pro-IL-1 β and the pore forming family of proteins known as gasdermins (84).

Results reported in Chapter 3 show that the intracellular perturbation caused by nsPEF serves as the specific trigger for the inflammasome (1). This recognition then prompts the activation of caspase-1 and the processing and release of the cytokine IL-1 β both *in vitro* and *in vivo* (Figs. 11 and 15).

Notably, inflammasome activation plays a crucial role in host defense against *S. aureus*, as it contributes to the mobilization, recruitment, and activation of essential immune cells, particularly neutrophils (19, 85-89). IL-1 β stimulates neutrophil recruitment while activating macrophages, and dendritic cells (19, 90-92). Additionally, IL-1 β induces IL-17-producing T-cells like T-helper-17 (Th17) cells and $\gamma\delta$ T-cells (19, 85-89, 91). These responses are crucial for an effective immune response against *S. aureus*. Individuals with elevated susceptibility to *S. aureus* skin infections often exhibit mutations leading to impaired interleukin-1 receptor (IL-1R) and/or Toll-like receptor (TLR) signaling, or impaired Th17 cell responses. Such impairments are frequently associated with recurrent and severe infections. (93-98). Experiments in mouse models of *S. aureus* skin infection emphasize the critical role of IL-1- and IL-17-mediated responses in promoting neutrophil abscess formation in the skin, a requirement for effective bacterial clearance (19, 85-88). The significance of the IL-1 β /IL-17 axis in *S. aureus* skin infection is further underscored by the multiple immune evasion mechanisms developed by *S.*

aureus to avoid inflammasome activation. O-acetylation of *S. aureus* peptidoglycan limits inflammasome activation and IL-1 β release, impairing the development of an effective Th17 response against reinfection (99, 100). More recently, adenosine synthase A (AdsA), a potent *S. aureus* virulence factor, was also found to dampen Th17 responses by interfering with inflammasome mediated IL-1 β production (101). These immune evasion mechanisms actively inhibit inflammasome activation (100, 101), therefore it is essential to understand if nsPEF can overcome these mechanisms to induce an anti-pathogen response.

Our preliminary results and the literature suggest that nsPEF could be a promising treatment option for enhancing the efficacy of clinically relevant antibiotics while also setting the stage for an enhanced immune response. This potential dual effect of nsPEF is particularly appealing given the absence of a licensed vaccine to prevent *S. aureus* infections. Therefore, we suggest using nsPEF to inactivate bacteria and enhance their susceptibility to antibiotics while also stimulating inflammasome activation to enhance the immune response necessary for innate immune cells to effectively combat *S. aureus* infection.

NANOSECOND PULSED ELECTRIC FIELDS INCREASE ANTIBIOTIC SUSCEPTIBILITY IN METHICILLIN-RESISTANT STAPHYLOCOCCUS AUREUS^{ab}

Introduction

The Gram-positive opportunistic pathogen *Staphylococcus aureus* (*S. aureus*) is the leading cause of skin and soft-tissue infections (SSTI) in the United States (102, 103). Patients with ulcers, commonly resulting from advanced complications of injuries, recent surgery, or indwelling medical devices, are particularly at risk. SSTI range from superficial infections such as impetigo, cellulitis, simple abscesses, and furuncles to deeper and more severe infections such as necrotizing infections, infected ulcers, infected burns, and major abscesses. Moreover, diabetic foot infections are similar to SSTI in pathophysiology, microbiology, and treatment and can be seen as a subset of SSTI (104). SSTI are common in ambulatory and inpatient settings, accounting for more than 14 million outpatient visits and 850,000 hospitalizations in the United States alone (105). Between 7-10% of hospitalized patients have SSTI, which are often hospital-acquired infections that complicate treatment of the original ailment (10, 106).

Treatment of SSTI varies based on clinical severity, patient comorbidities, admission status, and diagnosis. Uncomplicated SSTI are treated with topical or oral antibiotics while severe SSTI require early aggressive surgical debridement accompanied by antibiotic interventions (9). The history of *S. aureus* treatment is marked by the development of resistance to each new class of antimicrobial drugs, including penicillin, sulfonamides, tetracyclines,

^a This chapter is based on our manuscript titled “Nanosecond Pulsed Electric Fields Increase Antibiotic Susceptibility in Methicillin-Resistant *Staphylococcus aureus*,” which was originally published in *Microbiology Spectrum* on January 11, 2024. <https://doi.org/10.1128/spectrum.02992-23>. The manuscript has been modified for inclusion in this chapter and is reproduced here under copyright agreement.

^b This chapter includes experiments conducted in accordance to the guidelines set forth by the Institutional Biosafety Committee (IBC) and the Institutional Animal Care and Use Committee (IACUC) of Old Dominion University.

glycopeptides, and others, complicating therapy (107). Methicillin, which inhibits bacterial cell wall synthesis, was once a front-line treatment for *S. aureus* infections but this resulted in the development of methicillin-resistant strains of *S. aureus* (MRSA) (108). First reported in the 1960s (109), MRSA has become increasingly prevalent since the 1980s (110, 111) and is now endemic in many hospitals and even epidemic in some, with resistance in approximately 30% of all *S. aureus* infections in the United States (111). Vancomycin is the only antibiotic that can consistently successfully treat MRSA (112). However, the emergence of *S. aureus* infection with intermediate resistance to vancomycin in the United States suggests that *S. aureus* strains are constantly evolving, and full resistance may develop (113). Novel approaches to tackle this problem are urgently required.

Recently, the potential use of physical means as an aid to antibiotics in the battle against bacterial pathogens has been studied: photodynamic therapy (23, 24), ultrasound therapy (33-35), thermotherapy (25), and weak electric currents (26-30) are all being tested as treatment modalities against pathogenic microorganisms. The major drawback of these methods is their low therapeutic index due to high levels of heating (31) or production of reactive oxygen species, both of which can damage the tissues in and around the target area (32). Moreover, these methods usually require a long time of exposure and, for photodynamic therapy, a photosensitizer. As of today, none of the above-mentioned means has matured into an approved treatment modality against bacterial pathogens.

Pulsed electric fields (PEF) are successfully used in a wide range of clinical applications from cancer therapy to cardiac ablation (36, 37). The application of PEF disrupts cell plasma membranes in mammalian and bacterial cells and has been used for decades to promote bacterial uptake of exogenous DNA in laboratory settings (114, 115). This disruption of the membrane

barrier function, called electroporation, leads to multiple cyto-physiological effects, including calcium (Ca^{2+}) overload, efflux of ATP and other metabolites, and disturbances in transmembrane ion gradients (Na^+ , K^+ , Cl^-) required for maintenance of membrane resting potential and for osmotic and cell volume regulation (75, 76, 116-122). The biological effects of PEF can be tuned by adjusting pulse parameters such as pulse number, duration, and amplitude. In most protocols the rate of energy deposition is controlled so that the concurrent Joule heating does not cause thermal damage (120, 123-126). When the electroporative damage exceeds the cell repair capacity, PEF treatments cause cell death. The ability of pulsed electric fields (PEF) to inactivate microorganisms has been known for over 60 years (42). Indeed, PEF are among the most promising microbial inactivation methods for liquid, food (43) and wastewater (44, 45). Moreover, due to the physical nature of the main underlying mechanism - formation of aqueous pores in the plasma membrane- bacteria cannot easily develop resistance against it.

Recent research has extended PEF treatments to the nanosecond duration range (nsPEF). Because nsPEF use much shorter pulses (down to 10 ns), higher voltages can be applied with minimal thermal effects. Compared to micro- and millisecond pulses, permeabilization by nsPEF does not rely on charge movement or capacitive charging, resulting in a much more uniform/less localized poration pattern, or so-called "supra-electroporation"(127, 128). Moreover, nanosecond pulses permeabilize not only the outer membrane of the cell, but also intracellular membranes of eukaryotic organelles, such as the endoplasmic reticulum (ER) and the mitochondria (73, 75, 76, 129-131). nsPEF create nanopores with cross-section less than 1.5 nm with resulting cell permeabilization lifetimes on the order of seconds or minutes (121, 132, 133). Finally, treatment with nsPEF results in reduced neuromuscular stimulation as compared to μs -ms pulses. Pulses in the micro- to millisecond duration range trigger neuromuscular excitation, which causes severe

pain and involuntary muscle contractions (52-57). *In silico* models showed that standard 100 μ s electric pulses excites nerves at \sim 1,000-fold lower electric field than needed for ablation (134). While anesthesia and muscle relaxants offer a partial solution, the optimal solution is to minimize nerve excitation in the first place. Both theoretical and experimental research demonstrated that shortening the pulse duration into nanosecond range decreases neuromuscular response to PEF (57, 134-140). Specifically, Pakhomov's group recently published that 200 ns pulses can cause a 1000-fold reduction of the stimulated tissue compared to 100 μ s pulses (140).

In this study, we measured MRSA inactivation by nsPEF alone and in combination with antibiotics approved to treat SSTI, namely vancomycin, doxycycline and daptomycin. Previous studies were limited to testing the bacterial susceptibility to various antibiotics only after nsPEF were delivered (63-65). Here we directly compared the efficacy of multiple antibiotics administered either before or after the pulse treatment. Our results show that the treatment duration and order (nsPEF-antibiotics, antibiotics-nsPEF) is essential in determining the most effective result.

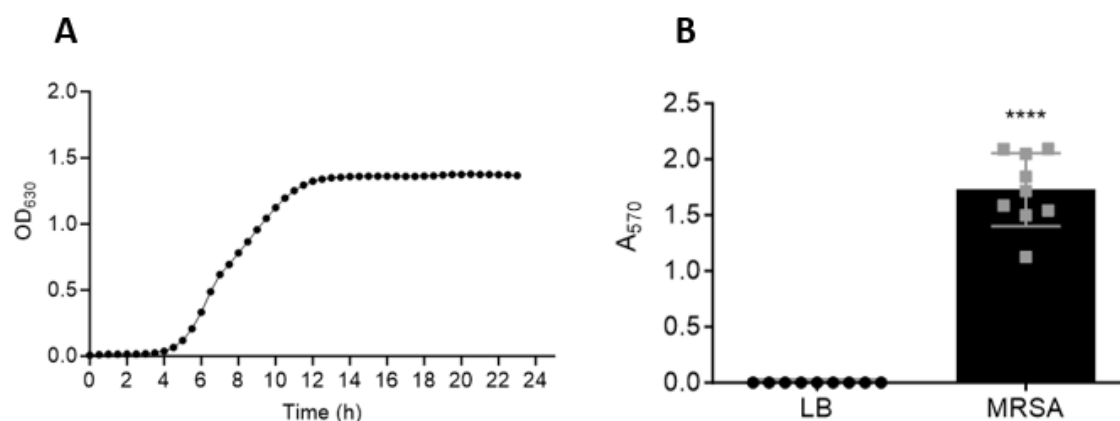


Figure 1. *S. aureus* growth in LB broth. (A) Planktonic MRSA cultures were diluted using a 1:20 ratio in LB broth in sterile 96-well plates. Plates were incubated at 37.0°C for 24 h in a microplate reader, which was set to constantly shake at medium intensity, and the optical density was recorded at 630 nm every 30 min. (B) Planktonic MRSA cultures were diluted 1:10 in LB broth in sterile 12-well plates. Plates were incubated at 37.0°C for 48 h before crystal violet staining was used to measure biofilm production. Shown are the means and standard deviations of nine samples. ****P < 0.0001. Figure is reproduced from Chittams-Miles AE, et al, 2024 (2).

Materials and Methods

Bacterial strains and growth conditions. All assays were conducted with *S. aureus* Xen 31 MRSA strain (Perkin Elmer, Waltham, MA). Bacterial colonies were maintained on LB plates containing 17 g/L agar (Fisher Scientific, Waltham, MA). Bacteria were grown in Luria Bertani Miller (LB-Miller; Fisher Scientific) broth at 37°C until they reached exponential phase (optical density of 0.4-0.7 at 600 nm) in a shaking incubator (New Brunswick Scientific, Edison, NJ) at 250 rpm. Bacterial growth was measured using the DU® 730 spectrophotometer (Beckman Coulter, Inc., Chaska, MN).

Growth curves. MRSA cultures were prepared by inoculating single colonies into 2 mL of LB broth and grown for 16 h at 37 °C with constant shaking at 250 rpm. The overnight cultures were diluted 1:20 into fresh LB broth, grown until they reached exponential phase (OD_{600nm} : 0.4-0.7) and diluted 1:10 into a sterile 96-well plate (Fisher Scientific) containing a range of antibiotic concentrations in LB broth. The antibiotics that were used were: vancomycin (VWR, Suwanee, GA), doxycycline (Cayman Chemicals, Ann Arbor, MI), and daptomycin (Fisher Scientific). Plates were incubated at 37.0°C for 24 h in a BioTek synergy microplate reader, which was set to constant shake at medium intensity and absorbance was recorded at 630 nm every 30 min.

Pulsed electric field exposure methods. MRSA cultures were prepared by inoculating single colonies into 2 mL of LB broth and grown for 18 h at 37°C with constant shaking. Starter cultures were diluted 1:20 into LB broth to reach exponential phase ($OD_{600} = 0.4-0.7$) and 90 μ L samples of this suspension were loaded into 1 mm gap electroporation cuvettes (BioSmith, Vandergrift, PA). Samples in electroporation cuvettes were exposed to nsPEF in LB broth with a conductivity of 1.73 S/m at room temperature. Trapezoidal pulses of 300 or 600 ns duration

were produced by a CellFX® generator (Pulse Biosciences Inc, Hayward, CA). The output stage of the pulse generator was optimized for the 10-ohm impedance presented by the cell suspensions in a 1 mm electroporation cuvette. The pulse amplitude and shape were monitored at the cuvette using a LeCroy WaveSurfer 3034z oscilloscope (Teledyne Lecroy, Chestnut Ridge, NY). Temperature changes were measured immediately after nsPEF using a thermocouple thermometer (Physitemp, Clifton, NJ). The nsPEF treated cells underwent a serial dilution in LB broth before being plated on LB agar plates. The plates were incubated at 37°C for 40 h before the number of colonies were counted. All experiments included an untreated ‘sham’ control that was prepared the same way as the experimental sample but not subjected to nsPEF treatment.

Antibiotic treatments. A schematic diagram of the experimental workflow is shown in Fig. S1. For short antibiotic incubations either pre- or post-nsPEF treatment, MRSA cultures in exponential growth phase ($OD_{600} = 0.4\text{--}0.7$) were treated with a range of concentrations for each of the antibiotics: 0-8 $\mu\text{g/mL}$ daptomycin, 0-32 $\mu\text{g/mL}$ doxycycline, and 0-32 $\mu\text{g/mL}$ vancomycin. Antibiotic exposure lasted 90 min at 37°C with constant shaking at 250 rpm. For prolonged antibiotic exposures, samples were exposed to nsPEF as described above, diluted, and spread on LB-agar plates containing the indicated concentrations of antibiotics. Plates were incubated at 37 °C for 40 h before the number of colonies were counted.

Replicate plating. Exponential phase cultures were exposed to 600 ns pulses (0, 60, and 120 pulses) and serially diluted in a sterile 96-well plate (ThermoFisher Scientific). A sterile replica plater (‘frogger’) for 96-well plate (Sigma Aldrich) was used to stamp the desired samples onto LB \pm antibiotic agar plates. The plates were incubated at 37°C for 24 h before being scanned on a ChemiDoc MP Imaging System (BioRad).

Biofilm formation, visualization, and quantification. A 12-well tissue culture treated plate (Fisher Scientific) containing 1.8 mL of fresh LB broth in each well was inoculated with 200 μ L of MRSA exponential phase cultures. The plate was then incubated at 37°C for 24 h. To quantify the biofilms, the supernatant from each well was removed by pipetting, the adhered biofilms were washed with 1 mL of 1X phosphate buffered saline (PBS) solution. The washed biofilms were then stained for 30 min with 1 mL of 0.1% crystal violet (Sigma Aldrich) and washed two additional times with 1X PBS. The adhered and stained biofilms were suspended in 70% ethanol. The plate was placed in the Bio-Tek synergy microplate reader (Marshall Scientific), which recorded the OD₅₇₀, after shaking the plate at medium intensity.

nsPEF and antibiotic treatment of biofilm derived cells. To treat biofilms, the supernatant was removed, biofilms were washed with 1X PBS, and adherent cells were manually scraped off the plastic surface with pipet tips and suspended in 1 mL of fresh LB broth. The sample was then vortexed to disrupt the biofilm structure. A 90 μ L aliquot of this sample was transferred to an electroporation cuvette for nsPEF as described above. After the nsPEF treatment, the sample was plated on LB \pm antibiotic (1 μ g/mL doxycycline or 1 μ g/mL vancomycin) agar plates. The plates were incubated at 37 °C for 40 h before the number of colonies were counted.

Determination of inactivation rates. Immediately after pulsing, 900 μ L of LB broth was added to each cuvette and mixed by pipetting. The resulting 1 mL samples were serially diluted up to 10⁻⁷ and 100 μ L of each sample was plated on duplicate LB agar plates and colonies were counted after 40 h incubation at 37 °C. Only counts between 0 and 300 CFU per plate were considered. Inactivation rates are expressed as log₁₀ (CFU/mL_{sham} - CFU/mL_{treated}).

Statistical analyses. Data are presented as mean \pm SD for n independent experiments. Statistical calculations, including data fits, and data plotting were accomplished using Prism (GraphPad). All quantitative experiments were performed in duplicate and repeated a minimum of three times.

Results

Sensitivity of planktonic MRSA to nsPEF treatments

Our initial experiments sought to establish optimal laboratory growth conditions for the planned experiments. MRSA (Xen 31) growth in liquid culture was assessed in different growth media commonly used to culture MRSA (data not shown). We found that MRSA grows rapidly and consistently in LB broth and reaches a stationary optical density of 1.2-1.4 within 12 h (Fig. 1A). 24 h was sufficient time for the growth of robust MRSA biofilms on plastic surfaces (Fig. 1B).

Inactivation by nsPEF of planktonic MRSA in exponential growth phase was measured using two different pulse durations, namely 300 ns, the shortest duration our generator can produce, and 600 ns (0-1000 pulses, 30 kV/cm, 1 Hz). Our results show that while MRSA was moderately affected by both pulse durations (Fig. 2), 600 ns pulses were more efficient at bacterial inactivation. Specifically, 250 pulses of 300 ns each caused a very modest 0.2 log₁₀ reduction in viability and increasing the number of pulses to 500 or 1000 only increased the killing effect to 0.3 and 0.5 log₁₀ reductions, respectively (Fig. 2A). Meanwhile, 60 pulses of 600 ns each caused a 0.4 log₁₀ reduction in viability, while increasing the number of pulses to 120 or 250 pulses did increase the killing effect to 0.5 and 1.1 log₁₀ reductions, respectively (Fig. 2B). Additionally, we calculated the energy between each set of pulse conditions with the highest 300 ns pulse condition (1000 pulses) being tested resulting in an energetic field of 270 J and the highest 600 ns pulse condition (250 pulses) resulting in an energetic field of 135 J. This shows that the 600 ns duration pulses generated a smaller energetic field while also creating a stronger inactivation effect. Therefore, we continued using the 600 ns pulse conditions.

PEF treatments are intended to be a non-thermal method to inactivate microorganisms. However, it is well known that an increase in temperature due to Joule heating can be associated with high pulse doses. Table 1 shows that the highest 600 ns pulse dose (250 pulses) increased the sample temperature from 24.4 ± 0.3 to $38.7 \pm 0.3^\circ\text{C}$ while 60 and 120 pulses increased the temperature to 28.6 ± 0.1 and 33.1 ± 0.2 , respectively.

Although *S. aureus* can grow over a wide range of temperature (6.5 – 46°C) with an optimal range between 30 – 37°C (141), we could not exclude that a rapid 14-degree rise in temperature during treatment affected the electroporation phenomenon and/or initiated stress responses. Therefore, to minimize the effect of heating, the condition utilizing 250 pulses at 600 ns pulse duration was discontinued. All subsequent experiments used 60 or 120 pulses with the 600 ns pulse duration, as indicated.

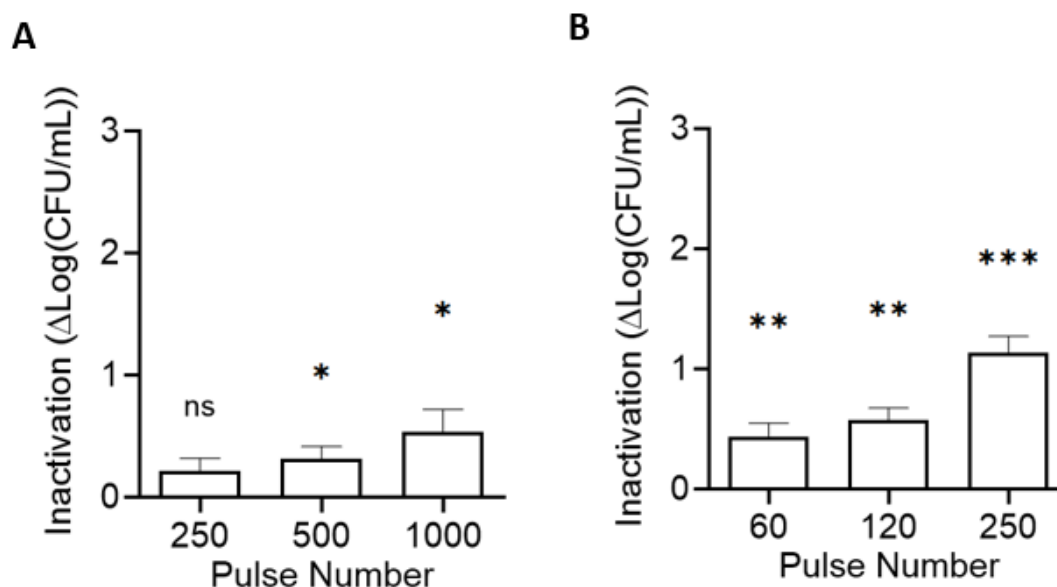


Figure 2. Effect of nsPEF on planktonic *S. aureus* viability. Cells in the exponential phase were treated with the indicated numbers of either (A) 300 or (B) 600 ns pulses. All pulses were 30 kV/cm, 1 Hz. Treated samples were plated in 10-fold dilutions on LB agar plates and colony-forming units were quantified 40 h post-treatment. Inactivation is quantified as $\log(\text{CFU/mL})_{\text{sham}} - \log(\text{CFU/mL})_{\text{nsPEF}}$ and is individually calculated for each sample. Shown are the means and standard deviations of at least three independent samples. n.s., not significant; * $P < 0.05$; ** $P < 0.01$; and *** $P < 0.001$. Figure is reproduced from Chittams-Miles AE, et al, 2024 (2).

# of Pulses	Temperature, °C
0	24.4 ± 0.3
60	28.6 ± 0.1
120	33.1 ± 0.2
250	38.7 ± 0.3

Table I. Temperatures measured immediately after the delivery of the indicated number of 600 ns pulses (30 kV/cm, 1Hz). Table is reproduced from Chittams-Miles AE, et al, 2024 (2).

nsPEF pre-treatment or post-treatment increases the antimicrobial effect of limited daptomycin exposure

Next, we asked whether nsPEF treatments could sensitize MRSA to a transient exposure to the SSTI-approved antibiotic daptomycin. Daptomycin is a lipophilic peptide that inserts into the bacterial cell membrane, causing rapid membrane depolarization and potassium ion efflux (142). We hypothesized that the membrane defects created by daptomycin would increase the efficacy of nsPEF treatment. To test this hypothesis, we first measured the ability of daptomycin to reduce the number of viable cells in exponentially growing MRSA cultures (for a schematic diagram of the experimental workflow see Fig. 3). As expected, daptomycin exposure reduced the number of colony forming units per mL in a dose-dependent manner, with a 90 min exposure to 8 µg/mL daptomycin, the highest concentration tested, leading to 3.3 log₁₀ reduction in viability (Fig. 4A). Next, we measured the effect of combining daptomycin with nsPEF (Fig. 4B). Cells were preincubated for 90 min with different sub-lethal doses of the antibiotic (0.5, 1 and 2 µg/mL), then treated with nsPEF (0, 60, 120 pulses 600 ns, 30 kV/cm, 1 Hz) and immediately plated on LB agar plates without antibiotic. Our results show that pretreatment with daptomycin significantly increased MRSA sensitivity to nsPEF (Fig. 4B). Combining 2 µg/mL of daptomycin with nsPEF caused nearly 3 log₁₀ reduction comparable to the effect of 8 µg/mL

of antibiotic alone. Similarly, at all of the antibiotic concentrations tested, antibiotics combined with pulses reduced culture viability significantly more than pulses alone (Fig. 4B). Next, we investigated whether the order in which the combined treatments were applied affected our results. Samples were either pretreated with 0.5 $\mu\text{g/mL}$ of daptomycin for 90 min and then exposed to nsPEF (600 ns, 30 kV/cm, 1 Hz) or exposed to nsPEF and then incubated with the antibiotic for 90 min. Our results show that regardless of the administration order, the co-treatment inactivates MRSA culture more strongly than either daptomycin or nsPEF alone (Fig. 5). Each of the monotherapies reduced culture viability by less than 1 log₁₀, while prior exposure to daptomycin allowed 60 or 120 pulses to reduce viability by 1.5 and 1.9 log₁₀, respectively. Pretreatment with 60 or 120 pulses sensitized the cells to daptomycin, allowing culture inactivation by 2.0 and 2.3 log₁₀, respectively (Fig. 5).

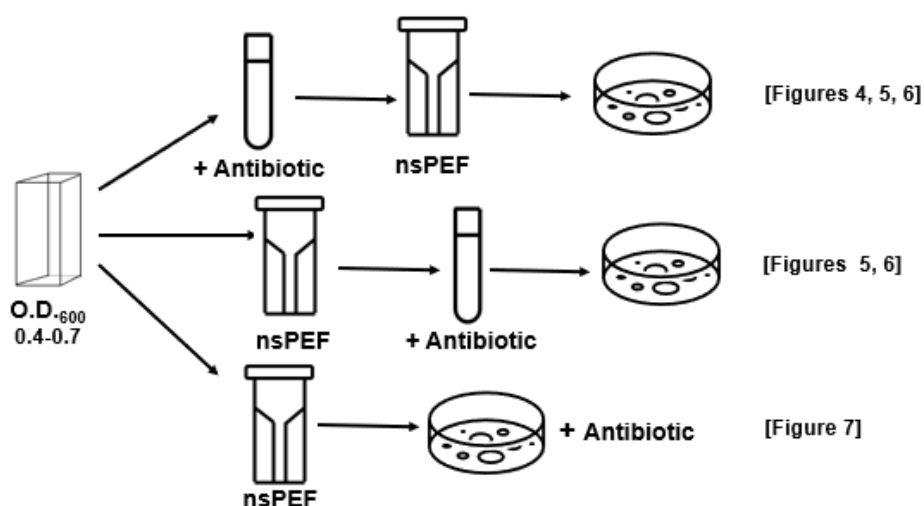


Figure 3. Schematic of experimental methods. MRSA cultures in exponential growth phase ($\text{OD}_{600} = 0.4-0.7$) were either transiently incubated with antibiotics for 90 minutes pre- or post nsPEF treatment and plated on plates without antibiotics or, for prolonged antibiotic exposure, treated with nsPEF and then plated on plates with antibiotics for 40 h. Figure is reproduced from Chittams-Miles AE, et al, 2024 (2).

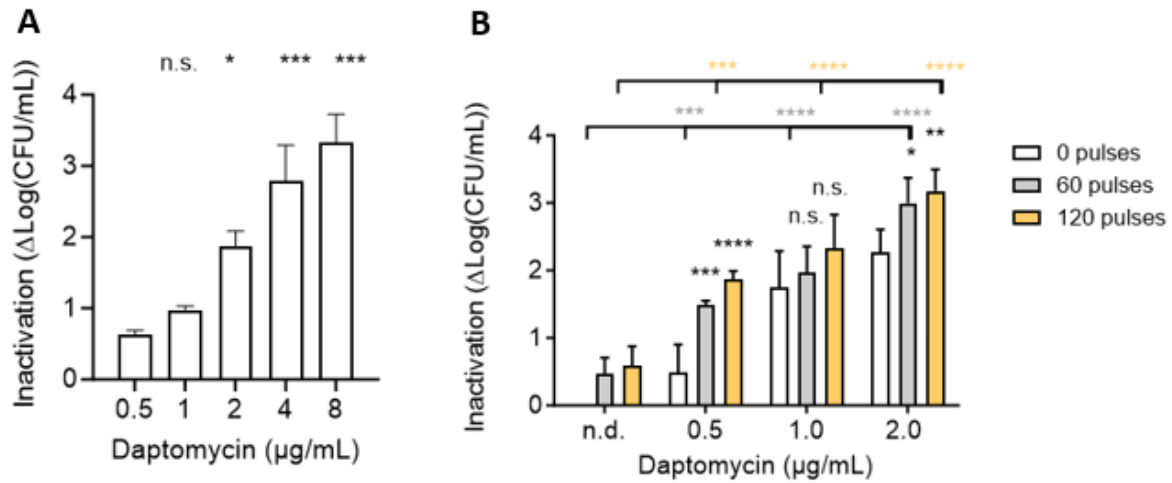


Figure 4. Pretreatment with daptomycin increases nsPEF cytotoxic effect. (A) Inactivation of exponentially growing MRSA cultures by 90 min of incubation with the indicated doses of daptomycin. Inactivation is quantified as $\log(\text{CFU/mL})_{\text{untreated}} - \log(\text{CFU/mL})_{\text{daptomycin}}$ and is individually calculated for each sample. Treated samples are compared to 0 (untreated control) by one-sample t-test. Numbers shown represent the means and standard deviations of at least three independent samples. (B) Inactivation of samples treated with the indicated concentrations of daptomycin for 90 min before exposure to 0, 60, or 120 pulses (600 ns, 30 kV/cm, 1 Hz). Inactivation is quantified as $\log(\text{CFU/mL})_{\text{untreated}} - \log(\text{CFU/mL})_{\text{treated}}$ and is individually calculated for each sample. Black asterisks: samples treated with daptomycin and pulses are compared to those treated with daptomycin alone by one-way ANOVA. Gray asterisks: samples treated with daptomycin and 60 pulses are compared to those treated with 60 pulses alone by one-way ANOVA. Orange asterisks: samples treated with daptomycin and 120 pulses are compared to those treated with 120 pulses alone by one-way ANOVA. Numbers shown represent the means and standard deviations of four independent samples. n.d., no drug; n.s., not significant; * $P < 0.05$; ** $P < 0.01$; *** $P < 0.001$; and **** $P < 0.0001$. Figure is reproduced from Chittams-Miles AE, et al, 2024 (2).

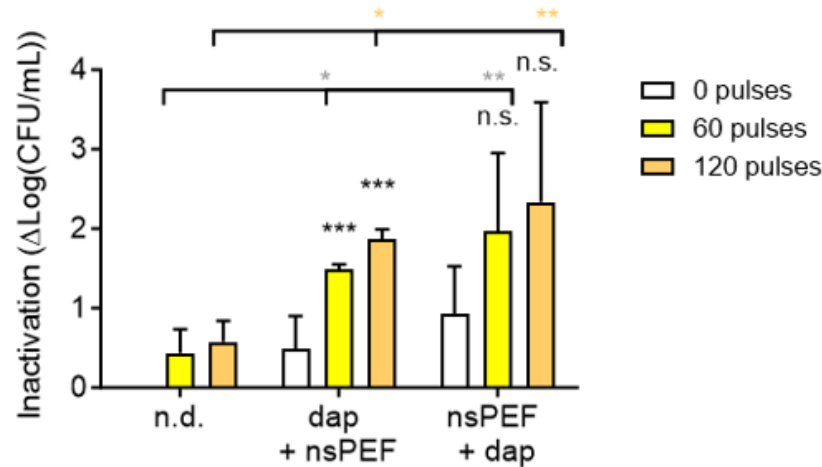


Figure 5. Daptomycin and nsPEF mutually enhance each other regardless of the order of application. Exponentially growing MRSA cultures were either pre-incubated with 0.5 $\mu\text{g/mL}$ daptomycin for 90 min and then exposed to 0, 60, and 120 pulses (Dap + nsPEF) or exposed to nsPEF and then incubated with the antibiotic (nsPEF + Dap). Inactivation is quantified as $\log(\text{CFU/mL})_{\text{untreated}} - \log(\text{CFU/mL})_{\text{treated}}$. Black asterisks: samples treated with daptomycin and pulses are compared to those treated with daptomycin alone. Gray asterisks: samples treated with daptomycin and 60 pulses are compared to those treated with 60 pulses alone. Orange asterisks: samples treated with daptomycin and 120 pulses are compared to those treated with 120 pulses alone. All treatment comparisons were analyzed using one-way ANOVA. Numbers shown represent the means and standard deviations of at least four independent samples. n.d., no drug; n.s., not significant; * $P < 0.05$; ** $P < 0.01$; and *** $P < 0.001$. Figure is reproduced from Chittams-Miles AE, et al, 2024 (2).

Only nsPEF pre-treatment sensitizes MRSA to doxycycline

Next, we asked whether nsPEF treatment would also enhance the effects of antibiotics with different mechanisms of action. Doxycycline inhibits bacterial protein synthesis by reversibly binding to the 30S ribosomal subunits, blocking the binding of the aminoacyl tRNA to the mRNA (143).

Unlike daptomycin, doxycycline must enter the cell to have an effect; the thick cell wall of Gram-positive pathogens such as MRSA can impede this. We therefore hypothesize that the damage created by nsPEF could increase MRSA permeability to doxycycline. As with daptomycin, we first measured the sensitivity of exponentially growing MRSA to doxycycline monotherapy. Interestingly, all tested doses (0-32 $\mu\text{g/mL}$) only mildly affected MRSA viability, suggesting that the 90 min contact time was not sufficient to cause significant bactericidal effects (Fig. 6A). Next, we measured the effect of combining doxycycline with nsPEF. Cells were incubated for 90 min with 4 $\mu\text{g/mL}$ doxycycline either before or after treatment with nsPEF (0, 60, 120 pulses 600 ns, 30 kV/cm, 1 Hz) and immediately plated on LB plates without antibiotic. Our results show that pretreating MRSA with doxycycline did not increase cells sensitivity to nsPEF, while nsPEF significantly potentiated MRSA susceptibility to consequent doxycycline incubation (Fig. 6B). Pre-treatment with doxycycline caused a small but significant enhancement to the effects of pulses, increasing the inactivation effect from 0.4 log₁₀ in the presence of doxycycline alone to 0.6 when doxycycline is followed by 60 or 120 pulses. Pulses sensitize MRSA to doxycycline much more strongly, as pre-treatment with 60 pulses increases culture inactivation by doxycycline from 0.6 to 1.3, and pre-treatment with 120 pulses increases it further to 1.5 (Fig. 6B). While the effect of the pulses on cells previously exposed to doxycycline was not significant compared to that of the pulses alone, pulses followed by doxycycline

exposure are much more lethal to the MRSA cultures than pulses alone (Fig. 6B). These results suggest that cell permeabilization by nsPEF enhances doxycycline penetration into the bacterial cytoplasm, while pretreatment with the antibiotic has no effect on the cellular response to nsPEF.

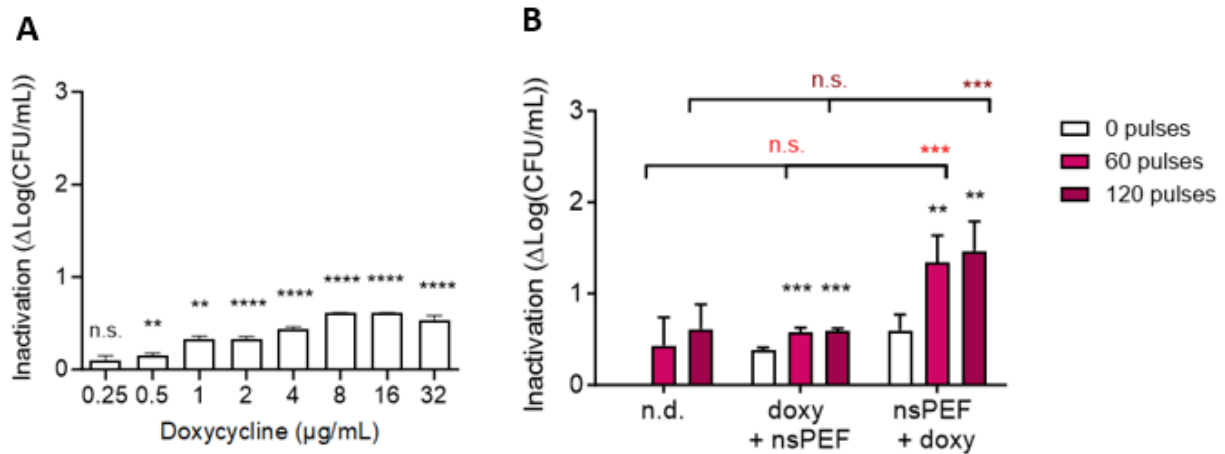


Figure 6. Pre-treatment with doxycycline does not increase nsPEF efficacy but nsPEF sensitizes MRSA to doxycycline. (A) Inactivation of exponentially growing MRSA cultures by 90 min of incubation with the indicated doses of doxycycline. Inactivation is quantified as $\log(\text{CFU/mL})_{\text{untreated}} - \log(\text{CFU/mL})_{\text{treated}}$ and is individually calculated for each sample. Treated samples are compared to 0 (untreated control) by one-sample t-test. Numbers shown represent the means and standard deviations of at least three independent samples. (B) Inactivation of exponentially growing MRSA cultures either pre-incubated with 4 $\mu\text{g/mL}$ doxycycline for 90 min and then exposed to 0, 60, and 120 pulses (doxy + nsPEF) or exposed to nsPEF and then incubated with the antibiotic (nsPEF + doxy). Inactivation is quantified as $\log(\text{CFU/mL})_{\text{untreated}} - \log(\text{CFU/mL})_{\text{treated}}$. Black asterisks: samples treated with doxycycline and pulses are compared to those treated with doxycycline alone. Light fuchsia symbols: samples treated with doxycycline and 60 pulses are compared to those treated with 60 pulses alone. Dark fuchsia symbols: samples treated with doxycycline and 120 pulses are compared to those treated with 120 pulses alone. All treatment comparisons were analyzed using one-way ANOVA. Numbers shown represent the means and standard deviations of at least three independent samples. n.d., no drug; n.s., not significant. * $P < 0.05$, ** $P < 0.01$, *** $P < 0.001$, and **** $P < 0.0001$. Figure is reproduced from Chittams-Miles AE, et al, 2024 (2).

nsPEF does not strongly affect the efficacy of a transient exposure to vancomycin ^c

Vancomycin is a glycopeptide antibiotic that exerts its bactericidal effect by inhibiting the polymerization of peptidoglycans in the bacterial cell wall, and is broadly effective against Gram positive bacteria (144). We hypothesized that the destabilization of the cell wall by vancomycin could enhance osmotic cell swelling and consequent cell death in electroporated MRSA. However, similar to doxycycline, incubation with all tested doses of vancomycin for 90 min did not result in substantial cytotoxic effects against exponentially growing cultures (data not shown). Consistent with this, transient exposure to vancomycin either before or after nsPEF treatment had not significant effect on MRSA inactivation (data not shown). Under our experimental conditions, it appears that antibiotic destabilization of the cell wall does not exhibit the same mutual enhancement with nsPEF treatment as antibiotic destabilization of the cell membrane.

nsPEF treatment sensitizes cells to prolonged antibiotic exposure

Because both doxycycline and vancomycin alone had only modest effects on MRSA viability after 90 min of exposure, we decided to test the effect of increased contact time with these antibiotics. To do this, we employed dilution plating on plates containing these antibiotics. After nsPEF treatment (0, 60, 120 pulses 600 ns, 30 kV/cm, 1 Hz), 10-fold serial dilutions of treated and untreated cells were spotted onto LB plates containing antibiotics (Fig. 7)^d. In samples with reduced viability, fewer dilutions are needed before no visible growth is detected after 24 h. Both doxycycline and vancomycin visibly reduced MRSA cell density on a serial

^c Results discussed in this subsection were generated by collaborator Areej Malik, who is also a Ph.D. student in the Biomedical Sciences Program at ODU

^d This was a collaborative study where results from vancomycin experiments reported in Figures 7 and 8 were generated by Areej Malik, who is also a Ph.D. student in the Biomedical Sciences Program at ODU.

dilution plate (compare yellow rectangles in Fig. 7A and 7C). The effect of nsPEF treatment alone was apparent on the dilution plates in the absence of antibiotics (Fig. 7A and 7C, see blue rectangles). However, the difference between nsPEF-treated and untreated cells was much more pronounced on plates containing antibiotics (Fig. 7A and 7C, red rectangles). The trends observed on the doxycycline plates were not statistically significant (Fig. 7B), but nsPEF combined with sustained vancomycin exposure inactivated MRSA significantly more than either treatment alone (Fig. 7D).

Plating nsPEF-treated MRSA on daptomycin plates led to inconclusive results as prolonged incubation of cells with this antibiotic caused either no effect or complete growth inhibition at all tested concentrations (data not shown).

Effect of nsPEF/antibiotics combined treatment of MRSA biofilm viability

Because *S. aureus* living within biofilms is more resistant to antibiotic than planktonic bacteria (145), we investigated the effect of combining nsPEF with either doxycycline or vancomycin on MRSA biofilms viability. Biofilms were washed and adherent cells were manually scraped from the plastic growth surface and resuspended into sterile LB broth. Cells were dispersed by vortexing and were aliquoted into electroporation cuvettes. After nsPEF treatment (0, 60, 120 pulses 600 ns, 30 kV/cm, 1 Hz), samples were plated on LB plates containing 1 μ g/mL of either doxycycline or vancomycin and colonies were counted in 40 h (Fig. 8). nsPEF treatment alone had very little effect on biofilm-grown cells, with 60 and 120 pulses reducing culture viability by less than 0.3 log₁₀ (Fig. 8). Doxycycline alone only reduced culture viability of 0.4 log₁₀, while pre-treatment with 60 or 120 pulses allowed doxycycline to impact the biofilm-grown cells by 0.5 and 0.6 log₁₀ (Fig. 8A). The effects of the co-treatment were significantly enhanced compared to either treatment alone, but their overall impact was

modest. Vancomycin treatment had more of an impact on the biofilm-grown cells, reducing viability by 1.1 log₁₀. Pre-treatment with 60 or 120 nsPEF pulses increased this effect to 1.8 and 1.9 log₁₀ (Fig. 8B). nsPEF enhancement of vancomycin treatment alone did not achieve statistical significance, but did trend upward, suggesting that investigation of vancomycin penetrance and efficacy in intact biofilms subjected to nsPEF treatment could be a promising area of future investigation.

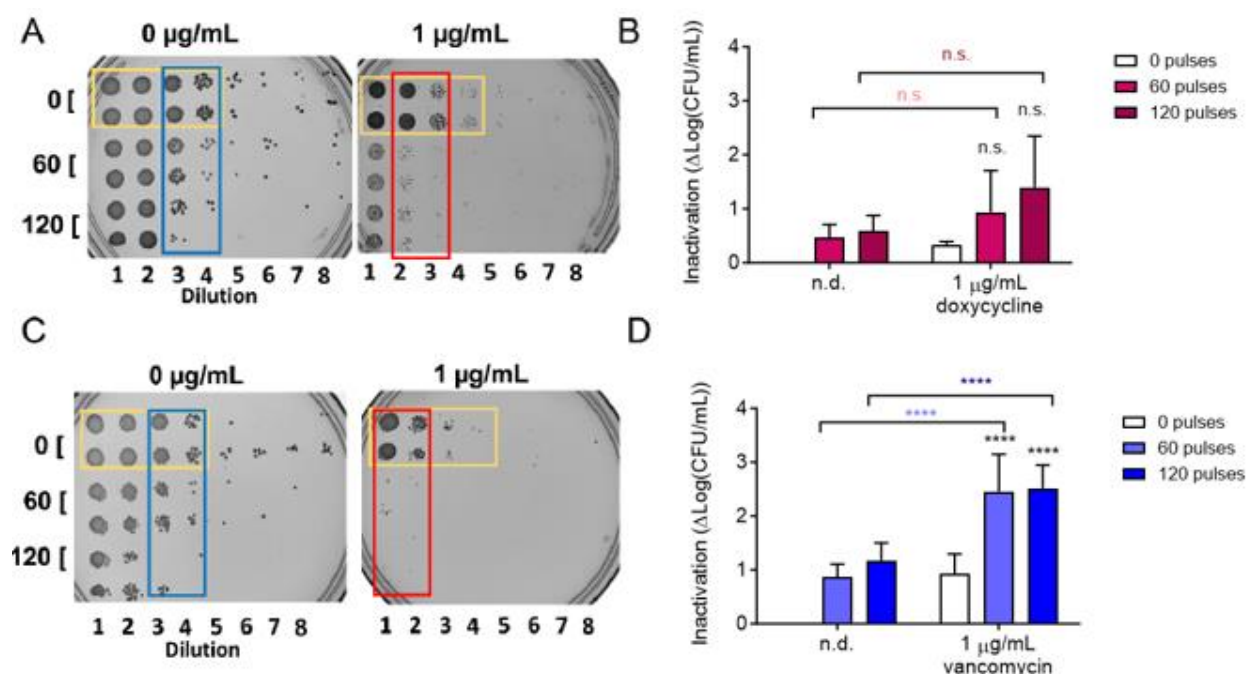


Figure 7. Effect of nsPEF and extended incubation with doxycycline (A, B) and vancomycin (C, D) on MRSA viability. In panels A and C, a replica plating device was used to reproducibly spot 10-fold serial dilutions onto agar plates. Shown are representative images of eight serial 10-fold dilutions of exponentially growing MRSA treated with 0, 60, or 120 pulses (600 ns, 30 kV/cm, 1 Hz) and then plated either on control LB plates (A and C left images) or plates containing 1 $\mu\text{g/mL}$ doxycycline (B) or vancomycin (D). Yellow and blue rectangles highlight the effect of the monotreatment with antibiotics and nsPEF, respectively. Red rectangles show the effect of the combined treatment (see text for details). In panels B and D, a quantification of the effects seen in panels A and C was done for one optimal dilution. Inactivation is quantified as $\log(\text{CFU/mL})_{\text{untreated}} - \log(\text{CFU/mL})_{\text{treated}}$. Black symbols: samples treated with antibiotics and pulses are compared to those treated with antibiotics alone by one-way ANOVA. Light fuchsia symbols: samples treated with doxycycline and 60 pulses are compared to those treated with 60 pulses alone. Dark fuchsia symbols: samples treated with doxycycline and 120 pulses are compared to those treated with 120 pulses alone. Light blue asterisks: samples treated with vancomycin and 60 pulses are compared to those treated with 60 pulses alone by one-way ANOVA. Dark blue asterisks: samples treated with vancomycin and 120 pulses are compared to those treated with 120 pulses alone. All treatment comparisons were analyzed using one-way ANOVA. Data shown represent the mean and standard deviation of at least three samples. n.d., no drug; n.s., not significant and **** $P < 0.0001$. Figure is reproduced from Chittams-Miles AE, et al, 2024 (2).

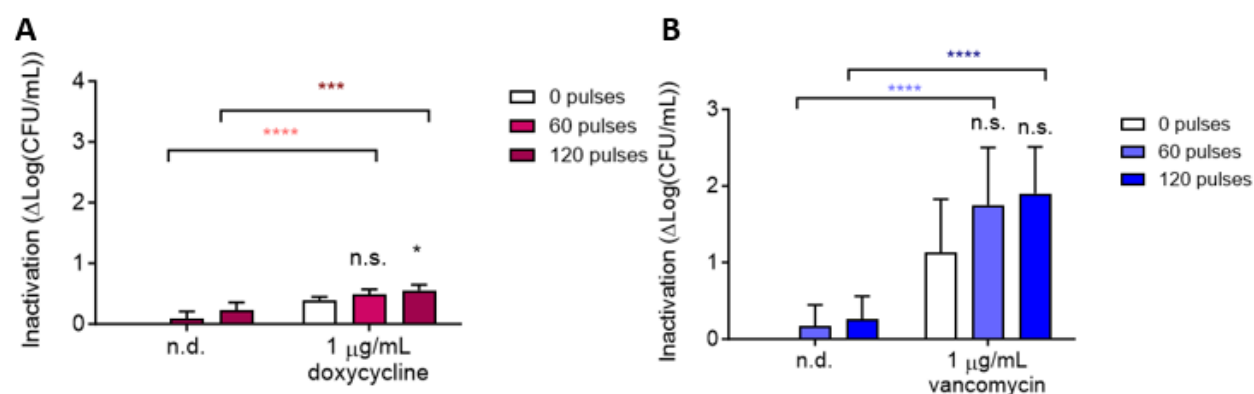


Figure 8. Effect of nsPEF on antibiotic susceptibility of biofilm-derived cells. MRSA cells scraped out of biofilms were homogenized in solution and treated with 0, 60, or 120 pulses before serial dilution plating on either control LB plates or plates containing 1 $\mu\text{g/mL}$ doxycycline (A) or 1 $\mu\text{g/mL}$ vancomycin (B). Inactivation is quantified as $\log(\text{CFU/mL})_{\text{untreated}} - \log(\text{CFU/mL})_{\text{treated}}$ and is individually calculated for each sample. Black asterisk: samples treated with antibiotics and pulses are compared to those treated with antibiotics alone. Light fuchsia asterisks: samples treated with doxycycline and 60 pulses are compared to those treated with 60 pulses alone. Dark fuchsia asterisks: samples treated with doxycycline and 120 pulses are compared to those treated with pulses alone. Light blue asterisks: samples treated with vancomycin and 60 pulses are compared to those treated with 60 pulses alone. Dark blue asterisks: samples treated with vancomycin and 120 pulses are compared to those treated with 120 pulses alone. All treatment comparisons were analyzed using one-way ANOVA. Data represent the means and standard deviations of at least five independent samples. n.d., no drug; n.s., not significant. * $P < 0.05$, *** $P < 0.001$, and **** $P < 0.0001$. Figure is reproduced from Chittams-Miles AE, et al, 2024 (2).

Discussion

S. aureus is a natural component of the commensal skin microbiota but can become an opportunistic pathogen when the skin, the first line of immune defense, is breached (15, 146, 147). Treatment of the resulting SSTI is complicated by the high prevalence of methicillin resistance among *S. aureus* strains (148). Many *S. aureus* infections, both methicillin-sensitive and methicillin-resistant, are currently treated using doxycycline, vancomycin, or daptomycin, alone or in tandem with physical debridement methods (149). However, resistance has also developed to these antibiotics (18-20). Effective methods of treatment are necessary to reduce the burden of *S. aureus* in healthcare settings (150).

This study makes use of nsPEF in combination with antibiotic treatments to inactivate MRSA. Pulsed electric fields (PEF) used for bacterial inactivation are traditionally of the microsecond duration and have been seen to impact bacterial viability with a range of pulse amplitudes (43, 151). Numerous studies have demonstrated that bacteria, when exposed to PEF, show both membrane and cell wall damage as well as subsequent cell death (42, 46, 152). While these studies are promising, few have investigated the synergistic effects of shorter nanosecond duration pulses in combination with antibiotics (63).

Our study shows that MRSA in exponential growth phase is mildly inactivated when treated with 300 or 600 nanosecond pulses with electric fields strength of 30 kV/cm, the maximum field we could reach with our setup. The inactivation observed is in line with previously completed studies on other Gram-positive bacterial species (63, 64). A previous study investigating the effects of 300 ns pulses on *S. aureus* viability showed an inactivation amount of 0.2 log₁₀ reduction using 1000 pulses at 20 kV/cm (63). These published results in addition to our own support the well-established notion that bacteria are more resilient to PEF than mammalian cells.

Additionally, our results indicate that MRSA biofilms are more resistant to nsPEF than the planktonic bacteria. This was expected as bacteria in a biofilm structure are well protected due to the surrounding extracellular polymeric matrix (EPS). EPS protects encased bacteria from the host immune response and prevents antimicrobials from effectively permeating into the biofilm structure (153). Previous work on another skin pathogen, *Cutibacterium acnes*, indicated that biofilm-grown cells and intact biofilm were more susceptible to inactivation by PEF than free-living planktonic cells (48). This result did not replicate with MRSA. This could be due to the bacterial species having different EPS components that are more or less conducive to electrical currents or could be due to a more robust staphylococcal genetic response to cell envelope damage. The *S. aureus* biofilm matrix is comprised largely of polysaccharides and proteins, although the components vary over time and differ depending on the nature of the biofilm substrate (154-156). To our knowledge, its conductive capacity has never been assessed. Similarly, this organism's transcriptional responses to stresses including heat shock, cold shock, starvation, DNA damage, and oxidative stress have been documented (157, 158), but to our knowledge the transcriptional response to PEF has not been documented in this or any other prokaryotic organism.

When planktonic MRSA is treated with both nsPEF and sub-lethal concentrations of clinically relevant antibiotics, we see more robust bacterial killing by the combinatorial treatment than by either treatment administered as monotherapies. In the case of daptomycin, the relative order of nsPEF and antibiotic application is unimportant, as prior nsPEF treatment sensitize cells to antibiotic, and prior antibiotic treatment appears to sensitize cells to nsPEF. This is consistent with a model in which nsPEF and daptomycin are both primarily active at the cell membrane, such that their effects reinforce each other regardless of which stress the cell encounters first.

Excitingly, combination with nsPEF gives 2 µg/mL daptomycin the same efficacy as 8 µg/mL of daptomycin applied alone. Doxycycline was modestly enhanced by combination with nsPEF, although the dual therapies depended on the order of administration. nsPEF treatment modestly sensitized MRSA to doxycycline but the antibiotic did not substantially sensitize the bacteria to subsequent nsPEF exposure. Similarly, pre-treatment with vancomycin did not sensitize MRSA to nsPEF but a prolonged exposure to the antibiotic after nsPEF greatly increased the efficacy of the combined treatment.

Our results suggest that nsPEF administered to surface accessible SSTIs could lower the effective dose of antibiotics needed to treat an infection, allowing more effective treatment without increasing the dose of antibiotic administered and risk of amplified side effects. By reducing the dose of antibiotic necessary to be effective, co-treatment with nsPEF could amplify the effects of standard antibiotic dosing to treat *S. aureus* infections, reducing the risk that tolerant persister cells could survive treatment and cause recurrent infection.

Future research will focus on testing the efficacy of nsPEF *in vivo* in a mouse model of SSTI. A range of PEF amplitudes and durations will be tested to minimize damage to healthy tissue and muscle contraction. If these results are replicated in animal and human studies, nsPEF co-treatment could allow treatment of suitable infections with lower antibiotic doses, reducing drug side effects. SSTI are accessible to physical intervention and are good candidates for nsPEF co-treatment, which could be adopted as a step-in wound and abscess debridement. Notably the CellFX pulse generator used in our experiments has already received clearance from the FDA, Europe, and Canada for the treatment of benign skin lesions.

Much more work will be needed before such possibilities can be realized, but here we report that nsPEF in combination with antibiotic treatments not only increases bacterial inactivation but

also reduces the concentration of antibiotics necessary for disinfection. Additionally, this is the first time that it has been shown that the order of antibiotic/PEF administration is important in bacterial inactivation, which will influence future treatment design.

INFLAMMASOME ACTIVATION AND IL-1 β RELEASE TRIGGERED BY NANOSECOND PULSED ELECTRIC FIELDS IN MURINE INNATE IMMUNE CELLS AND SKIN ^{ef}

Introduction

Treatments with intense pulsed electric fields (PEF) are central for many existing and emerging medical applications including tumor treatment (66, 68, 125, 137, 159-161), vaccination (162-165), cardiac ablation (166, 167), and gene therapy (168-170). In these treatments the delivery of electrical energy causes cell membrane permeabilization in the treated area (120, 123-126). Depending on the application, this disruption of the membrane barrier function, called electroporation (or electropermeabilization), can be either reversible or irreversible. Protocols causing reversible electroporation, in which permeabilizing structures are transient and membrane integrity is quickly recovered, are used in ECT and GET to introduce into cells substances which are otherwise impermeant, such as drugs, proteins, and nucleic acids (171, 172). Conversely, irreversible electroporation (IRE) creates damage that exceeds the cell's membrane repair capacity and cause cell death. The primary factors causing irreversible changes in homeostasis are, calcium (Ca²⁺) overload, efflux of ATP and other metabolites, and disturbances in transmembrane ion gradients (Na⁺, K⁺, Cl⁻) required for maintenance of membrane resting potential and for osmotic and cell volume regulation (75, 76, 116-122).

^e This chapter is based on the manuscript titled “Inflammasome Activation and IL-1 β Release Triggered by Nanosecond Pulsed Electric Fields in Murine Innate Immune Cells and Skin.” Which was originally published in The Journal of Immunology on January 15, 2024.

<https://doi.org/10.4049/jimmunol.2200881>. The manuscript has been modified for inclusion in this chapter and is reproduced here under copyright agreement.

^f This chapter includes experiments conducted in accordance to the guidelines set forth by the Institutional Biosafety Committee (IBC) and the Institutional Animal Care and Use Committee (IACUC) of Old Dominion University.

Lethal PEF applications such as IRE and nsPEF cause both immediate and delayed cell death by multiple mechanisms, still incompletely defined (116, 125, 159, 173, 174).

PEF protocols currently in use in the clinic were developed to maximize tumor tissue ablation (IRE and nsPEF) or to achieve the highest drug uptake or the most persistent gene expression (ECT and GET). Recent research in both healthy and tumor tissue indicates that PEF have a potent immune stimulatory effect (66-69, 175, 176), a novel dimension which merits consideration during treatment planning. Activation of a robust immune response against cancerous cells or a pathogen antigen can be a significant advantage for any anticancer therapeutic modality or vaccine. Conversely, PEF-induced immune activation can be harmful for other applications such as cardiac ablation and gene therapy. Understanding the mechanisms responsible for PEF-induced immune stimulation, and their dependence on pulse parameters, is essential for the improvement of existing PEF applications and the development of new ones.

The immune system detects threats like tissue damage, infections, and metabolic stress through pattern recognition receptors (PRRs). The nucleotide-binding domain, leucine-rich repeat (LRR)-containing receptors (NLRs) are PRRs that initiate inflammatory responses (177). NLRs are typically formed by three components: a sensor, an adaptor, and an effector. Following activation, these subunits combine to form a pro-inflammatory, multiprotein complex named the inflammasome. Activation of the inflammasome promotes the secretion of pro-inflammatory cytokines and induces pyroptosis. Among the multiple NLRs, the NLRP3 has been the most extensively studied (81, 82). The NLRP3 inflammasome is regulated by a two-step process; a “priming” stimulus is required to initiate expression of key inflammasome components, followed by a secondary “activating” stimulus that results in assembly of the inflammasome complex (81,

82). This process involves the oligomerization of NLRP3 proteins, which then recruit the adaptor apoptosis-associated speck-like protein containing a CARD (ASC) and caspase-1. Autocatalytic activation and cleavage of caspase-1 enables cleavage of pro-inflammatory cytokines IL-1 β and IL-18, as well as the pore-forming protein gasdermin D (GSDMD). IL-1 β is released through GSDMD pores, and in larger amounts during pyroptosis, the lytic cell death that often follows GSDMD pore formation (81, 82). IL-1 β and IL-18 are involved in the innate immune response to infection and trauma, creating a generalized pro-inflammatory environment. Detection of active caspase-1, and mature IL-1 β and IL-18 are commonly utilized in research as indicators of NLRP3 activation (178).

The NLRP3 inflammasome sensor is activated by several chemically and structurally diverse triggers, including markers of cell damage (e.g., ATP), environmental pollutants like silica, and pore-forming toxins (81, 82). Since a direct interaction with each activator is unlikely, it is assumed that the NLRP3 inflammasome either senses a common secondary activator downstream of these stimuli or responds to cellular stress signals associated with infection or damage. For instance, a feature common to all NLRP3 stimuli is potassium (K⁺) efflux, an indicator of cell membrane permeabilization. Other signals proposed to be critical for NLRP3 activation include reactive oxygen species (ROS), cell volume changes, elevation of intracellular calcium levels, mitochondria destabilization, and endoplasmic reticulum (ER) stress (81, 82, 179, 180). Interestingly, several of these mechanisms mirror PEF bio-effects, especially responses to nanosecond pulses used in nsPEF. Unlike the micro- and millisecond PEF, nanosecond pulses permeabilize not only the outer (plasma) membrane of the cell, but also intracellular membranes of organelles such as the endoplasmic reticulum (ER) and the mitochondria, and these “ultrashort” pulses deposit proportionally more energy in intracellular membranes than in plasma

membranes (73, 75, 76, 129, 130, 181). Membrane permeabilization by nsPEF causes K^+ efflux (74), intracellular Ca^{2+} mobilization (75-78), and cell swelling (73). Moreover, cell damage by nsPEF has also been found to increase ROS production and trigger ER stress (66, 79, 80).

In this study we investigated whether the damage created by nsPEF is sensed intracellularly by the NLRP3 inflammasome. We show that nsPEF trigger caspase-1 activation and IL-1 β release both in innate immune cells *in vitro* and *in vivo* in mouse skin. We also found that longer, microsecond duration pulses are less effective at stimulating inflammasome activation. Finally, while IL-1 β release in response to nsPEF was blocked in cells treated with the NLRP3 inhibitor MCC950, its release was not impaired in bone marrow derived macrophages (BMDM) from NLRP3 knockout animals (NLRP3-KO). These results suggest that nsPEF generate a set of stimuli for the inflammasome which are sensed by the NLRP3 but also by other yet unknown sensors.

Materials and Methods

Cell culture and stable cell lines. Murine macrophages J774A.1 cells (TIB-67) and human embryonic kidney cells HEK 293 T (CRL-3216) were obtained from ATCC (Manassas, VA). Cells were cultured in high-glucose Dulbecco's modified Eagle's medium (DMEM) (Corning, New York, NY) supplemented with L-glutamine (ATCC), 10% fetal bovine serum (FBS; Atlanta Biologicals, Norcross, GA), 100 U/mL penicillin and 0.1 mg/mL streptomycin (Gibco, Gaithersburg, MD) at 37°C and 5% CO₂.

Wild-type, NLRP3-KO BMDM were differentiated as previously described (182). Briefly, female BALB/c or C57BL/6 (NLRP3-KO) mice (Jackson Laboratory, Bar Harbor, ME) were euthanized and contents of femurs and tibiae were flushed with cold medium using a 5 mL syringe and a 25-gauge needle. Cells were plated at $6-8 \times 10^6$ cells/plate in 7 mL DMEM with

20% FBS, 100 U/mL penicillin and 0.1 mg/mL streptomycin, 25 mM Hepes, and 30 ng/mL recombinant murine macrophage colony stimulating factor (M-CSF; Peprotech, Cranbury, NJ). On day 3, 3 mL of the same medium were added to BMDM cultures. Cells were used for experiments at day 7. BMDM phenotype was confirmed by flow cytometry analysis using specific macrophage (CD11b and F4/80) markers (data not shown).

J774A.1 cells overexpressing ASC fused to GFP (J774A.1 ASC-GFP) were generated by lentiviral transduction using a pLEX-MCS-ASC-GFP construct (Addgene, Watertown, MA). Viral particles were produced in HEK 293T cells using a Lenti-X Packaging Single Shot kit (Takara, San Jose, CA) according to the manufacturer's instruction. J774A.1 cells were transduced with 2 mL of HEK 293T viral particle-containing supernatant in presence of 5 µg/mL polybrene (Sigma-Aldrich, St. Louis, MO) for 18 h. After 72 h, cells expressing ASC-GFP were selected with 2 µg/mL puromycin (Sigma-Aldrich).

Inflammasome priming, activation and inhibition. All cell types were primed with 1 µg/mL LPS from *Escherichia coli* 0111:B4 (Sigma-Aldrich) for 4 hrs to induce the expression of pro-IL-1β and NLRP3 inflammasome precursors. Because intracellular delivery of LPS by electroporation is a widely used method for non-canonical activation of the NLRP3 inflammasome (183, 184), the extracellular LPS was removed by three washes with PBS. Cells were then detached, centrifuged, and resuspended in growth medium for PEF exposure. ATP (5 mM; Sigma-Aldrich) for either 30 or 60 min was used as positive control for caspase-1 activation or IL-1β release, respectively. MCC950 (75 nM; InvivoGen, San Diego, CA) was used to inhibit the NLRP3 inflammasome. The incubation with the inhibitor started 30 min before stimulation of the inflammasome.

PEF exposure methods. In experiments *in vitro* PEF were delivered to cells either attached to cover glasses or in suspension in electroporation cuvettes. Both methods have been previously described (66, 185).

Trapezoidal 200 ns pulses were produced by either a custom pulse generation system with an output impedance of 100 Ω , adjustable pulse amplitude (up to 15 kV), duration (200 to 1000 ns) and frequency (1 to 100 Hz; Pulse Biosciences, Inc., Hayward, CA) (48) or from an AVTECH AVOZ-D2-B-ODA generator (AVTECH Electrosystems, Ottawa, Ontario, Canada). 200 ns pulse waveforms from each generator are shown in Supplemental Fig. 1A. To deliver trains of 100 μ s pulses (rectangular) we used an ECM 830 square wave electroporation system (BTX Harvard Apparatus, Holliston, MA).

For exposure of cells in cuvettes, samples were resuspended at 1.2 to 2×10^6 cell/mL in the growth medium, loaded in 1 mm gap electroporation cuvettes (BioSmith, San Diego, CA, USA) and subjected to either nsPEF (0 to 300 pulses, 200 ns, 10 Hz, 9 kV/cm) or sham exposure at RT.

To treat the skin *in vivo*, mice were anesthetized by inhalation of 3% isoflurane in oxygen (Patterson Veterinary, Devens, MA). Pulses of 200 ns duration (50-200, 15 kV, 4 Hz) were applied by sandwiching the skin of the mouse between a flat round silicon stage and a plastic ring into which a needle electrode array made of two parallel rows of six needles, 4.5 mm apart, was inserted through the skin into the underneath silicon support (Supplementary Fig. 1B, I and II). To ensure an efficient electrical continuity, electrodes were covered with Vaseline. The electric field was calculated by 2D numerical simulations using a finite element analysis software COMSOL Multiphysics®, Release 5.0 (COMSOL Inc., Stockholm, Sweden). The electric field distribution was modeled under static conditions and the electrical conductivity was

assigned to 0.148 S/m [<https://itis.swiss/virtual-population/tissue-properties/database/low-frequency-conductivity/>]. Supplementary Fig. 1B, III shows that the electric field is homogeneous in the area bounded by the two rows of electrodes and its value is 30 kV/cm for 15 kV applied. Animals in the sham control group underwent anesthesia and the probe insertion procedure but no nsPEF delivery.

The pulse amplitude and shape were monitored in all experiments using a LeCroy WaveSurfer 3034z oscilloscope (Teledyne Lecroy, Chestnut Ridge, NY).

Viability and ELISA assays. Immediately after PEF application, cell samples were plated in triplicate at 0.03×10^6 cell/well in black wall 96-well plates (ThermoFisher) and viability was measured by Presto Blue assay after 24h (ThermoFisher). For the ELISA assays, cell samples were seeded at 0.6×10^6 cell/well in 48 well plates immediately after PEF. 1 h post-treatment, the supernatant was harvested, centrifuged at 200 x g for 5 minutes at 4 °C and IL- β was measured using a mouse-specific ELISA kit according to the manufacturer's instructions (88-7013-88; ThermoFisher) (186-189). TNF- α was also measured 1 h after treatment using a mouse-specific ELISA kit (887324-22; ThermoFisher) (188, 189).

Western blot analysis. The Western blot procedure was described previously (66, 190). Either 30 min (for caspase-1 and -11) or 1 h (GSDMD) post nsPEF treatment, cells were washed twice with ice-cold PBS and lysed for 30 min in a buffer containing 20 mM Tris-HCl (pH 7.5), 150 mM NaCl, 1 mM Na₂EDTA, 1 mM EGTA, 1% Triton, 2.5 mM sodium pyrophosphate, 1 mM beta-glycerophosphate, 1 mM Na₃VO₄, 1 μ g/mL leupeptin (Cell Signaling Technology, Danvers, MA) and 1 mM phenylmethylsulfonyl fluoride (PMSF; Sigma-Aldrich) added immediately before use. For IL-1 β detection both supernatants and cell lysates were collected at 1 h post nsPEF treatment. Supernatants were concentrated 10 times using centrifugal filter

devices (ThermoFisher). Protein concentration was measured by BCA assay (ThermoFisher), 20 µg of lysate (or supernatant) per sample were separated by SDS-PAGE and transferred onto polyvinylidene difluoride (PVDF) membranes. Membranes were bathed in 5% BSA Tris-buffered saline with 0.1% Tween (TBS-T) solution for 1 h at RT and then incubated overnight at 4 °C and for 1 h at RT with primary and secondary antibodies, respectively. Anti-caspase-1 (p20) (AG-20B-0042-C100; Adipogen, San Diego, CA)(191-193) was used at 1:1000 and 1:2500 dilution for BMDM and skin lysates, respectively. Anti-GSDMD (ab209845; Abcam, Cambridge, MA)(191), anti-IL-1β (AF-401-NA; R&D Systems, Minneapolis, MN) (186, 191, 192, 194, 195), anti-Caspase 11 (NB120-10454; Novus Biologicals, Englewood, CO) (196) and anti-vinculin primary antibodies (ab129002, Abcam) were used at 1:1000 dilution. A rabbit anti-mouse IgG (ab6728, Abcam) was used to detect caspase-1 while a goat anti-rabbit IgG (7074, Cell Signaling Technology) was used for GSDMD and vinculin detection. IL-1β and Caspase-11 were detected using a rabbit anti-goat IgG (HAF017; Novus Biologicals) and goat anti-rat IgG (7077; Cell Signaling) antibody, respectively. Images were captured with a ChemiDoc MP Imaging System (Bio-Rad, Hercules, CA).

Quantification of band intensities was conducted in ImageJ (ImageJ-win64). The fraction of the cleaved protein (IL-1β, caspase-1 and GSDMD) was calculated as: $K = 100 \times S / (S + L)$ where L and S are the intensities of the full-length protein and of the cleaved fragment, respectively.

***In vivo* study.** Four- to six- week-old BalbC female mice (Jackson Laboratory) were housed in group of 5 animals in individually ventilated cages under pathogen-free conditions. The flank skin was treated with nsPEF as described above. As a positive control for the activation of the inflammasome *in vivo*, animals were injected subcutaneously with 10 mg/kg

LPS. After 1 h, mice were humanly euthanized, and skin samples were collected and snap-frozen in liquid nitrogen. After 24 h, the tissue was weighed and sonicated in lysis buffer to measure IL-1 β and TNF- α release by ELISA (ThermoFisher) and caspase-1 activation by western blot analysis as above described.

Statistical analysis. Data are presented as mean \pm standard error for n independent experiments with data points overlap. Statistical analyses were performed using either a two-tailed t test or a one-way ANOVA, where $p < 0.05$ was considered statistically significant. Statistical calculations, including data fits and data plotting were carried out in Grapher 11 (Golden Software, Golden, CO) and Prism (GraphPad, San Diego, CA).

Results

Nanosecond electric pulses activate the inflammasome and trigger GSDMD independent IL-1 β release ^g

The effect of PEF on inflammasome activation was measured using 200 ns duration pulses in innate immune cells that express the NLRP3 inflammasome, namely macrophages. Previous studies reported profound differences in sensitivity of various cell types when exposed to nsPEF (197). Therefore, to identify electric pulse doses causing comparable damage across multiple cell types, we investigated the sensitivity to nsPEF of J774A.1 macrophages and bone marrow-derived macrophages (BMDMs) (Fig. 9, top panels). We identified 25 and 50 pulses for J774A.1, and 25 and 100 pulses for BMDMs, as iso-effective 200 ns pulse doses (9 kV/cm, 10 Hz) causing 0-10% (low dose) and 35-45% (high dose) cell death at 24 h, respectively.

^g The experiments in Figures 9, 10, 11, 13, and 15 were completed by Dr. Flavia Mazzarda, Mrs. Julia Pittaluga and Alexandra Chittams-Miles.

Notice that for each cell type the above indicated pulse numbers will be referred to as high dose and low dose throughout the study.

Inflammasome activation was monitored by measuring the secretion of IL-1 β in cells primed with LPS. For each cell type the higher pulse dose triggered statistically significant IL-1 β release as measured by ELISA at 1 h (Fig. 9, bottom panels).

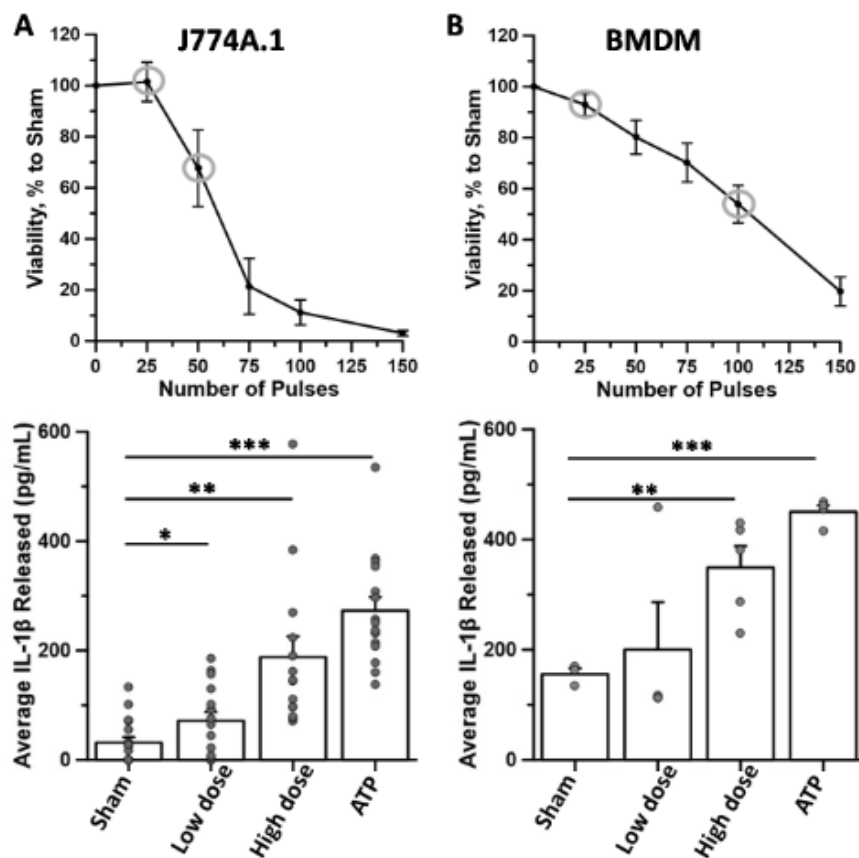


Figure 9. nsPEF trigger IL-1 β release in J774A.1 (A), BMDM (B). Cells were primed by incubation with LPS (1 μ g/mL). After 4 h samples were washed with PBS three times, detached, resuspended in growth medium and either treated with the indicated numbers of 200 ns pulses (9 kV/cm, 10 Hz) or subject to a sham exposure. Viability was measured at 24 h post nsPEF by Presto blue assay and is reported as % to sham exposed parallel control (top graphs). Grey circles identify iso-effective pulse doses causing 0-10% (low dose; 25 pulses) and 35-45% (high dose; 50 and 100 pulses for J774A.1 and BMDM respectively) cell death at 24 h. Bottom graphs report IL-1 β measured in the cell supernatant by ELISA 1 h after treatment with the above indicated iso-effective nsPEF doses. As positive control for inflammasome induction, cells were treated with 5 mM ATP for 1h. Mean \pm s.e., n = 5-16. *p < 0.05, **p < 0.01, ***p < 0.001. Figure is reproduced from Mazzarda, F, et al, 2024 (1).

We further investigate the role of the pulse dose in BMDM and found that nsPEF doses causing 80% cell death at 24h, namely 150 pulses (200 ns, 9 kV/cm, 10 Hz) did not cause IL-1 β release (Fig. 10A). These results can be explained by the fact that incrementing the number of pulses beyond a certain limit increases the percentage of cells dying immediately of primary necrosis due to irreversible permeabilization of the cell plasma membrane. In this scenario most cells don't have time to activate the inflammasome, while at lower doses a higher percentage of cells can repair the electroporation damage and cope with it by activating stress responses including the inflammasome. We further confirm the presence of the active form of IL-1 β (p17) in the supernatant of treated cells by western blot analysis (Fig. 10B). Moreover, the release of the inflammasome-independent marker TNF- α was not affected suggesting that nsPEF specifically stimulates IL-1 β release (Fig. 10C).

Most inflammasomes comprise members of the NLRP family of intracellular pathogen receptors that associate with the ASC adaptor protein to recruit caspase-1. ASC-dependent inflammasome activation is accompanied by rapid relocation of NLR and ASC into a singular, perinuclear, punctate "speck" structure of approximately 1 μ m that can be observed with fluorescence microscopy (198). To visualize the formation of ASC specks in response to inflammasome activation, we generated a J774A.1 cell line stably expressing ASC fused to GFP (J774A.1 ASC-GFP). To test the functionality of this cell line, ASC speck formation was monitored in response to extracellular ATP. As expected, ATP triggered the aggregation of ASC in LPS-treated cells while it failed to do so in cells that were not primed (Fig. 11A). Notably, ASC specks formed also in response to 200 ns pulses (50 pulses, 9 kV/m, 10 Hz) (Fig. 11A).

In nsPEF-treated cells clustering of the ASC adaptor correlated with the activation caspase-1 (Fig. 11B) while caspase-11 (data not shown) was not affected suggesting that these short electrical stimuli activate the canonical inflammasome.

Although secretion of IL-1 β typically requires formation of membrane pores by GSDMD, we did not measure cleavage of GSDMD in response to nsPEF (Fig. 11C). Our results are consistent with previous reports of IL-1 β secretion through GSDMD-independent pathways controlled by caspase-1, such as exocytosis of secretory lysosomes and microvesicle shedding (199-202).

Altogether, our data show that nanosecond pulses induce ASC specks formation, caspase-1 activation, and seemingly unconventional secretion of IL-1 β .

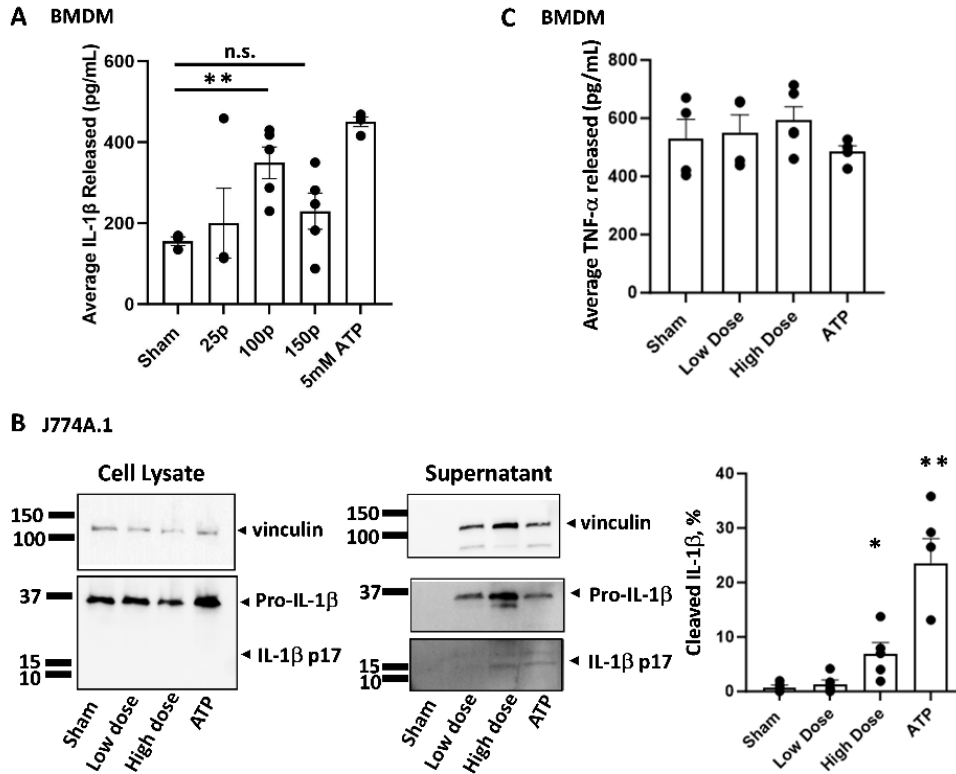


Figure 10. The nsPEF dose affects IL-1 β release (A, B) but does not impact TNF- α release (C). In **A** LPS-primed BMDM were treated with the indicated numbers of 200 ns pulses (9 kV/cm, 10 Hz) and IL-1 β released in the supernatant was measured in 1 h by ELISA assay. In **B** LPS-primed J774A.1 cells were exposed to either a low (25 pulses) or a high (50 pulses) nsPEF dose (200 ns, 9 kV/cm, 10 Hz). Cell lysates and supernatants were assessed for IL-1 β in 1 h by western blot analysis. The bar graph on the right is a quantification of active IL-1 β (p17) over total IL-1 β released in the supernatant. Notice that samples treated with the high nsPEF dose consistently had more vinculin and pro-IL-1 β suggesting that intracellular proteins are passively released by a fraction of cells dying instantaneously of primary necrosis. Vinculin was used as housekeeping control. In **C** LPS-primed BMDM were treated with either 25 (low dose) or 100 (high dose) pulses (200 ns, 9 kV/cm, 10 Hz) and TNF- α was measured by ELISA in 1h. As positive control for inflammasome induction, cells were treated with 5 mM ATP for 1 h. Mean \pm s.e., n=3 (A), 5 (B), and 4-5 (C). * p < 0.05, ** p < 0.01. Figure is reproduced from Mazzarda, F, et al, 2024 (1).

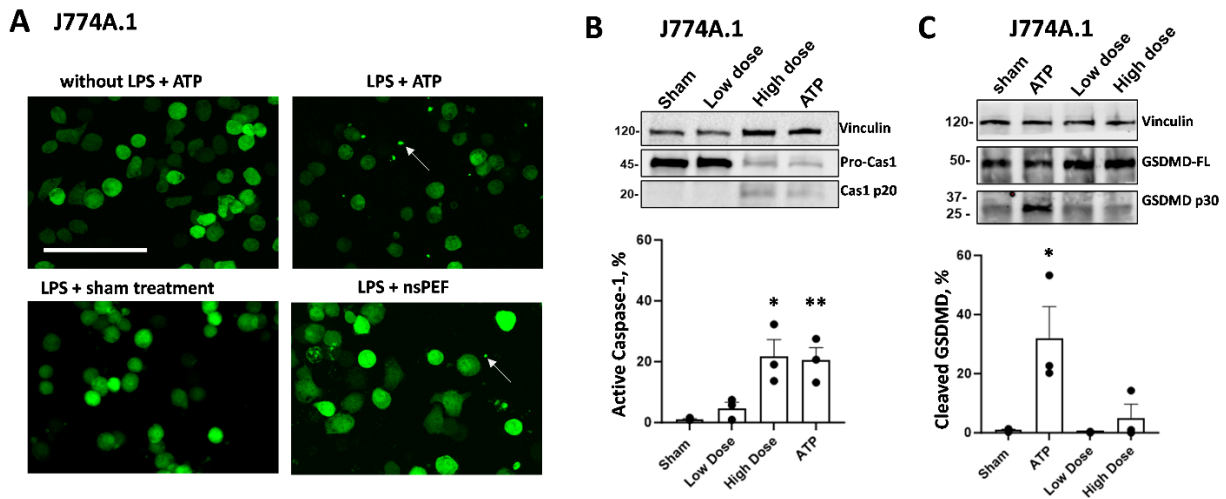


Figure 11. nsPEF trigger ASC specks formation (A) and caspase-1 activation (B) but not GSDMD cleavage (C). **A.** Representative fluorescence images of LPS-primed J774A.1 cells expressing ASC-GFP and treated with either 5 mM ATP or 50, 200 ns pulses (9 kV/cm, 10 Hz). As negative controls, cells were either treated with ATP without priming with LPS or exposed to a sham exposure. Characteristic fluorescence changes from cytosolic diffuse to granular specks are indicated by the white arrows. Scale bar: 100 μ m. **B** and **C** show representative western blot images and quantifications for caspase-1 and GSDMD cleavage measured in J774A.1 at 30 min and 1h post nsPEF, respectively. Low dose and high dose correspond to 25 and 50 pulses (200 ns, 9 kV/cm, 10 Hz) causing 0-10% and 35-45% cell death (Fig. 10A), respectively. Vinculin was used as housekeeping control. Mean \pm s.e., n=3. *p< 0.05, **p< 0.01. Figure is reproduced from Mazzarda, F, et al, 2024 (1).

Microsecond duration pulses are less effective at activating the inflammasome

Next, we asked whether the damage created by longer pulses such as the 100 μ s pulses used in IRE and ECT was also sensed by the inflammasome. For direct comparison with nsPEF experiments, we measured IL-1 β release in cells treated with 100 μ s pulse doses (1 kV/cm, 5 Hz) causing either 0-10% (low dose) or 35-45% (high dose) cell death, namely 2 and 15 pulses and 2 and 7 pulses for BMDMs and J774A.1, respectively (**Fig. 12**, top panels). Compared to the 200 ns pulses used in our nsPEF experiments, 100 μ s pulses failed to trigger the release of IL-1 β in BMDMs and have a weaker effect in J774A.1 cells (**Fig. 12**, bottom panels).

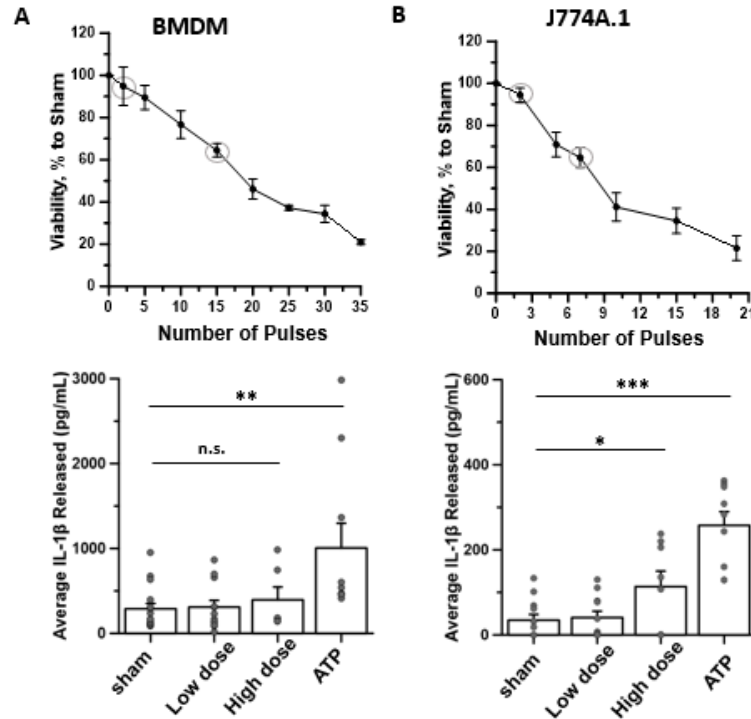


Figure 12. 100 μ s pulses are weaker activators of the inflammasome. Primed BMDMs (**A**) and J774A.1 (**B**) were treated with the indicated numbers of 100 μ s pulses (1 kV/cm, 5 Hz) or subject to a sham exposure. Top panels show viability measured by Presto blue assay at 24 h post treatment. Viability is reported as % to sham exposed parallel control, grey circles identify iso-effective 100 μ s pulse doses causing 0-10% (low dose, 2 pulses for both BMDM and J774A.1 cells) and 35-45% (high dose; 15 and 7 pulses for BMDM and J774A.1 cells, respectively) cell death. Bottom graphs report IL-1 β measured in the cell supernatant by ELISA 1 h after treatment with the above indicated iso-effective low and high pulse doses. Mean \pm s.e., $n = 6-10$ * $p < 0.05$, ** $p < 0.01$, *** $p < 0.001$, n.s. non statistically significant differences. Figure is reproduced from Mazzarda, F, et al, 2024 (1).

The damage created by nsPEF alarm the NLRP3 inflammasome but can also trigger other sensors

To assess the relevance of the NLRP3 inflammasome sensor we initially tested whether IL-1 β release in response to nsPEF was affected by treatment with the NLRP3 inhibitor MCC950 (195). 75 nM MCC950 blocked IL-1 β release in both LPS-primed BMDM and J774A.1 cells (Fig. 13A). In addition, MCC950 rescued 200 ns treated J774A.1 cells from death (Fig. 13B), while it did not protect 100 μ s treated cells (Fig. 13C). These results suggested that nsPEF triggered the NLRP3 inflammasome causing the release of IL-1 β and cell death.

To further investigate the role of the NLRP3 inflammasome sensor, we used BMDM from NLRP3-KO mice. As expected, the lack of NLRP3 expression completely blocked IL-1 β release in response to ATP (Fig. 14). However, contrary to our results with the MCC950 inhibitor, the lack of NLRP3 expression did not impair IL-1 β release in response to nsPEF. These results suggested that either nsPEF trigger another inflammasome sensor in NLRP3-KO cells or MCC950 has an off-target effect that impacts both IL-1 β release and viability. To distinguish between these two scenarios, we measured the effect of MCC950 on nsPEF-treated NLRP3-KO cells. Notably, MCC950 did not block IL-1 β in NLRP3 deficient cells ruling out the possibility of an off-target effect (Fig. 14).

Altogether our results show that the nsPEF damage is sensed intracellularly by the NLRP3 inflammasome, but other sensors can be activated when the NLRP3 is not expressed.

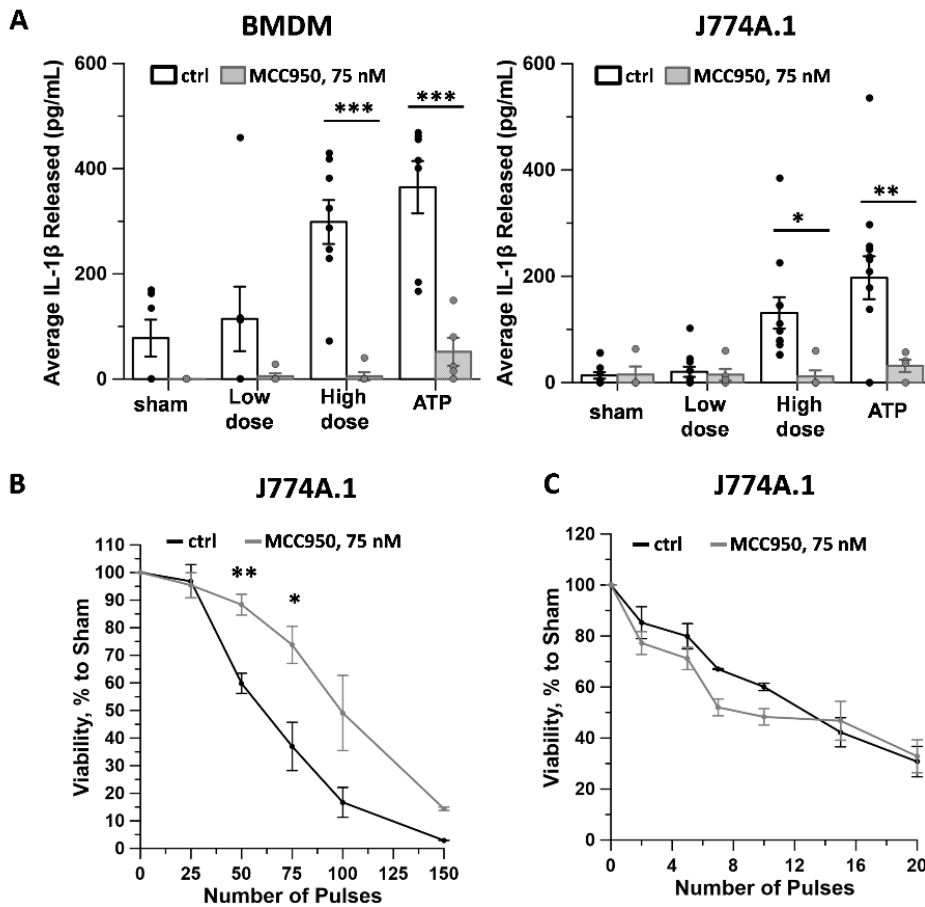


Figure 13. MCC950 blocks IL-1 β release and rescued cells treated with nsPEF. In **A** BMDMs (left panel) and J774A.1 (right panel) were primed by incubation with LPS (1 μ g/mL) for 4 h. Treatment with the NLRP3 inflammasome inhibitor MCC950 (75 nM) started 30 min before the indicated nsPEF treatments (200 ns, 9 kV/cm, 10 Hz) and IL-1 β was measured in 1 h. In **B** and **C**, J774A.1 cells were primed, incubated with MCC950 (75 nM) for 30 min before nsPEF (200 ns, 9 kV/cm, 10 Hz) (**B**) or 100 μ s (1 kV/cm, 5 Hz) (**C**) pulse treatments. Viability was measured in 24h. Mean \pm s.e., n=3-8 (A), 8 (B) and 6 (C). *p< 0.05, **p< 0.01, ***p< 0.001. Figure is reproduced from Mazzarda, F, et al, 2024 (1).

nsPEF triggers IL-1 β release *in vivo* in mouse skin

The activation of the inflammasome *in vivo* in response to nsPEF was monitored in mice skin, which is easy to access and highly infiltrated by innate immune cells. Electric pulses were delivered to the mouse's flank skin using a needle electrode array as described in Materials and Methods. To address the inherent uncertainty of the extrapolation of nsPEF efficacy from *in vitro* to *in vivo*, we tested three pulse number doses delivered at 30 kV/cm, an electric field that is widely used in preclinical and clinical settings (71, 203-205). 1 h post-nsPEF, all tested pulse doses (50, 100 and 200 pulses, 200 ns, 30 kV/cm, 4 Hz) activated the inflammasome as measured by caspase-1 activation (Fig. 15A) and increased concentration IL-1 β in skin tissue lysates (Fig. 15B). Notably TNF- α , another proinflammatory cytokine produced by macrophages, was not affected by the pulse treatment, suggesting that nsPEF selectively induces the release of IL-1 β (Fig. 15B).

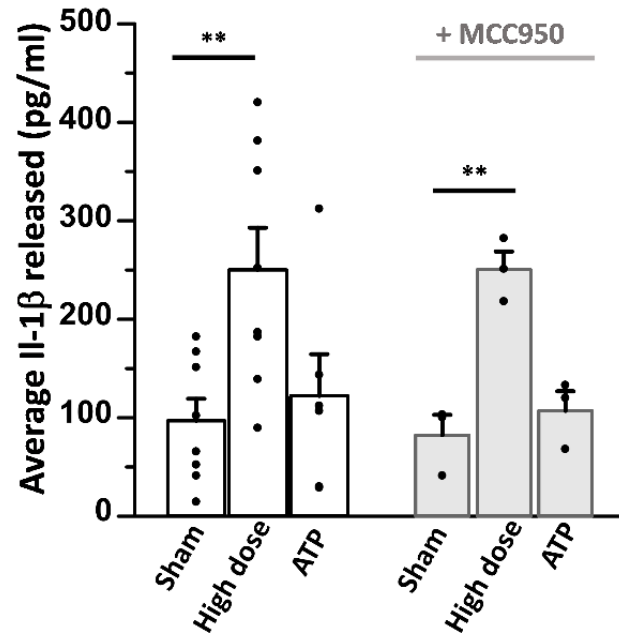


Figure 14. Relevance of NLRP3 expression for nsPEF-induced IL-1 β release. NLRP3-KO BMDM were primed by incubation with LPS (1 μ g/mL). After 4 h cells were treated with a high 200 ns pulse dose (100 pulses, 9 kV/cm, 10 Hz) and IL-1 β was measured by ELISA in 1 h. In selected experiments, treatment with the NLRP3 inflammasome inhibitor MCC950 (75 nM) started 30 min before nsPEF treatments (grey bars). As control for NLRP3 inflammasome induction, cells were treated with 5 mM ATP for 1 h. Mean \pm s.e., n=3-8. ** p<0.01. Figure is reproduced from Mazzarda, F, et al, 2024 (1).

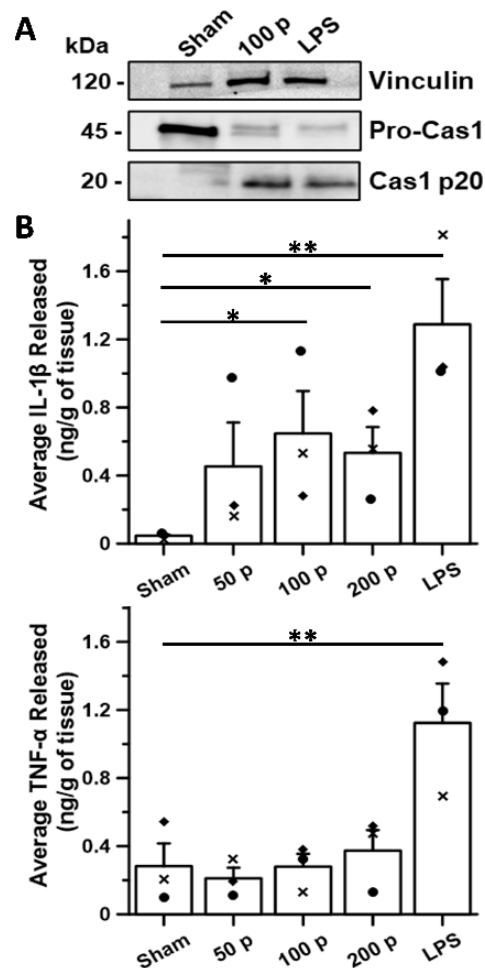


Figure 15. 200 ns pulses activate the inflammasome in mouse skin. Mice skin (3 animals per group) was either treated with nsPEF (50,100, and 200 pulses, 200 ns, 30 kV/cm, 4 Hz) or left untreated. As a positive control for inflammasome activation, animals were injected intradermally with LPS (10 mg/kg). 1 h post treatment, all mice were humanely euthanized to collect the skin. Tissue lysates were analyzed for caspase-1 activation (**A**) and IL-1 β and TNF- α concentration (**B**). Symbols identify animal per condition done in parallel. Mean \pm s.e., n = 3. *p < 0.05, **p < 0.01. Figure is reproduced from Mazzarda, F, et al, 2024 (1).

Discussion

We have presented evidence here that the damage created by PEF activates the NLRP3 inflammasome initiating IL-1 β release. These effects are better seen when using pulses of nanosecond duration compared to equivalent treatments with longer (100 μ s) electric pulses. Experiments using the NLRP3 inhibitor MCC950 also highlight the relevance of the pulse duration. Pre-incubation with the inhibitor protects J774A.1 cells from 200 ns pulses but not from 100 μ s pulses (Fig. 13 B and C). Notably, the effect of the inhibitor is best seen at doses that also cause IL-1 β secretion.

Why are shorter pulses more effective at activating the inflammasome? Unlike electroporative pulses with durations in the micro- and millisecond range, which produce voltages across the cytoplasmic membrane with no direct effects on the cell interior, pulses with rise and fall times faster than the membrane charging time constant (<1 μ s for tightly packed cells in a tissue) (206), generate an electric field in the cytoplasm, and across the intracellular membranes of the nucleus, mitochondria, and other organelles (207, 208). For nanosecond pulses the cytoplasmic membrane appears electrically transparent, and, if the pulse amplitude is large enough, depolarizing and porating electric fields can appear across internal organelles and dissipate before plasma membrane charges redistribute on the plasma membrane to shield the cell interior. Multiple studies showed that nsPEF permeabilize intracellular structures (75, 76, 129-131, 208) including mitochondria (129, 209), endoplasmic reticulum (73, 76, 130, 210, 211), and nuclei (212).

This organelle-penetrating property of nsPEF may explain why their damage is sensed by inflammasomes, the guardians of cytosolic integrity. Mitochondria contain several DAMPs for inflammasome activation (213). For instance, oxidized mitochondrial DNA (mtDNA)

released into the cytosol upon mitochondrial dysfunction is a potent NLRP3 inflammasome activator (214-216). MtDNA also activates inflammasomes that use absent in melanoma 2 (AIM2) as a sensing component (217). Notably, AIM2 can also sense alteration of nuclear envelope integrity by detecting nuclear DNA in the cytosol (218). Our results showing that the lack of NLRP3 expression did not impair nsPEF-induced IL-1 β release (Fig. 14) indicate that nsPEF generate a set of stimuli that can trigger more than one inflammasome sensor. While it has been reported that nsPEF cause cytochrome c release (130, 219, 220) and reduction of mitochondrial membrane potential (129), no one yet has looked for evidence of mitochondrial DNA in the cytoplasm. More research is needed to define the minimal requirements needed to trigger the inflammasome with nsPEF. These short pulses initiate multiple interrelated cellular events — membrane permeabilization, mitochondrial damage, and ROS production — complicating the distinction between bystander and causative events.

Unexpectedly, we found that GSDMD is not activated by nsPEF, at least not at 1 h post treatment where we measured significant IL-1 β release in the supernatant of treated cells (Fig. 11C). IL-1 β lacks a secretory signal and is synthesized as a precursor, pro-IL-1 β , which requires cleavage for activation. Pro-IL-1 β is cleaved by caspase-1, which enables its secretion (81, 82). Caspase-1 also cleaves GSDMD, triggering the formation of GSDMD pores in the plasma membrane and pyroptosis (81, 82). Cell lysis and active IL-1 β secretion are temporally associated (221-223), therefore IL-1 β is often proposed to be passively released during cell rupture (224). However, a growing number of studies report IL-1 β release from living cells (186, 225, 226) and various cell lysis-independent secretion mechanisms have been reported including through GSDMD pores, secretory lysosomes, and microvesicle shedding (186, 199-202).

Lipid electropores (nanopores) are too small to conduct IL-1 β (73, 227). But Pakhomova and colleagues have reported that an initial pulse-induced opening of nanopores minimally permeable to propidium (Pr) is followed by an abrupt Pr inflow which can occur tens of minutes after the exposure(228). This increase in permeability was shown to be due to a sudden pore dilation or perhaps *de novo* opening of larger pores (228). These events are followed by characteristic and irreversible changes in cell appearance (granulation, pyknosis, loss of differential interference contrast and volume changes), and could be regarded as a sign of cell death. IL-1 β could then be released through either dilated nanopores or during cell lysis.

One more intriguing hypothesis is that the release of IL-1 β , which localizes to the plasma membrane after maturation (200) and can also be packed into lysosomes (202), occurs in connection with the active membrane repair initiated to restore membrane integrity after electroporation. Membrane repair mechanisms involve outward vesiculation or shedding of damaged membranes (229, 230) and exocytosis of lysosomes (231) and inflammasome activity correlates with enhanced secretion of extracellular vesicles containing IL-1 β (201). Notably, the repair by lysosomal exocytosis was demonstrated in epithelial cells and fibroblasts treated by milli- and microsecond pulses (232), while we found that Annexin V, a protein that self-assembles into lattices and is involved in patch resealing through vesicle fusion, is activated by nsPEF and contribute to the membrane resealing (233).

Another key question is whether inflammasome activation and cell death are linked or independent processes in nsPEF-treated cells. The lack of GSDMD cleavage suggests that inflammasome activation is not triggering *bona fide* pyroptosis, but why is cell death blocked by the NLRP3 inflammasome inhibitor MCC950? Several studies have shown that caspase-1- or GSDMD-deficient cells are still susceptible to inflammasome-driven cell death (199, 234-236).

In this setting the inflammasome triggers apoptotic Caspases (Caspase-8 and -3) and, according to Schneider *et al.*, initiates an alternative lytic cell death pathway which contributes to immunity against infections (199). Future experiments will be examining these phenomena.

Finally, what are the implications of inflammasome activation for PEF applications? Inflammasome-mediated inflammation can be beneficial for PEF applications such as tumor ablation. Our results, showing higher efficiency of short pulses at inducing the inflammasome suggest that the immunogenicity of the PEF treatment may be increased by shortening the pulse duration. For instance, the release of inflammatory cytokines such as IL-1 β and damage-associated molecular patterns (DAMPs) can create an immune-adjuvanted environment within which tumor antigens are released. While longer pulses of 100 μ s duration are routinely used in the clinic for cancer applications including IRE and ECT (120), treatment with nsPEF is a newer technology which has been investigated mostly in preclinical settings using pulse durations ranging from 100 to 300 ns (120). Multiple studies, including ours, have shown that nsPEF induce an immunogenic form of cell death which assists tumor eradication and prevents the formation of new tumors (66-69, 71, 237-242). Although the inflammasome has been investigated most often in the context of inflammation and innate immunity, there is growing evidence that inflammasome products, particularly IL-1 family cytokines, have an essential role in stimulating adaptive immune responses, including those involved in anti-cancer immunosurveillance (243). For instance, Ghiringhelli and colleagues reported that the activation of the NLRP3 inflammasome in dendritic cells (DCs) is critical for the priming of IFN- γ -producing, tumor-antigen-specific CD8 T cells (244).

Conversely, an enhanced inflammatory response may be harmful to other PEF applications such as cardiac ablation for the treatment of atrial fibrillation (AF) (166, 167).

Cardiomyocytes, cardiac fibroblasts and cardiac macrophages express inflammasome sensors including NLRP3 (245), AIM2 (246) and NLRC4 (246) suggesting that ablation of cardiac tissue may potentially trigger inflammation via inflammasome activation. Notably, an increase in inflammatory markers such as high-sensitivity C-reactive protein (hs-CRP), troponin-T, and fibrinogen are predictive of early recurrence of atrial arrhythmias after radiofrequency ablation (247). Hence anti-inflammatory agents such as corticosteroids and colchicine are currently being tested for their efficacy at preventing AF recurrence (248-251).

Current research is focused on identifying the stimuli that trigger the inflammasome as well as the executors of cell death in nsPEF-treated cells. A better understanding of these responses will facilitate optimization of the treatment conditions to achieve the desired outcome, whether it is exploiting the immune adjuvant effects of PEF or avoiding them.

CONCLUSIONS AND FUTURE DIRECTIONS

Conclusion

In this study we evaluated the use of nanosecond pulsed electric fields (nsPEF) in two ways: uncovering its potential as a bacterial inactivator and as a method of sensitizing methicillin-resistant *Staphylococcus aureus* (MRSA) to widely used antibiotics, while concurrently revealing the immune stimulatory effects in innate immune cells through the activation of the NLRP3 inflammasome.

The initial study explored the sensitivity of MRSA to nsPEF treatment. *S. aureus* is a gram-positive opportunistic and is the leading cause of SSTI (102, 103) *S. aureus* has increasingly developed resistance to varying classes of antibiotics including vancomycin, often considered the first line treatment (107, 113). The development of treatment alternatives is imperative to reduce the burden of *S. aureus* infections in healthcare settings.

In the study we first treated MRSA with 300 and 600 ns pulses with electric field strength of 30 kV/cm and determined that both pulse durations generated a modest inactivation effect in planktonic MRSA. As we saw a stronger inactivation effect with 600 ns pulses, we continued using this pulse duration. The study further investigated the impact of dual treatment of nsPEF and clinically relevant antibiotics (vancomycin, doxycycline, and daptomycin). When compared to monotherapies, co-treatment of nsPEF and daptomycin showed significant inactivation effects regardless of treatment order (nsPEF/daptomycin or daptomycin/nsPEF). Interestingly, while administering doxycycline and vancomycin prior to pulse exposure showed a mild inactivation effect, reversing treatment order with nsPEF being applied before antibiotic exposure provided a

much more robust inactivation response. This indicates that treatment order plays a pivotal role in the inactivation of MRSA.

In parallel, this study sought to understand the immune stimulatory mechanisms of nsPEF treatments by investigating the activation of the inflammasome. We found that nsPEF, rather than the more conventional μ sPEF, stimulated NLRP3 inflammasome activation. This can be attributed to nsPEF's ability to permeabilize intracellular organelles including the mitochondria and endoplasmic reticulum not seen in pulses of microsecond or millisecond duration (73, 75, 129-131, 252). These effects of nsPEF may lead to the release of additional inflammasome stimuli. For instance, oxidized mitochondrial DNA (mtDNA) released into the cytosol upon mitochondrial dysfunction is a potent NLRP3 inflammasome activator (214-216).

Our results show that nsPEF stimulated the cleavage of Caspase-1 and IL-1 β in immortal and bone marrow-derived macrophages and in the murine skin. However, cleaved Gasdermin-D (GSDMD) was not detected in nsPEF treated samples. This indicated that nsPEF does not stimulate pyroptosis. Though we don't see GSDMD cleavage, we do see rescue from cell death when cells are pre-treated with MCC950, suggesting that inflammasome activation and cell death are hand-in-hand processes. Notably, recent studies have proposed an alternative method of cell death which requires inflammasome activation, but it is independent from GSDMD pore formation. These studies suggest that secondary pyroptosis may occur through the activation of caspase-3 and subsequent activation of caspase-8 (199, 253, 254). However, the mechanisms of this process are still unclear. We hypothesize that a secondary pathway of pyroptosis is being activated by making use of apoptotic caspases.

To further prove that nsPEF activate the NLRP3 inflammasome, we repeated the same experiments using bone marrow-derived macrophages (BMDM) differentiated from NLRP3 KO

mice. Surprisingly, when the NLRP3 KO BMDM were treated with nsPEF, IL-1 β was still detected via ELISA. Having ruled out an off-target effect of the NLRP3 inflammasome inhibitor, our working hypothesis is that nsPEF generate an array of stimuli and that multiple inflammasome sensors can potentially be engaged.

Overall, the combined research underscores the potential of nsPEF as a versatile tool in combating antibiotic-resistant pathogens and highlights the importance of further investigation into its mechanisms of action and therapeutic applications.

Future Directions

Our findings have spurred numerous inquiries, paving the way for future research.

Skin and Soft Tissue Infection

Determine the sensitivity of *S. aureus* clinical isolates to nsPEF. In chapter 2, we explored the inactivation effects of nsPEF and antibiotic single and combination treatments on the Xen 31 *S. aureus* strain. Future studies should investigate whether this result is applicable to other more clinically relevant strains of *S. aureus*, most importantly USA300, which is quickly becoming the predominant strain in the US (255). While cell sensitivity to PEF treatment has been documented to be cell dependent in mammalian cells (197, 256, 257), to date, no research has been done investigating the variance in sensitivity of prokaryotic cells to PEF treatment. Therefore, it is imperative that we determine the effects of PEF across multiple clinical *S. aureus* strains. We expect to observe similar inactivation effects as previously seen due to the similarities in bacterial cell shape and size, despite a difference in virulence factors, antibiotic resistance and genome variances (255, 258). This expanded scope will make the study more pertinent to strains commonly encountered in clinical settings.

Measure the antimicrobial effect of nsPEF in SSTI *in vivo*. Our next steps will be to establish the effects of nsPEF on *in vivo* SSTI models in mice. Initially, we need to assess the potential skin damaging effects of pulse treatment. Achieving a delicate equilibrium between the potential skin ablation effects and the bacterial inactivation effects is essential. To achieve this, we will explore multiple pulse conditions testing varying pulse numbers and pulse durations, namely 200 ns and 600 ns) while maintaining a pulse amplitude of 30 kV/cm.

Measure the antimicrobial effect of nsPEF and antibiotic combination treatments *in vivo*. Moving forward, we aim to explore the synergistic effects of nsPEF and antibiotic combination treatments *in vivo*, namely daptomycin and vancomycin. As previously outlined, daptomycin and vancomycin showed encouraging inactivation effects when combined with pulse treatments *in vitro*. Briefly, nsPEF showed an enhanced inactivation effect when combined with antibiotics that targeted similar regions, in this case the bacterial plasma membrane and the cell wall. We predict that *in vivo* nsPEF and antibiotic cotreatment will hasten infection healing and bolster the host immune response. We anticipate that this response will be mediated by the release of pro-inflammatory cytokines and antigens induced by antibacterial therapy, coupled with the enhanced immune activation triggered by nsPEF treatment.

Inflammasome

Establish which nsPEF generated stimuli activates the inflammasome. In chapter 3, we explored the effects of nsPEF in stimulating the inflammasome. Future studies should investigate which nsPEF generated stimuli activates the inflammasome specifically. Literature indicates that multiple stimuli can initiate inflammasome activation including K⁺ efflux, Ca²⁺ influx, ROS formation and intracellular double stranded-DNA (81, 82, 179, 214-216). Although not presented in this thesis work, we performed a study to determine the effects of nsPEF on K⁺

efflux and subsequent IL-1 β release. Briefly, we exposed J774A. 1 cells to nsPEF in a high K⁺ solution and measured IL-1 β release after 1 h. In these results we saw that IL-1 β release was reduced but not blocked (1). In future, we are going to investigate the effects of nsPEF on other known triggers of the inflammasome, namely the influx of Ca²⁺ and ROS. To investigate the impact of Ca⁺ influx, we will treat the cells in calcium-free DMEM and measure IL-1 β release 1 h after pulse treatment. To investigate the role of ROS, we will block ROS formation using the ROS inhibitor NAC, and measure IL-1 β release after 1 h.

Determine the alternative inflammasome sensor that is being activated by nsPEF. In chapter 3, we uncovered that when the NLRP3 inflammasome is unavailable, we still see release of IL-1 β indicating that a secondary inflammasome is activated. We aim to explore secondary inflammasome sensor activation in response to nsPEF-derived stimuli. Of particular interest is the absent in melanoma 2 (AIM2) inflammasome. The AIM2 inflammasome is primarily activated by the presence of intracellular double stranded DNA, including self-DNA like mitochondrial DNA (mtDNA) and nuclear DNA (217, 218). Research has indicated that nsPEF treatment stimulates the release of cytochrome-c from the mitochondria (130, 219, 220), showing mitochondrial damage, however to date, no one has investigated the potential release of mtDNA into the cytosol after nsPEF treatment..

In these experiments we aim to test the AIM2 inhibitor, A151 (259), on wild type BMDM, J774A.1 cell line and NLRP3 KO BMDM. Subsequently we will be testing the effects of nsPEF on both AIM2 and ASC KO BMDM. In these experiments we hope to show that AIM2 and other ASC-dependent inflammasomes can also be activated in response to nsPEF treatment.

Determine how cells die in response to nsPEF. In our study we did not observe GDMD activation following nsPEF treatment, indicating that the inflammatory cell death pathway,

pyroptosis, is not triggered. However, the literature suggests that GSDMD-deficient cells are still capable of undergoing inflammasome-driven cell death through the activation of apoptotic caspases and members of the gasdermin family outside of GSDMD (199, 234-236, 260). Consequently, we propose investigating the activation of varying apoptotic caspases, most importantly Caspase-3 and Caspase-8, and alternative members of the gasdermin family in response to nsPEF treatment.

Investigate other cell types that are targeted by PEF treatment. NsPEF induced inflammasome activation could be of benefit for many applications such as tumor ablation, however, in certain circumstances could be harmful such as in the case of cardiac ablation (166, 167). In future, we hope to expand our study to investigate the specific cellular effects of nsPEF triggered inflammasome activation in varying cell types. Due to the wide range of applications, we hope to explore the effects of inflammasome activating nsPEF treatments in cell types that are present in potential treatment regions like cancer cells, epithelial cells, and muscle cells.

REFERENCES

1. Mazzarda, F., A. E. Chittams-Miles, J. Pittaluga, E. B. Sozer, P. T. Vernier, and C. Muratori. 2023. Inflammasome Activation and IL-1 β Release Triggered by Nanosecond Pulsed Electric Fields in Murine Innate Immune Cells and Skin. *J Immunol*.
2. Chittams-Miles, A. E., A. Malik, E. B. Purcell, and C. Muratori. 2023. Nanosecond pulsed electric fields increase antibiotic susceptibility in methicillin-resistant *Staphylococcus aureus*. *Microbiol Spectr*: e0299223.
3. McMenemy, K. 2017. Skin and Soft Tissue Infections. *Physician Assistant Clinics* 2: 165-176.
4. Lowy, F. D. 1998. *Staphylococcus aureus* infections. *N Engl J Med* 339: 520-532.
5. Malachowa, N., S. D. Kobayashi, J. Lovaglio, and F. R. DeLeo. 2019. Mouse Model of *Staphylococcus aureus* Skin Infection. *Methods Mol Biol* 1960: 139-147.
6. Moran, G. J., A. Krishnadasan, R. J. Gorwitz, G. E. Fosheim, L. K. McDougal, R. B. Carey, D. A. Talan, and E. M. I. N. S. Group. 2006. Methicillin-resistant *S. aureus* infections among patients in the emergency department. *N Engl J Med* 355: 666-674.
7. Daum, R. S. 2007. Clinical practice. Skin and soft-tissue infections caused by methicillin-resistant *Staphylococcus aureus*. *N Engl J Med* 357: 380-390.
8. DeLeo, F. R., M. Otto, B. N. Kreiswirth, and H. F. Chambers. 2010. Community-associated methicillin-resistant *Staphylococcus aureus*. *Lancet* 375: 1557-1568.
9. Stevens, D. L., A. L. Bisno, H. F. Chambers, E. P. Dellinger, E. J. Goldstein, S. L. Gorbach, J. V. Hirschmann, S. L. Kaplan, J. G. Montoya, J. C. Wade, and A. Infectious Diseases Society of. 2014. Practice guidelines for the diagnosis and management of skin and soft tissue infections: 2014 update by the Infectious Diseases Society of America. *Clin Infect Dis* 59: e10-52.
10. Ki, V., and C. Rotstein. 2008. Bacterial skin and soft tissue infections in adults: A review of their epidemiology, pathogenesis, diagnosis, treatment and site of care. *Can J Infect Dis Med Microbiol* 19: 173-184.
11. Kwiecinski, J., G. Kahlmeter, and T. Jin. 2015. Biofilm Formation by *Staphylococcus aureus* Isolates from Skin and Soft Tissue Infections. *Curr Microbiol* 70: 698-703.
12. Archer, N. K., M. J. Mazaitis, J. W. Costerton, J. G. Leid, M. E. Powers, and M. E. Shirtliff. 2011. *Staphylococcus aureus* biofilms: properties, regulation, and roles in human disease. *Virulence* 2: 445-459.
13. Hoiby, N., T. Bjarnsholt, C. Moser, G. L. Bassi, T. Coenye, G. Donelli, L. Hall-Stoodley, V. Høla, C. Imbert, K. Kirketerp-Møller, D. Lebeaux, A. Oliver, A. J. Ullmann, C. Williams, E. S. G. f. Biofilms, and Z. Consulting External Expert Werner. 2015. ESCMID guideline for the diagnosis and treatment of biofilm infections 2014. *Clin Microbiol Infect* 21 Suppl 1: S1-25.
14. Donlan, R. M. 2002. Biofilms: microbial life on surfaces. *Emerg Infect Dis* 8: 881-890.
15. Idrees, M., S. Sawant, N. Karodia, and A. Rahman. 2021. *Staphylococcus aureus* Biofilm: Morphology, Genetics, Pathogenesis and Treatment Strategies. *Int J Environ Res Public Health* 18.
16. Pillet, F. 2017. Electroporation of Biofilms. In *Handbook of Electroporation*. D. Miklavčič, ed. Springer International Publishing, Cham. 403-416.
17. Donlan, R. M., and J. W. Costerton. 2002. Biofilms: survival mechanisms of clinically relevant microorganisms. *Clin Microbiol Rev* 15: 167-193.
18. Bal, A. M., and I. M. Gould. 2005. Antibiotic resistance in *Staphylococcus aureus* and its relevance in therapy. *Expert Opin Pharmacother* 6: 2257-2269.
19. Miller, L. S., E. M. Pietras, L. H. Uricchio, K. Hirano, S. Rao, H. Lin, R. M. O'Connell, Y. Iwakura, A. L. Cheung, G. Cheng, and R. L. Modlin. 2007. Inflammasome-mediated production of IL-1 β is required for neutrophil recruitment against *Staphylococcus aureus* in vivo. *J Immunol* 179: 6933-6942.

20. Jackson, N., L. Czaplewski, and L. J. V. Piddock. 2018. Discovery and development of new antibacterial drugs: learning from experience? *J Antimicrob Chemother* 73: 1452-1459.
21. Miller, L. S., V. G. Fowler, S. K. Shukla, W. E. Rose, and R. A. Proctor. 2020. Development of a vaccine against *Staphylococcus aureus* invasive infections: Evidence based on human immunity, genetics and bacterial evasion mechanisms. *FEMS Microbiol Rev* 44: 123-153.
22. Clegg, J., E. Soldaini, R. M. McLoughlin, S. Rittenhouse, F. Bagnoli, and S. Phogat. 2021. *Staphylococcus aureus* Vaccine Research and Development: The Past, Present and Future, Including Novel Therapeutic Strategies. *Front Immunol* 12: 705360.
23. Jori, G., C. Fabris, M. Soncin, S. Ferro, O. Coppellotti, D. Dei, L. Fantetti, G. Chiti, and G. Roncucci. 2006. Photodynamic therapy in the treatment of microbial infections: basic principles and perspective applications. *Lasers Surg Med* 38: 468-481.
24. Willis, J. A., V. Cheburkanov, S. Chen, J. M. Soares, G. Kassab, K. C. Blanco, V. S. Bagnato, P. de Figueiredo, and V. V. Yakovlev. 2022. Breaking down antibiotic resistance in methicillin-resistant *Staphylococcus aureus*: Combining antimicrobial photodynamic and antibiotic treatments. *Proc Natl Acad Sci U S A* 119: e2208378119.
25. Reithinger, R., M. Mohsen, M. Wahid, M. Bismullah, R. J. Quinnell, C. R. Davies, J. Kolaczinski, and J. R. David. 2005. Efficacy of thermotherapy to treat cutaneous leishmaniasis caused by *Leishmania tropica* in Kabul, Afghanistan: a randomized, controlled trial. *Clin Infect Dis* 40: 1148-1155.
26. Niepa, T. H., J. L. Gilbert, and D. Ren. 2012. Controlling *Pseudomonas aeruginosa* persister cells by weak electrochemical currents and synergistic effects with tobramycin. *Biomaterials* 33: 7356-7365.
27. Jass, J., and H. M. Lappin-Scott. 1996. The efficacy of antibiotics enhanced by electrical currents against *Pseudomonas aeruginosa* biofilms. *J Antimicrob Chemother* 38: 987-1000.
28. Giladi, M., Y. Porat, A. Blatt, E. Shmueli, Y. Wasserman, E. D. Kirson, and Y. Palti. 2010. Microbial growth inhibition by alternating electric fields in mice with *Pseudomonas aeruginosa* lung infection. *Antimicrob Agents Chemother* 54: 3212-3218.
29. Costerton, J. W., B. Ellis, K. Lam, F. Johnson, and A. E. Khoury. 1994. Mechanism of electrical enhancement of efficacy of antibiotics in killing biofilm bacteria. *Antimicrob Agents Chemother* 38: 2803-2809.
30. Blenkinsopp, S. A., A. E. Khoury, and J. W. Costerton. 1992. Electrical enhancement of biocide efficacy against *Pseudomonas aeruginosa* biofilms. *Appl Environ Microbiol* 58: 3770-3773.
31. Zolfaghari, P. S., S. Packer, M. Singer, S. P. Nair, J. Bennett, C. Street, and M. Wilson. 2009. In vivo killing of *Staphylococcus aureus* using a light-activated antimicrobial agent. *BMC Microbiol* 9: 27.
32. Oleinick, N. L., and H. H. Evans. 1998. The photobiology of photodynamic therapy: cellular targets and mechanisms. *Radiat Res* 150: S146-156.
33. Ensing, G. T., B. L. Roeder, J. L. Nelson, J. R. van Horn, H. C. van der Mei, H. J. Busscher, and W. G. Pitt. 2005. Effect of pulsed ultrasound in combination with gentamicin on bacterial viability in biofilms on bone cements in vivo. *J Appl Microbiol* 99: 443-448.
34. Rediske, A. M., B. L. Roeder, M. K. Brown, J. L. Nelson, R. L. Robison, D. O. Draper, G. B. Schaalje, R. A. Robison, and W. G. Pitt. 1999. Ultrasonic enhancement of antibiotic action on *Escherichia coli* biofilms: an in vivo model. *Antimicrob Agents Chemother* 43: 1211-1214.
35. Rediske, A. M., N. Rapoport, and W. G. Pitt. 1999. Reducing bacterial resistance to antibiotics with ultrasound. *Lett Appl Microbiol* 28: 81-84.
36. Geboers, B., H. J. Scheffer, P. M. Graybill, A. H. Ruarus, S. Nieuwenhuizen, R. S. Puijk, P. M. van den Tol, R. V. Davalos, B. Rubinsky, T. D. de Gruijl, D. Miklavcic, and M. R. Meijerink. 2020. High-Voltage Electrical Pulses in Oncology: Irreversible Electroporation, Electrochemotherapy, Gene Electrottransfer, Electrofusion, and Electroimmunotherapy. *Radiology* 295: 254-272.

37. Maor, E., A. Sugrue, C. Witt, V. R. Vaidya, C. V. DeSimone, S. J. Asirvatham, and S. Kapa. 2019. Pulsed electric fields for cardiac ablation and beyond: A state-of-the-art review. *Heart Rhythm* 16: 1112-1120.
38. Beebe, S. J., P. M. Fox, L. J. Rec, K. Somers, R. H. Stark, and K. H. Schoenbach. 2002. Nanosecond pulsed electric field (nsPEF) effects on cells and tissues: apoptosis induction and tumor growth inhibition. *IEEE Transactions on Plasma Science* 30: 286-292.
39. Buchmann, L., and A. Mathys. 2019. Perspective on Pulsed Electric Field Treatment in the Bio-based Industry. *Front Bioeng Biotechnol* 7: 265.
40. Novickij, V., A. Zinkeviciene, E. Perminaitė, R. Cesna, E. Lastauskiene, A. Paskevicius, J. Svediene, S. Markovskaja, J. Novickij, and I. Girkontaite. 2018. Non-invasive nanosecond electroporation for biocontrol of surface infections: an in vivo study. *Sci Rep* 8: 14516.
41. Zhang, K., J. Guo, Z. Ge, and J. Zhang. 2014. Nanosecond pulsed electric fields (nsPEFs) regulate phenotypes of chondrocytes through Wnt/beta-catenin signaling pathway. *Sci Rep* 4: 5836.
42. Sale, A. J. H., and W. A. Hamilton. 1967. Effect of high electric fields on microorganism. I. Killing of bacteria and yeast. *Biochimica et Biophysica Acta* 15: 1031-1037.
43. Mahnic-Kalamiza, S., E. Vorobiev, and D. Miklavcic. 2014. Electroporation in food processing and biorefinery. *J Membr Biol* 247: 1279-1304.
44. Rieder, A., T. Schwartz, K. Schon-Holz, S. M. Marten, J. Suss, C. Gusbeth, W. Kohnen, W. Swoboda, U. Obst, and W. Frey. 2008. Molecular monitoring of inactivation efficiencies of bacteria during pulsed electric field treatment of clinical wastewater. *J Appl Microbiol* 105: 2035-2045.
45. Gusbeth, C., W. Frey, H. Volkmann, T. Schwartz, and H. Bluhm. 2009. Pulsed electric field treatment for bacteria reduction and its impact on hospital wastewater. *Chemosphere* 75: 228-233.
46. Pillet, F., C. Formosa-Dague, H. Baaziz, E. Dague, and M. P. Rols. 2016. Cell wall as a target for bacteria inactivation by pulsed electric fields. *Sci Rep* 6: 19778.
47. Khan, S. I., G. Blumrosen, D. Vecchio, A. Golberg, M. C. McCormack, M. L. Yarmush, M. R. Hamblin, and W. G. Austen, Jr. 2016. Eradication of multidrug-resistant pseudomonas biofilm with pulsed electric fields. *Biotechnol Bioeng* 113: 643-650.
48. Poudel, A., A. Oludiran, E. B. Sozer, M. Casciola, E. B. Purcell, and C. Muratori. 2021. Growth in a biofilm sensitizes *Cutibacterium acnes* to nanosecond pulsed electric fields. *Bioelectrochemistry* 140: 107797.
49. Yano, K.-i., and K. Morotomi-Yano. 2016. Cell Stress Responses to Pulsed Electric Fields. In *Handbook of Electroporation*. D. Miklavcic, ed. Springer International Publishing, Cham. 1-17.
50. Ruiz-Fernandez, A. R., L. Campos, S. E. Gutierrez-Maldonado, G. Nunez, F. Villanelo, and T. Perez-Acle. 2022. Nanosecond Pulsed Electric Field (nsPEF): Opening the Biotechnological Pandora's Box. *Int J Mol Sci* 23.
51. Hall, E. H., K. H. Schoenbach, and S. J. Beebe. 2005. Nanosecond pulsed electric fields (nsPEF) induce direct electric field effects and biological effects on human colon carcinoma cells. *DNA Cell Biol* 24: 283-291.
52. Thomson, K. R., W. Cheung, S. J. Ellis, D. Federman, H. Kavnoudias, D. Loader-Oliver, S. Roberts, P. Evans, C. Ball, and A. Haydon. 2011. Investigation of the safety of irreversible electroporation in humans. *J Vasc Interv Radiol* 22: 611-621.
53. Zupanic, A., S. Ribaric, and D. Miklavcic. 2007. Increasing the repetition frequency of electric pulse delivery reduces unpleasant sensations that occur in electrochemotherapy. *Neoplasma* 54: 246-250.
54. Miklavcic, D., G. Pucihar, M. Pavlovec, S. Ribaric, M. Mali, A. Macek-Lebar, M. Petkovsek, J. Nastran, S. Kranjc, M. Cemazar, and G. Sersa. 2005. The effect of high frequency electric pulses on muscle contractions and antitumor efficiency in vivo for a potential use in clinical electrochemotherapy. *Bioelectrochemistry* 65: 121-128.

55. Scheffer, H. J., K. Nielsen, M. C. de Jong, A. A. van Tilborg, J. M. Vieveen, A. R. Bouwman, S. Meijer, C. van Kuijk, P. M. van den Tol, and M. R. Meijerink. 2014. Irreversible electroporation for nonthermal tumor ablation in the clinical setting: a systematic review of safety and efficacy. *J Vasc Interv Radiol* 25: 997-1011; quiz 1011.
56. Ball, C., K. R. Thomson, and H. Kavnoudias. 2010. Irreversible electroporation: a new challenge in "out of operating theater" anesthesia. *Anesth Analg* 110: 1305-1309.
57. Fusco, R., E. Di Bernardo, V. D'Alessio, S. Salati, and M. Cadossi. 2021. Reduction of muscle contraction and pain in electroporation-based treatments: An overview. *World J Clin Oncol* 12: 367-381.
58. Pakhomova, O. N., B. W. Gregory, I. Semenov, and A. G. Pakhomov. 2013. Two modes of cell death caused by exposure to nanosecond pulsed electric field. *PLoS One* 8: e70278.
59. Nuccitelli, R. 2019. Application of Pulsed Electric Fields to Cancer Therapy. *Bioelectricity* 1: 30-34.
60. Pakhomova, O., E. Gianulis, and A. G. Pakhomov. 2017. Different Cell Sensitivity to Pulsed Electric Field. In *Handbook of Electroporation*. D. Miklavcic, ed. Springer International Publishing, Cham. 1-17.
61. Novickij, V., A. Zinkeviciene, R. Staneviciene, R. Gruskiene, E. Serviene, I. Vepstaite-Monstavice, T. Krivorotova, E. Lastauskiene, J. Sereikaite, I. Girkontaite, and J. Novickij. 2018. Inactivation of Escherichia coli Using Nanosecond Electric Fields and Nisin Nanoparticles: A Kinetics Study. *Front Microbiol* 9: 3006.
62. Yan, Z., L. Yin, C. Hao, K. Liu, and J. Qiu. 2021. Synergistic effect of pulsed electric fields and temperature on the inactivation of microorganisms. *AMB Express* 11: 47.
63. Vadlamani, A., D. A. Detwiler, A. Dhanabal, and A. L. Garner. 2018. Synergistic bacterial inactivation by combining antibiotics with nanosecond electric pulses. *Appl Microbiol Biotechnol* 102: 7589-7596.
64. Martens, S. L., S. Klein, R. A. Barnes, P. TrejoSanchez, C. C. Roth, and B. L. Ibey. 2020. 600-ns pulsed electric fields affect inactivation and antibiotic susceptibilities of Escherichia coli and Lactobacillus acidophilus. *AMB Express* 10: 55.
65. Vadlamani, R. A., A. Dhanabal, D. A. Detwiler, R. Pal, J. McCarthy, M. N. Seleem, and A. L. Garner. 2020. Nanosecond electric pulses rapidly enhance the inactivation of Gram-negative bacteria using Gram-positive antibiotics. *Appl Microbiol Biotechnol* 104: 2217-2227.
66. Rossi, A., O. N. Pakhomova, P. A. Mollica, M. Casciola, U. Mangalanathan, A. G. Pakhomov, and C. Muratori. 2019. Nanosecond Pulsed Electric Fields Induce Endoplasmic Reticulum Stress Accompanied by Immunogenic Cell Death in Murine Models of Lymphoma and Colorectal Cancer. *Cancers (Basel)* 11.
67. Nuccitelli, R., J. C. Berridge, Z. Mallon, M. Kreis, B. Athos, and P. Nuccitelli. 2015. Nanoelectroablation of murine tumors triggers a CD8-dependent inhibition of secondary tumor growth. *PLoS One* 10: e0134364.
68. Guo, S., Y. Jing, N. I. Burcus, B. P. Lassiter, R. Tanaz, R. Heller, and S. J. Beebe. 2018. Nanopulse stimulation induces potent immune responses, eradicating local breast cancer while reducing distant metastases. *Int J Cancer* 142: 629-640.
69. Chen, R., N. M. Sain, K. T. Harlow, Y. J. Chen, P. K. Shires, R. Heller, and S. J. Beebe. 2014. A protective effect after clearance of orthotopic rat hepatocellular carcinoma by nanosecond pulsed electric fields. *European journal of cancer* 50: 2705-2713.
70. Hanahan, D., and R. A. Weinberg. 2011. Hallmarks of cancer: the next generation. *Cell* 144: 646-674.
71. Rossi, A., O. N. Pakhomova, A. G. Pakhomov, S. Weygandt, A. A. Bulysheva, L. E. Murray, P. A. Mollica, and C. Muratori. 2019. Mechanisms and immunogenicity of nsPEF-induced cell death in B16F10 melanoma tumors. *Sci Rep* 9: 431.

72. Koga, T., K. Morotomi-Yano, T. Sakugawa, H. Saitoh, and K. I. Yano. 2019. Nanosecond pulsed electric fields induce extracellular release of chromosomal DNA and histone citrullination in neutrophil-differentiated HL-60 cells. *Sci Rep* 9: 8451.
73. Nesin, O. M., O. N. Pakhomova, S. Xiao, and A. G. Pakhomov. 2011. Manipulation of cell volume and membrane pore comparison following single cell permeabilization with 60- and 600-ns electric pulses. *Biochim Biophys Acta* 1808: 792-801.
74. Saulis, G., S. Satkauskas, and R. Praneviciute. 2007. Determination of cell electroporation from the release of intracellular potassium ions. *Analytical biochemistry* 360: 273-281.
75. Semenov, I., S. Xiao, and A. G. Pakhomov. 2013. Primary pathways of intracellular Ca(2+) mobilization by nanosecond pulsed electric field. *Biochim Biophys Acta* 1828: 981-989.
76. Semenov, I., S. Xiao, O. N. Pakhomova, and A. G. Pakhomov. 2013. Recruitment of the intracellular Ca by ultrashort electric stimuli: The impact of pulse duration. *Cell calcium* 54: 145-150.
77. Vernier, P. T., Y. Sun, M. T. Chen, M. A. Gundersen, and G. L. Craviso. 2008. Nanosecond electric pulse-induced calcium entry into chromaffin cells. *Bioelectrochemistry* 73: 1-4.
78. Craviso, G. L., S. Choe, P. Chatterjee, I. Chatterjee, and P. T. Vernier. 2010. Nanosecond electric pulses: A novel stimulus for triggering Ca²⁺ influx into chromaffin cells via voltage-gated Ca²⁺ channels. *Cell Mol Neurobiol* 30: 1259-1265.
79. Pakhomova, O. N., V. A. Khorokhorina, A. M. Bowman, R. Rodaite-Riseviciene, G. Saulis, S. Xiao, and A. G. Pakhomov. 2012. Oxidative effects of nanosecond pulsed electric field exposure in cells and cell-free media. *Arch Biochem Biophys* 527: 55-64.
80. Nuccitelli, R., K. Lui, M. Kreis, B. Athos, and P. Nuccitelli. 2013. Nanosecond pulsed electric field stimulation of reactive oxygen species in human pancreatic cancer cells is Ca(2+)-dependent. *Biochem Biophys Res Commun* 435: 580-585.
81. Swanson, K. V., M. Deng, and J. P. Ting. 2019. The NLRP3 inflammasome: molecular activation and regulation to therapeutics. *Nat Rev Immunol* 19: 477-489.
82. He, Y., H. Hara, and G. Nunez. 2016. Mechanism and Regulation of NLRP3 Inflammasome Activation. *Trends Biochem Sci* 41: 1012-1021.
83. Gong, T., Y. Yang, T. Jin, W. Jiang, and R. Zhou. 2018. Orchestration of NLRP3 Inflammasome Activation by Ion Fluxes. *Trends Immunol* 39: 393-406.
84. Coll, R. C., K. Schroder, and P. Pelegrin. 2022. NLRP3 and pyroptosis blockers for treating inflammatory diseases. *Trends Pharmacol Sci* 43: 653-668.
85. Miller, L. S., R. M. O'Connell, M. A. Gutierrez, E. M. Pietras, A. Shahangian, C. E. Gross, A. Thirumala, A. L. Cheung, G. Cheng, and R. L. Modlin. 2006. MyD88 mediates neutrophil recruitment initiated by IL-1R but not TLR2 activation in immunity against *Staphylococcus aureus*. *Immunity* 24: 79-91.
86. Munoz-Planillo, R., L. Franchi, L. S. Miller, and G. Nunez. 2009. A critical role for hemolysins and bacterial lipoproteins in *Staphylococcus aureus*-induced activation of the Nlrp3 inflammasome. *J Immunol* 183: 3942-3948.
87. Cho, J. S., E. M. Pietras, N. C. Garcia, R. I. Ramos, D. M. Farzam, H. R. Monroe, J. E. Magorien, A. Blauvelt, J. K. Kolls, A. L. Cheung, G. Cheng, R. L. Modlin, and L. S. Miller. 2010. IL-17 is essential for host defense against cutaneous *Staphylococcus aureus* infection in mice. *J Clin Invest* 120: 1762-1773.
88. Ishigame, H., S. Kakuta, T. Nagai, M. Kadoki, A. Nambu, Y. Komiyama, N. Fujikado, Y. Tanahashi, A. Akitsu, H. Kotaki, K. Sudo, S. Nakae, C. Sasakawa, and Y. Iwakura. 2009. Differential roles of interleukin-17A and -17F in host defense against mucocutaneous bacterial infection and allergic responses. *Immunity* 30: 108-119.
89. Martynova, E., A. Rizvanov, R. A. Urbanowicz, and S. Khaiboullina. 2022. Inflammasome Contribution to the Activation of Th1, Th2, and Th17 Immune Responses. *Front Microbiol* 13: 851835.

90. Dinarello, C. A. 2011. Interleukin-1 in the pathogenesis and treatment of inflammatory diseases. *Blood* 117: 3720-3732.
91. Liu, Q., M. Mazhar, and L. S. Miller. 2018. Immune and Inflammatory Responses to Staphylococcus aureus Skin Infections. *Curr Dermatol Rep* 7: 338-349.
92. Sims, J. E., and D. E. Smith. 2010. The IL-1 family: regulators of immunity. *Nat Rev Immunol* 10: 89-102.
93. Picard, C., A. Puel, M. Bonnet, C. L. Ku, J. Bustamante, K. Yang, C. Soudais, S. Dupuis, J. Feinberg, C. Fieschi, C. Elbim, R. Hitchcock, D. Lamm, G. Davies, A. Al-Ghonaïm, H. Al-Rayes, S. Al-Jumaah, S. Al-Hajjar, I. Z. Al-Mohsen, H. H. Frayha, R. Rucker, T. R. Hawn, A. Aderem, H. Tufenkeji, S. Haraguchi, N. K. Day, R. A. Good, M. A. Gougerot-Pocidalo, A. Ozinsky, and J. L. Casanova. 2003. Pyogenic bacterial infections in humans with IRAK-4 deficiency. *Science* 299: 2076-2079.
94. von Bernuth, H., C. Picard, Z. Jin, R. Pankla, H. Xiao, C. L. Ku, M. Chrabieh, I. B. Mustapha, P. Ghandil, Y. Camcioglu, J. Vasconcelos, N. Sirvent, M. Guedes, A. B. Vitor, M. J. Herrero-Mata, J. I. Arostegui, C. Rodrigo, L. Alsina, E. Ruiz-Ortiz, M. Juan, C. Fortuny, J. Yague, J. Anton, M. Pascal, H. H. Chang, L. Janniere, Y. Rose, B. Z. Garty, H. Chapel, A. Issekutz, L. Marodi, C. Rodriguez-Gallego, J. Banchereau, L. Abel, X. Li, D. Chaussabel, A. Puel, and J. L. Casanova. 2008. Pyogenic bacterial infections in humans with MyD88 deficiency. *Science* 321: 691-696.
95. Ku, C. L., H. von Bernuth, C. Picard, S. Y. Zhang, H. H. Chang, K. Yang, M. Chrabieh, A. C. Issekutz, C. K. Cunningham, J. Gallin, S. M. Holland, C. Roifman, S. Ehl, J. Smart, M. Tang, F. J. Barrat, O. Levy, D. McDonald, N. K. Day-Good, R. Miller, H. Takada, T. Hara, S. Al-Hajjar, A. Al-Ghonaïm, D. Speert, D. Sanlaville, X. Li, F. Geissmann, E. Vivier, L. Marodi, B. Z. Garty, H. Chapel, C. Rodriguez-Gallego, X. Bossuyt, L. Abel, A. Puel, and J. L. Casanova. 2007. Selective predisposition to bacterial infections in IRAK-4-deficient children: IRAK-4-dependent TLRs are otherwise redundant in protective immunity. *J Exp Med* 204: 2407-2422.
96. Milner, J. D., J. M. Brechley, A. Laurence, A. F. Freeman, B. J. Hill, K. M. Elias, Y. Kanno, C. Spalding, H. Z. Elloumi, M. L. Paulson, J. Davis, A. Hsu, A. I. Asher, J. O'Shea, S. M. Holland, W. E. Paul, and D. C. Douek. 2008. Impaired T(H)17 cell differentiation in subjects with autosomal dominant hyper-IgE syndrome. *Nature* 452: 773-776.
97. Ma, C. S., G. Y. Chew, N. Simpson, A. Priyadarshi, M. Wong, B. Grimbacher, D. A. Fulcher, S. G. Tangye, and M. C. Cook. 2008. Deficiency of Th17 cells in hyper IgE syndrome due to mutations in STAT3. *J Exp Med* 205: 1551-1557.
98. Renner, E. D., S. Rylaarsdam, S. Anover-Sombke, A. L. Rack, J. Reichenbach, J. C. Carey, Q. Zhu, A. F. Jansson, J. Barboza, L. F. Schimke, M. F. Leppert, M. M. Getz, R. A. Seger, H. R. Hill, B. H. Belohradsky, T. R. Torgerson, and H. D. Ochs. 2008. Novel signal transducer and activator of transcription 3 (STAT3) mutations, reduced T(H)17 cell numbers, and variably defective STAT3 phosphorylation in hyper-IgE syndrome. *J Allergy Clin Immunol* 122: 181-187.
99. Sanchez, M., S. L. Kolar, S. Muller, C. N. Reyes, A. J. Wolf, C. Ogawa, R. Singhania, D. D. De Carvalho, M. Arditi, D. M. Underhill, G. A. Martins, and G. Y. Liu. 2017. O-Acetylation of Peptidoglycan Limits Helper T Cell Priming and Permits Staphylococcus aureus Reinfection. *Cell Host Microbe* 22: 543-551 e544.
100. Shimada, T., B. G. Park, A. J. Wolf, C. Brikos, H. S. Goodridge, C. A. Becker, C. N. Reyes, E. A. Miao, A. Aderem, F. Gotz, G. Y. Liu, and D. M. Underhill. 2010. Staphylococcus aureus evades lysozyme-based peptidoglycan digestion that links phagocytosis, inflammasome activation, and IL-1 β secretion. *Cell Host Microbe* 7: 38-49.
101. Deng, J., B. Z. Zhang, H. Chu, X. L. Wang, Y. Wang, H. R. Gong, R. Li, D. Yang, C. Li, Y. Dou, P. Gao, J. P. Cai, M. Jin, Q. Du, J. F. Chan, R. Y. Kao, K. Y. Yuen, and J. D. Huang. 2021. Adenosine synthase A contributes to recurrent Staphylococcus aureus infection by dampening protective immunity. *EBioMedicine* 70: 103505.

102. Silva-Santana, G., G. G. Cabral-Oliveira, D. R. Oliveira, B. A. Nogueira, P. M. A. Pereira-Ribeiro, and A. L. Mattos-Guaraldi. 2021. Staphylococcus aureus biofilms: an opportunistic pathogen with multidrug resistance. *Reviews and Research in Medical Microbiology* 32.
103. Tong, S. Y., J. S. Davis, E. Eichenberger, T. L. Holland, and V. G. Fowler, Jr. 2015. Staphylococcus aureus infections: epidemiology, pathophysiology, clinical manifestations, and management. *Clin Microbiol Rev* 28: 603-661.
104. Lipsky, B. A., M. H. Silverman, and W. S. Joseph. 2017. A Proposed New Classification of Skin and Soft Tissue Infections Modeled on the Subset of Diabetic Foot Infection. *Open Forum Infect Dis* 4: ofw255.
105. Edelsberg, J., C. Taneja, M. Zervos, N. Haque, C. Moore, K. Reyes, J. Spalding, J. Jiang, and G. Oster. 2009. Trends in US hospital admissions for skin and soft tissue infections. *Emerg Infect Dis* 15: 1516-1518.
106. Shen, H. N., and C. L. Lu. 2010. Skin and soft tissue infections in hospitalized and critically ill patients: a nationwide population-based study. *BMC Infect Dis* 10: 151.
107. Neu, H. C. 1992. The crisis in antibiotic resistance. *Science* 257: 1064-1073.
108. Stapleton, P. D., and P. W. Taylor. 2002. Methicillin resistance in Staphylococcus aureus: mechanisms and modulation. *Science progress* 85: 57-72.
109. Barrett, F. F., R. F. McGehee, Jr., and M. Finland. 1968. Methicillin-resistant Staphylococcus aureus at Boston City Hospital. Bacteriologic and epidemiologic observations. *N Engl J Med* 279: 441-448.
110. Boyce, J. M. 1990. Increasing prevalence of methicillin-resistant Staphylococcus aureus in the United States. *Infect Control Hosp Epidemiol* 11: 639-642.
111. Panlilio, A. L., D. H. Culver, R. P. Gaynes, S. Banerjee, T. S. Henderson, J. S. Tolson, and W. J. Martone. 1992. Methicillin-resistant Staphylococcus aureus in U.S. hospitals, 1975-1991. *Infect Control Hosp Epidemiol* 13: 582-586.
112. Choo, E. J., and H. F. Chambers. 2016. Treatment of methicillin-resistant Staphylococcus aureus bacteremia. *Infection & chemotherapy* 48: 267-273.
113. David, M. Z., and R. S. Daum. 2017. Treatment of Staphylococcus aureus Infections. *Curr Top Microbiol Immunol* 409: 325-383.
114. Calvin, N. M., and P. C. Hanawalt. 1988. High-efficiency transformation of bacterial cells by electroporation. *J Bacteriol* 170: 2796-2801.
115. Neumann, E., M. Schaefer-Ridder, Y. Wang, and P. H. Hofschneider. 1982. Gene transfer into mouse lymphoma cells by electroporation in high electric fields. *EMBO J* 1: 841-845.
116. Batista Napotnik, T., M. Rebersek, P. T. Vernier, B. Mali, and D. Miklavcic. 2016. Effects of high voltage nanosecond electric pulses on eukaryotic cells (in vitro): A systematic review. *Bioelectrochemistry* 110: 1-12.
117. Teissie, J. 2007. Biophysical effects of electric fields on membrane water interfaces: a mini review. *Eur Biophys J* 36: 967-972.
118. Teissie, J., M. Golzio, and M. P. Rols. 2005. Mechanisms of cell membrane electroporation: a minireview of our present (lack of ?) knowledge. *Biochim Biophys Acta* 1724: 270-280.
119. Weaver, J. C., and Y. A. Chizmadzhev. 1996. Theory of electroporation: A review. *Bioelectrochemistry and Bioenergetics* 41: 135-160.
120. Pakhomov, A. G., D. Miklavcic, and M. S. Markov, eds. 2010. *Advanced Electroporation Techniques in Biology in Medicine*. CRC Press, Boca Raton.
121. Pakhomov, A. G., A. M. Bowman, B. L. Ibey, F. M. Andre, O. N. Pakhomova, and K. H. Schoenbach. 2009. Lipid nanopores can form a stable, ion channel-like conduction pathway in cell membrane. *Biochem Biophys Res Commun* 385: 181-186.
122. Sozer, E. B., and P. T. Vernier. 2019. Modulation of biological responses to 2ns electrical stimuli by field reversal. *Biochim Biophys Acta Biomembr* 1861: 1228-1239.

123. Sukhorukov, V. L., H. Mussauer, and U. Zimmermann. 1998. The effect of electrical deformation forces on the electroporabilization of erythrocyte membranes in low- and high-conductivity media. *J Membr Biol* 163: 235-245.
124. Neumann, E., A. E. Sowers, and C. A. Jordan, eds. 1989. *Electroporation and Electrofusion in Cell Biology*. Plenum, New York.
125. Rubinsky, B., ed. 2010. *Irreversible Electroporation*. Springer-Verlag, Berlin Heidelberg.
126. Zimmermann, U. N., G.A. 1996. *Electromanipulation of cells*. CRC Press, Boca Raton.
127. Gowrishankar, T. R., and J. C. Weaver. 2006. Electrical behavior and pore accumulation in a multicellular model for conventional and supra-electroporation. *Biochem Biophys Res Commun* 349: 643-653.
128. Semenov, I., C. Zemlin, O. N. Pakhomova, S. Xiao, and A. G. Pakhomov. 2015. Diffuse, non-polar electroporabilization and reduced propidium uptake distinguish the effect of nanosecond electric pulses. *Biochim Biophys Acta* 1848: 2118-2125.
129. Batista Napotnik, T., Y. H. Wu, M. A. Gundersen, D. Miklavcic, and P. T. Vernier. 2012. Nanosecond electric pulses cause mitochondrial membrane permeabilization in Jurkat cells. *Bioelectromagnetics* 33: 257-264.
130. Beebe, S. J., P. M. Fox, L. J. Rec, E. L. Willis, and K. H. Schoenbach. 2003. Nanosecond, high-intensity pulsed electric fields induce apoptosis in human cells. *FASEB journal : official publication of the Federation of American Societies for Experimental Biology* 17: 1493-1495.
131. White, J. A., P. F. Blackmore, K. H. Schoenbach, and S. J. Beebe. 2004. Stimulation of capacitative calcium entry in HL-60 cells by nanosecond pulsed electric fields. *The Journal of biological chemistry* 279: 22964-22972.
132. Bowman, A. M., O. M. Nesin, O. N. Pakhomova, and A. G. Pakhomov. 2010. Analysis of plasma membrane integrity by fluorescent detection of Tl(+) uptake. *J Membr Biol* 236: 15-26.
133. Pakhomov, A. G., J. F. Kolb, J. A. White, R. P. Joshi, S. Xiao, and K. H. Schoenbach. 2007. Long-lasting plasma membrane permeabilization in mammalian cells by nanosecond pulsed electric field (nsPEF). *Bioelectromagnetics* 28: 655-663.
134. Mercadal, B., C. B. Arena, R. V. Davalos, and A. Ivorra. 2017. Avoiding nerve stimulation in irreversible electroporation: a numerical modeling study. *Phys Med Biol* 62: 8060-8079.
135. Long, G., P. K. Shires, D. Plescia, S. J. Beebe, J. F. Kolb, and K. H. Schoenbach. 2011. Targeted tissue ablation with nanosecond pulses. *IEEE Trans Biomed Eng* 58: 2161-2167.
136. Sano, M. B., C. B. Arena, K. R. Bittleman, M. R. DeWitt, H. J. Cho, C. S. Szot, D. Saur, J. M. Cissell, J. Robertson, Y. W. Lee, and R. V. Davalos. 2015. Bursts of Bipolar Microsecond Pulses Inhibit Tumor Growth. *Sci Rep* 5: 14999.
137. Arena, C. B., M. B. Sano, J. H. Rossmeisl, Jr., J. L. Caldwell, P. A. Garcia, M. N. Rylander, and R. V. Davalos. 2011. High-frequency irreversible electroporation (H-FIRE) for non-thermal ablation without muscle contraction. *Biomedical engineering online* 10: 102.
138. Sano, M. B., R. E. Fan, K. Cheng, Y. Saenz, G. A. Sonn, G. L. Hwang, and L. Xing. 2018. Reduction of Muscle Contractions during Irreversible Electroporation Therapy Using High-Frequency Bursts of Alternating Polarity Pulses: A Laboratory Investigation in an Ex Vivo Swine Model. *J Vasc Interv Radiol* 29: 893-898 e894.
139. Dong, S. L., C. G. Yao, Y. J. Zhao, Y. P. Lv, and H. M. Liu. 2018. Parameters Optimization of Bipolar High Frequency Pulses on Tissue Ablation and Inhibiting Muscle Contraction. *Ieee T Dielect El In* 25: 207-216.
140. Gudvangen, E., V. Kim, V. Novickij, F. Battista, and A. G. Pakhomov. 2022. Electroporation and cell killing by milli- to nanosecond pulses and avoiding neuromuscular stimulation in cancer ablation. *Sci Rep* 12: 1763.
141. Onyango, L. A., R. H. Dunstan, J. Gottfries, C. von Eiff, and T. K. Roberts. 2012. Effect of low temperature on growth and ultra-structure of *Staphylococcus* spp. *PLoS One* 7: e29031.
142. Jung, D., A. Rozek, M. Okon, and R. E. Hancock. 2004. Structural transitions as determinants of the action of the calcium-dependent antibiotic daptomycin. *Chem Biol* 11: 949-957.

143. Chopra, I., and M. Roberts. 2001. Tetracycline antibiotics: mode of action, applications, molecular biology, and epidemiology of bacterial resistance. *Microbiology and molecular biology reviews* 65: 232-260.
144. Koyama, N., J. Inokoshi, and H. Tomoda. 2012. Anti-infectious agents against MRSA. *Molecules* 18: 204-224.
145. Olsen, I. 2015. Biofilm-specific antibiotic tolerance and resistance. *European Journal of Clinical Microbiology & Infectious Diseases* 34: 877-886.
146. Silverberg, B. 2021. A Structured Approach to Skin and Soft Tissue Infections (SSTIs) in an Ambulatory Setting. *Clin Pract* 11: 65-74.
147. Thammavongsa, V., H. K. Kim, D. Missiakas, and O. Schneewind. 2015. Staphylococcal manipulation of host immune responses. *Nat Rev Microbiol* 13: 529-543.
148. Lee, A. S., H. De Lencastre, J. Garau, J. Kluytmans, S. Malhotra-Kumar, A. Peschel, and S. Harbarth. 2018. Methicillin-resistant *Staphylococcus aureus*. *Nature reviews Disease primers* 4: 1-23.
149. World Health, O. 2019. *Critically important antimicrobials for human medicine*. World Health Organization, Geneva.
150. World Health, O. 2017. Ranking of other drug-resistant bacterial infections. In *PRIORITIZATION OF PATHOGENS TO GUIDE DISCOVERY, RESEARCH AND DEVELOPMENT OF NEW ANTIBIOTICS FOR DRUG-RESISTANT BACTERIAL INFECTIONS, INCLUDING TUBERCULOSIS*. World Health Organization. 25-87.
151. Hulsheger, H., J. Potel, and E. G. Niemann. 1983. Electric field effects on bacteria and yeast cells. *Radiat Environ Biophys* 22: 149-162.
152. Hamilton, W. A., and A. J. H. Sale. 1967. Effects of high electric fields on microorganisms: II. Mechanism of action of the lethal effect. *Biochimica et Biophysica Acta (BBA) - General Subjects* 148: 789-800.
153. Vestby, L. K., T. Grønseth, R. Simm, and L. L. Nesse. 2020. Bacterial Biofilm and its Role in the Pathogenesis of Disease. *Antibiotics (Basel)* 9.
154. Foulston, L., A. K. Elsholz, A. S. DeFrancesco, and R. Losick. 2014. The extracellular matrix of *Staphylococcus aureus* biofilms comprises cytoplasmic proteins that associate with the cell surface in response to decreasing pH. *MBio* 5: e01667-01614.
155. Hiltunen, A. K., K. Savijoki, T. A. Nyman, I. Miettinen, P. Ihalainen, J. Peltonen, and A. Fallarero. 2019. Structural and functional dynamics of *Staphylococcus aureus* biofilms and biofilm matrix proteins on different clinical materials. *Microorganisms* 7: 584.
156. Hobley, L., C. Harkins, C. E. MacPhee, and N. R. Stanley-Wall. 2015. Giving structure to the biofilm matrix: an overview of individual strategies and emerging common themes. *FEMS microbiology reviews* 39: 649-669.
157. Anderson, K. L., C. Roberts, T. Disz, V. Vonstein, K. Hwang, R. Overbeek, P. D. Olson, S. J. Projan, and P. M. Dunman. 2006. Characterization of the *Staphylococcus aureus* heat shock, cold shock, stringent, and SOS responses and their effects on log-phase mRNA turnover. *Journal of bacteriology* 188: 6739-6756.
158. Pandey, S., G. S. Sahukhal, and M. O. Elasri. 2019. The msaABCR operon regulates the response to oxidative stress in *Staphylococcus aureus*. *Journal of bacteriology* 201: e00417-00419.
159. Davalos, R. V., I. L. Mir, and B. Rubinsky. 2005. Tissue ablation with irreversible electroporation. *Ann Biomed Eng* 33: 223-231.
160. Sanchez-Velazquez, P., Q. Castellvi, A. Villanueva, R. Quesada, C. Panella, M. Caceres, D. Dorcaratto, A. Andaluz, X. Moll, M. Trujillo, J. M. Burdio, E. Berjano, L. Grande, A. Ivorra, and F. Burdio. 2016. Irreversible electroporation of the liver: is there a safe limit to the ablation volume? *Sci Rep* 6: 23781.
161. Nuccitelli, R., U. Pliquett, X. Chen, W. Ford, R. James Swanson, S. J. Beebe, J. F. Kolb, and K. H. Schoenbach. 2006. Nanosecond pulsed electric fields cause melanomas to self-destruct. *Biochem Biophys Res Commun* 343: 351-360.

162. Sardesai, N. Y., and D. B. Weiner. 2011. Electroporation delivery of DNA vaccines: prospects for success. *Curr Opin Immunol* 23: 421-429.
163. Song, J. M., Y. C. Kim, E. O. R. W. Compans, M. R. Prausnitz, and S. M. Kang. 2012. DNA vaccination in the skin using microneedles improves protection against influenza. *Mol Ther* 20: 1472-1480.
164. Heller, R., Y. Cruz, L. C. Heller, R. A. Gilbert, and M. J. Jaroszeski. 2010. Electrically mediated delivery of plasmid DNA to the skin, using a multielectrode array. *Hum Gene Ther* 21: 357-362.
165. Xia, D., R. Jin, G. Byagathvalli, H. Yu, L. Ye, C. Y. Lu, M. S. Bhamla, C. Yang, and M. R. Prausnitz. 2021. An ultra-low-cost electroporator with microneedle electrodes (ePatch) for SARS-CoV-2 vaccination. *Proc Natl Acad Sci U S A* 118.
166. Xie, F., F. Varghese, A. G. Pakhomov, I. Semenov, S. Xiao, J. Philpott, and C. Zemlin. 2015. Ablation of Myocardial Tissue With Nanosecond Pulsed Electric Fields. *PLoS One* 10: e0144833.
167. Varghese, F., J. M. Philpott, J. U. Neuber, B. Hargrave, and C. W. Zemlin. 2022. Surgical Ablation of Cardiac Tissue with Nanosecond Pulsed Electric Fields in Swine. *Cardiovasc Eng Technol*.
168. Lucas, M. L., and R. Heller. 2003. IL-12 gene therapy using an electrically mediated nonviral approach reduces metastatic growth of melanoma. *DNA Cell Biol* 22: 755-763.
169. Lucas, M. L., L. Heller, D. Coppola, and R. Heller. 2002. IL-12 plasmid delivery by in vivo electroporation for the successful treatment of established subcutaneous B16.F10 melanoma. *Mol Ther* 5: 668-675.
170. Lucas, M. L., and R. Heller. 2001. Immunomodulation by electrically enhanced delivery of plasmid DNA encoding IL-12 to murine skeletal muscle. *Mol Ther* 3: 47-53.
171. Sersa, G., D. Miklavcic, M. Cemazar, Z. Rudolf, G. Pucihar, and M. Snoj. 2008. Electrochemotherapy in treatment of tumours. *Eur J Surg Oncol* 34: 232-240.
172. Rosazza, C., S. H. Meglic, A. Zumbusch, M. P. Rols, and D. Miklavcic. 2016. Gene Electrotransfer: A Mechanistic Perspective. *Curr Gene Ther* 16: 98-129.
173. Al-Sakere, B., F. Andre, C. Bernat, E. Connault, P. Opolon, R. V. Davalos, B. Rubinsky, and L. M. Mir. 2007. Tumor ablation with irreversible electroporation. *PLoS ONE* 2: e1135.
174. Chopinet, L., and M. P. Rols. 2015. Nanosecond electric pulses: A mini-review of the present state of the art. *Bioelectrochemistry* 103: 2-6.
175. Babiuk, S., M. E. Baca-Estrada, M. Foldvari, D. M. Middleton, D. Rabussay, G. Widera, and L. A. Babiuk. 2004. Increased gene expression and inflammatory cell infiltration caused by electroporation are both important for improving the efficacy of DNA vaccines. *J Biotechnol* 110: 1-10.
176. Zhao, J., X. Wen, L. Tian, T. Li, C. Xu, X. Wen, M. P. Melancon, S. Gupta, B. Shen, W. Peng, and C. Li. 2019. Irreversible electroporation reverses resistance to immune checkpoint blockade in pancreatic cancer. *Nat Commun* 10: 899.
177. Davis, B. K., H. Wen, and J. P. Ting. 2011. The inflammasome NLRs in immunity, inflammation, and associated diseases. *Annu Rev Immunol* 29: 707-735.
178. Gross, O. 2012. Measuring the inflammasome. *Methods Mol Biol* 844: 199-222.
179. Menu, P., A. Mayor, R. Zhou, A. Tardivel, H. Ichijo, K. Mori, and J. Tschopp. 2012. ER stress activates the NLRP3 inflammasome via an UPR-independent pathway. *Cell Death Dis* 3: e261.
180. Zhou, Y., Z. Tong, S. Jiang, W. Zheng, J. Zhao, and X. Zhou. 2020. The Roles of Endoplasmic Reticulum in NLRP3 Inflammasome Activation. *Cells* 9.
181. White, J. A., P. F. Blackmore, K. H. Schoenbach, and S. J. Beebe. 2004. Stimulation of capacitative calcium entry in HL-60 cells by nanosecond pulsed electric fields. *J Biol Chem* 279: 22964-22972.
182. Weischenfeldt, J., and B. Porse. 2008. Bone Marrow-Derived Macrophages (BMM): Isolation and Applications. *CSH Protoc* 2008: pdb prot5080.
183. Kayagaki, N., M. T. Wong, I. B. Stowe, S. R. Ramani, L. C. Gonzalez, S. Akashi-Takamura, K. Miyake, J. Zhang, W. P. Lee, A. Muszynski, L. S. Forsberg, R. W. Carlson, and V. M. Dixit.

2013. Noncanonical inflammasome activation by intracellular LPS independent of TLR4. *Science* 341: 1246-1249.
184. Hagar, J. A., D. A. Powell, Y. Achoui, R. K. Ernst, and E. A. Miao. 2013. Cytoplasmic LPS activates caspase-11: implications in TLR4-independent endotoxic shock. *Science* 341: 1250-1253.
185. Sozer, E. B., C. F. Pocetti, and P. T. Vernier. 2018. Transport of charged small molecules after electroporation - drift and diffusion. *BMC Biophys* 11: 4.
186. Evavold, C. L., J. Ruan, Y. Tan, S. Xia, H. Wu, and J. C. Kagan. 2018. The Pore-Forming Protein Gasdermin D Regulates Interleukin-1 Secretion from Living Macrophages. *Immunity* 48: 35-44 e36.
187. Hirano, S., Q. Zhou, A. Furuyama, and S. Kanno. 2017. Differential Regulation of IL-1 β and IL-6 Release in Murine Macrophages. *Inflammation* 40: 1933-1943.
188. Zanoni, I., Y. Tan, M. Di Gioia, J. R. Springstead, and J. C. Kagan. 2017. By Capturing Inflammatory Lipids Released from Dying Cells, the Receptor CD14 Induces Inflammasome-Dependent Phagocyte Hyperactivation. *Immunity* 47: 697-709 e693.
189. Zhivaki, D., F. Borriello, O. A. Chow, B. Doran, I. Fleming, D. J. Theisen, P. Pallis, A. K. Shalek, C. L. Sokol, I. Zanoni, and J. C. Kagan. 2020. Inflammasomes within Hyperactive Murine Dendritic Cells Stimulate Long-Lived T Cell-Mediated Anti-tumor Immunity. *Cell Rep* 33: 108381.
190. Muratori, C., A. G. Pakhomov, E. C. Gianulis, S. D. Jensen, and O. N. Pakhomova. 2016. The cytotoxic synergy of nanosecond electric pulses and low temperature leads to apoptosis. *Sci Rep* 6: 36835.
191. Chen, K. W., B. Demarco, R. Heilig, K. Shkarina, A. Boettcher, C. J. Farady, P. Pelczar, and P. Broz. 2019. Extrinsic and intrinsic apoptosis activate pannexin-1 to drive NLRP3 inflammasome assembly. *EMBO J* 38.
192. Carty, M., J. Kearney, K. A. Shanahan, E. Hams, R. Sugisawa, D. Connolly, C. G. Doran, N. Munoz-Wolf, C. Gurtler, K. A. Fitzgerald, E. C. Lavelle, P. G. Fallon, and A. G. Bowie. 2019. Cell Survival and Cytokine Release after Inflammasome Activation Is Regulated by the Toll-IL-1R Protein SARM. *Immunity* 50: 1412-1424 e1416.
193. Kang, R., L. Zeng, S. Zhu, Y. Xie, J. Liu, Q. Wen, L. Cao, M. Xie, Q. Ran, G. Kroemer, H. Wang, T. R. Billiar, J. Jiang, and D. Tang. 2018. Lipid Peroxidation Drives Gasdermin D-Mediated Pyroptosis in Lethal Polymicrobial Sepsis. *Cell Host Microbe* 24: 97-108 e104.
194. Gross, O., A. S. Yazdi, C. J. Thomas, M. Masin, L. X. Heinz, G. Guarda, M. Quadroni, S. K. Drexler, and J. Tschopp. 2012. Inflammasome activators induce interleukin-1 α secretion via distinct pathways with differential requirement for the protease function of caspase-1. *Immunity* 36: 388-400.
195. Coll, R. C., A. A. Robertson, J. J. Chae, S. C. Higgins, R. Munoz-Planillo, M. C. Innes, I. Vetter, L. S. Dungan, B. G. Monks, A. Stutz, D. E. Croker, M. S. Butler, M. Haneklaus, C. E. Sutton, G. Nunez, E. Latz, D. L. Kastner, K. H. Mills, S. L. Masters, K. Schroder, M. A. Cooper, and L. A. O'Neill. 2015. A small-molecule inhibitor of the NLRP3 inflammasome for the treatment of inflammatory diseases. *Nat Med* 21: 248-255.
196. Kayagaki, N., S. Warming, M. Lamkanfi, L. Vande Walle, S. Louie, J. Dong, K. Newton, Y. Qu, J. Liu, S. Heldens, J. Zhang, W. P. Lee, M. Roose-Girma, and V. M. Dixit. 2011. Non-canonical inflammasome activation targets caspase-11. *Nature* 479: 117-121.
197. Gianulis, E. C., C. Labib, G. Saulis, V. Novickij, O. N. Pakhomova, and A. G. Pakhomov. 2017. Selective susceptibility to nanosecond pulsed electric field (nsPEF) across different human cell types. *Cell Mol Life Sci* 74: 1741-1754.
198. Bryan, N. B., A. Dorfleutner, Y. Rojanasakul, and C. Stehlik. 2009. Activation of inflammasomes requires intracellular redistribution of the apoptotic speck-like protein containing a caspase recruitment domain. *J Immunol* 182: 3173-3182.

199. Schneider, K. S., C. J. Gross, R. F. Dreier, B. S. Saller, R. Mishra, O. Gorka, R. Heilig, E. Meunier, M. S. Dick, T. Cikovic, J. Sodenkamp, G. Medard, R. Naumann, J. Ruland, B. Kuster, P. Broz, and O. Gross. 2017. The Inflammasome Drives GSDMD-Independent Secondary Pyroptosis and IL-1 Release in the Absence of Caspase-1 Protease Activity. *Cell Rep* 21: 3846-3859.
200. Monteleone, M., A. C. Stanley, K. W. Chen, D. L. Brown, J. S. Bezbradica, J. B. von Pein, C. L. Holley, D. Boucher, M. R. Shakespear, R. Kapetanovic, V. Rolfes, M. J. Sweet, J. L. Stow, and K. Schroder. 2018. Interleukin-1beta Maturation Triggers Its Relocation to the Plasma Membrane for Gasdermin-D-Dependent and -Independent Secretion. *Cell Rep* 24: 1425-1433.
201. MacKenzie, A., H. L. Wilson, E. Kiss-Toth, S. K. Dower, R. A. North, and A. Surprenant. 2001. Rapid secretion of interleukin-1beta by microvesicle shedding. *Immunity* 15: 825-835.
202. Semino, C., S. Carta, M. Gattorno, R. Sitia, and A. Rubartelli. 2018. Progressive waves of IL-1beta release by primary human monocytes via sequential activation of vesicular and gasdermin D-mediated secretory pathways. *Cell Death Dis* 9: 1088.
203. Nuccitelli, R. 2019. Nano-Pulse Stimulation Therapy for the Treatment of Skin Lesions. *Bioelectricity* 1: 235-239.
204. Nuccitelli, R., R. Wood, M. Kreis, B. Athos, J. Huynh, K. Lui, P. Nuccitelli, and E. H. Epstein, Jr. 2014. First-in-human trial of nanoelectroablation therapy for basal cell carcinoma: proof of method. *Exp Dermatol* 23: 135-137.
205. Nuccitelli, R., K. Tran, S. Sheikh, B. Athos, M. Kreis, and P. Nuccitelli. 2010. Optimized nanosecond pulsed electric field therapy can cause murine malignant melanomas to self-destruct with a single treatment. *Int J Cancer* 127: 1727-1736.
206. Schoenbach, K. H. 2010. Bioelectric effect of intense nanosecond pulses. In *Advanced Electroporation Techniques in Biology and Medicine*. A. G. Pakhomov, D. Miklavcic, and M. S. Markov, eds. Taylor and Francis Group, Boca Raton. 19-50.
207. Sher, L. D., E. Kresch, and H. P. Schwan. 1970. On the possibility of nonthermal biological effects of pulsed electromagnetic radiation. *Biophys J* 10: 970-979.
208. Schoenbach, K. H., S. J. Beebe, and E. S. Buescher. 2001. Intracellular effect of ultrashort electrical pulses. *Bioelectromagnetics* 22: 440-448.
209. Vernier, P. T. 2011. Mitochondrial membrane permeabilization with nanosecond electric pulses. *Annu Int Conf IEEE Eng Med Biol Soc* 2011: 743-745.
210. Vernier, P. T., Y. Sun, L. Marcu, S. Salemi, C. M. Craft, and M. A. Gundersen. 2003. Calcium bursts induced by nanosecond electric pulses. *Biochem. Biophys. Res. Commun* 310: 286-295.
211. White, J. A., P. F. Blackmore, K. H. Schoenbach, and S. J. Beebe. 2004. Stimulation of capacitative calcium entry in HL-60 cells by nanosecond pulsed electric fields. *J. Biol. Chem* 279: 22964-22972.
212. Thompson, G. L., C. C. Roth, M. A. Kuipers, G. P. Tolstikh, H. T. Beier, and B. L. Ibey. 2016. Permeabilization of the nuclear envelope following nanosecond pulsed electric field exposure. *Biochem. Biophys. Res. Commun* 470: 35-40.
213. Marchi, S., E. Guilbaud, S. W. G. Tait, T. Yamazaki, and L. Galluzzi. 2023. Mitochondrial control of inflammation. *Nat Rev Immunol* 23: 159-173.
214. Zhou, R., A. S. Yazdi, P. Menu, and J. Tschopp. 2011. A role for mitochondria in NLRP3 inflammasome activation. *Nature* 469: 221-225.
215. Nakahira, K., J. A. Haspel, V. A. Rathinam, S. J. Lee, T. Dolinay, H. C. Lam, J. A. Englert, M. Rabinovitch, M. Cernadas, H. P. Kim, K. A. Fitzgerald, S. W. Ryter, and A. M. Choi. 2011. Autophagy proteins regulate innate immune responses by inhibiting the release of mitochondrial DNA mediated by the NALP3 inflammasome. *Nat Immunol* 12: 222-230.
216. Shimada, K., T. R. Crother, J. Karlin, J. Dagvadorj, N. Chiba, S. Chen, V. K. Ramanujan, A. J. Wolf, L. Vergnes, D. M. Ojcius, A. Rentsendorj, M. Vargas, C. Guerrero, Y. Wang, K. A. Fitzgerald, D. M. Underhill, T. Town, and M. Arditi. 2012. Oxidized mitochondrial DNA activates the NLRP3 inflammasome during apoptosis. *Immunity* 36: 401-414.

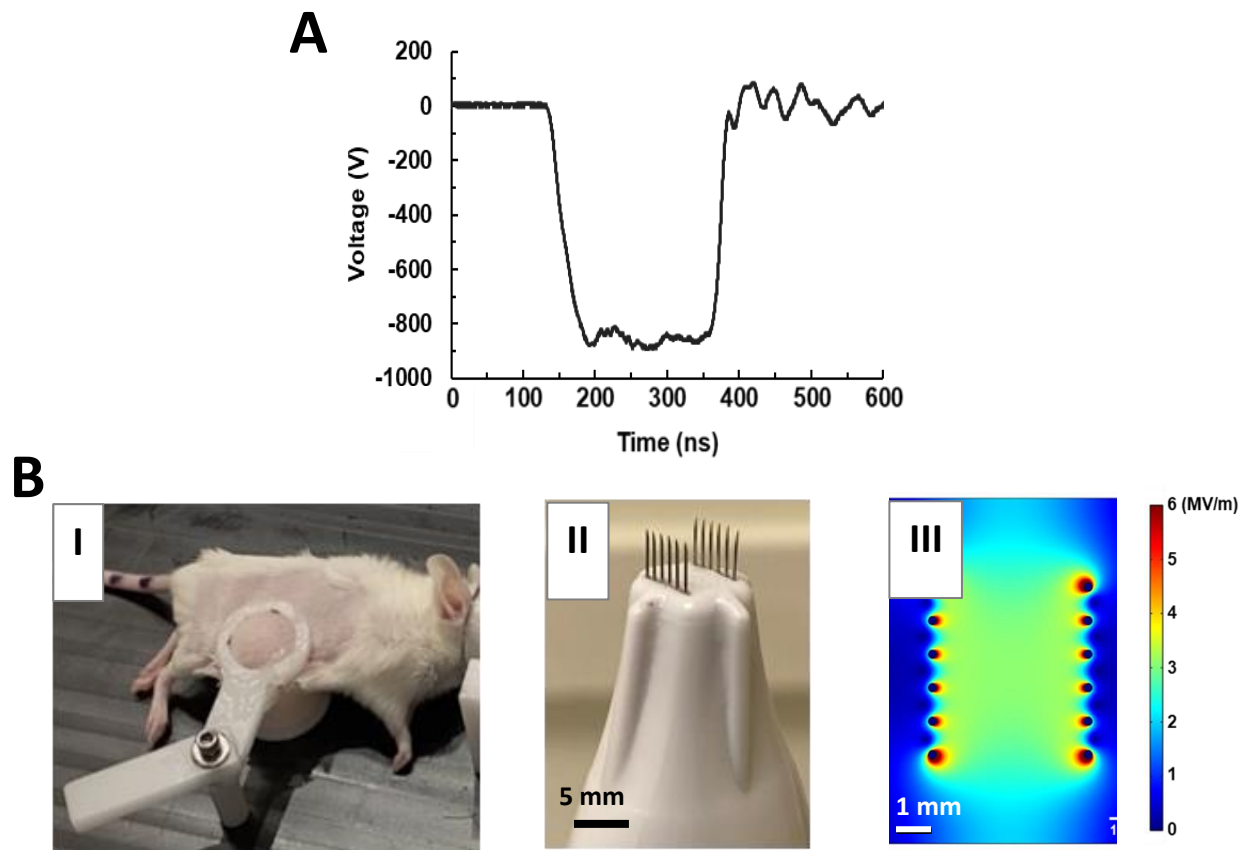
217. Dang, E. V., J. G. McDonald, D. W. Russell, and J. G. Cyster. 2017. Oxysterol Restraint of Cholesterol Synthesis Prevents AIM2 Inflammasome Activation. *Cell* 171: 1057-1071 e1011.
218. Di Micco, A., G. Frera, J. Lugrin, Y. Jamilloux, E. T. Hsu, A. Tardivel, A. De Gassart, L. Zaffalon, B. Bujisic, S. Siegert, M. Quadroni, P. Broz, T. Henry, C. A. Hrycyna, and F. Martinon. 2016. AIM2 inflammasome is activated by pharmacological disruption of nuclear envelope integrity. *Proc Natl Acad Sci U S A* 113: E4671-4680.
219. Hall, E. H., K. H. Schoenbach, and S. J. Beebe. 2007. Nanosecond pulsed electric fields induce apoptosis in p53-wildtype and p53-null HCT116 colon carcinoma cells. *Apoptosis* 12: 1721-1731.
220. Ren, W., and S. J. Beebe. 2011. An apoptosis targeted stimulus with nanosecond pulsed electric fields (nsPEFs) in E4 squamous cell carcinoma. *Apoptosis* 16: 382-393.
221. Brough, D., and N. J. Rothwell. 2007. Caspase-1-dependent processing of pro-interleukin-1beta is cytosolic and precedes cell death. *J Cell Sci* 120: 772-781.
222. Cullen, S. P., C. J. Kearney, D. M. Clancy, and S. J. Martin. 2015. Diverse Activators of the NLRP3 Inflammasome Promote IL-1beta Secretion by Triggering Necrosis. *Cell Rep* 11: 1535-1548.
223. Liu, T., Y. Yamaguchi, Y. Shirasaki, K. Shikada, M. Yamagishi, K. Hoshino, T. Kaisho, K. Takemoto, T. Suzuki, E. Kuranaga, O. Ohara, and M. Miura. 2014. Single-cell imaging of caspase-1 dynamics reveals an all-or-none inflammasome signaling response. *Cell Rep* 8: 974-982.
224. Monteleone, M., J. L. Stow, and K. Schroder. 2015. Mechanisms of unconventional secretion of IL-1 family cytokines. *Cytokine* 74: 213-218.
225. Gaidt, M. M., T. S. Ebert, D. Chauhan, T. Schmidt, J. L. Schmid-Burgk, F. Rapino, A. A. Robertson, M. A. Cooper, T. Graf, and V. Hornung. 2016. Human Monocytes Engage an Alternative Inflammasome Pathway. *Immunity* 44: 833-846.
226. Zanoni, I., Y. Tan, M. Di Gioia, A. Broggi, J. Ruan, J. Shi, C. A. Donado, F. Shao, H. Wu, J. R. Springstead, and J. C. Kagan. 2016. An endogenous caspase-11 ligand elicits interleukin-1 release from living dendritic cells. *Science* 352: 1232-1236.
227. Sozer, E. B., Y. H. Wu, S. Romeo, and P. T. Vernier. 2017. Nanometer-Scale Permeabilization and Osmotic Swelling Induced by 5-ns Pulsed Electric Fields. *J Membr Biol* 250: 21-30.
228. Pakhomova, O. N., B. Gregory, I. Semenov, and A. G. Pakhomov. 2014. Calcium-mediated pore expansion and cell death following nanoelectroporation. *Biochim Biophys Acta* 1838: 2547-2554.
229. Romero, M., M. Keyel, G. Shi, P. Bhattacharjee, R. Roth, J. E. Heuser, and P. A. Keyel. 2017. Intrinsic repair protects cells from pore-forming toxins by microvesicle shedding. *Cell Death Differ* 24: 798-808.
230. Jimenez, A. J., P. Maiuri, J. Lafaurie-Janvore, S. Divoux, M. Piel, and F. Perez. 2014. ESCRT machinery is required for plasma membrane repair. *Science* 343: 1247136.
231. Reddy, A., E. V. Caler, and N. W. Andrews. 2001. Plasma membrane repair is mediated by Ca(2+)-regulated exocytosis of lysosomes. *Cell* 106: 157-169.
232. Huynh, C., D. Roth, D. M. Ward, J. Kaplan, and N. W. Andrews. 2004. Defective lysosomal exocytosis and plasma membrane repair in Chediak-Higashi/beige cells. *Proc Natl Acad Sci U S A* 101: 16795-16800.
233. Muratori, C., G. Silkuniene, P. A. Mollica, A. G. Pakhomov, and O. N. Pakhomova. 2021. The role of ESCRT-III and Annexin V in the repair of cell membrane permeabilization by the nanosecond pulsed electric field. *Bioelectrochemistry* 140: 107837.
234. Tsuchiya, K., S. Nakajima, S. Hosojima, D. Thi Nguyen, T. Hattori, T. Manh Le, O. Hori, M. R. Mahib, Y. Yamaguchi, M. Miura, T. Kinoshita, H. Kushiya, M. Sakurai, T. Shiroishi, and T. Suda. 2019. Caspase-1 initiates apoptosis in the absence of gasdermin D. *Nat Commun* 10: 2091.
235. Taabazuing, C. Y., M. C. Okondo, and D. A. Bachovchin. 2017. Pyroptosis and Apoptosis Pathways Engage in Bidirectional Crosstalk in Monocytes and Macrophages. *Cell Chem Biol* 24: 507-514 e504.

236. Antonopoulos, C., H. M. Russo, C. El Sanadi, B. N. Martin, X. Li, W. J. Kaiser, E. S. Mocarski, and G. R. Dubyak. 2015. Caspase-8 as an Effector and Regulator of NLRP3 Inflammasome Signaling. *The Journal of biological chemistry* 290: 20167-20184.
237. Skeate, J. G., D. M. Da Silva, E. Chavez-Juan, S. Anand, R. Nuccitelli, and W. M. Kast. 2018. Nano-Pulse Stimulation induces immunogenic cell death in human papillomavirus-transformed tumors and initiates an adaptive immune response. *PLoS One* 13: e0191311.
238. Nuccitelli, R., A. McDaniel, S. Anand, J. Cha, Z. Mallon, J. C. Berridge, and D. Uecker. 2017. Nano-Pulse Stimulation is a physical modality that can trigger immunogenic tumor cell death. *J Immunother Cancer* 5: 32.
239. Lassiter, B. P., S. Guo, and S. J. Beebe. 2018. Nano-Pulse Stimulation Ablates Orthotopic Rat Hepatocellular Carcinoma and Induces Innate and Adaptive Memory Immune Mechanisms that Prevent Recurrence. *Cancers (Basel)* 10.
240. Guo, S., N. I. Burcus, J. Hornef, Y. Jing, C. Jiang, R. Heller, and S. J. Beebe. 2018. Nano-Pulse Stimulation for the Treatment of Pancreatic Cancer and the Changes in Immune Profile. *Cancers (Basel)* 10.
241. Beebe, S. J., B. P. Lassiter, and S. Guo. 2018. Nanopulse Stimulation (NPS) Induces Tumor Ablation and Immunity in Orthotopic 4T1 Mouse Breast Cancer: A Review. *Cancers (Basel)* 10.
242. Liu, J., X. Chen, and S. Zheng. 2021. Immune response triggered by the ablation of hepatocellular carcinoma with nanosecond pulsed electric field. *Front Med* 15: 170-177.
243. Eisenbarth, S. C., and R. A. Flavell. 2009. Innate instruction of adaptive immunity revisited: the inflammasome. *EMBO Mol Med* 1: 92-98.
244. Ghiringhelli, F., L. Apetoh, A. Tesniere, L. Aymeric, Y. Ma, C. Ortiz, K. Vermaelen, T. Panaretakis, G. Mignot, E. Ullrich, J. L. Perfettini, F. Schlemmer, E. Tasdemir, M. Uhl, P. Genin, A. Civas, B. Ryffel, J. Kanellopoulos, J. Tschopp, F. Andre, R. Lidereau, N. M. McLaughlin, N. M. Haynes, M. J. Smyth, G. Kroemer, and L. Zitvogel. 2009. Activation of the NLRP3 inflammasome in dendritic cells induces IL-1 β -dependent adaptive immunity against tumors. *Nat Med* 15: 1170-1178.
245. Chen, G., M. G. Chelu, D. Dobrev, and N. Li. 2018. Cardiomyocyte Inflammasome Signaling in Cardiomyopathies and Atrial Fibrillation: Mechanisms and Potential Therapeutic Implications. *Front Physiol* 9: 1115.
246. Onodi, Z., M. Ruppert, D. Kucsera, A. A. Sayour, V. E. Toth, G. Koncsos, J. Novak, G. B. Brenner, A. Makkos, T. Baranyai, Z. Gircz, A. Gorbe, P. Leszek, M. Gyongyosi, I. G. Horvath, R. Schulz, B. Merkely, P. Ferdinandy, T. Radovits, and Z. V. Varga. 2021. AIM2-driven inflammasome activation in heart failure. *Cardiovasc Res* 117: 2639-2651.
247. Lim, H. S., C. Schultz, J. Dang, M. Alasady, D. H. Lau, A. G. Brooks, C. X. Wong, K. C. Roberts-Thomson, G. D. Young, M. I. Worthley, P. Sanders, and S. R. Willoughby. 2014. Time course of inflammation, myocardial injury, and prothrombotic response after radiofrequency catheter ablation for atrial fibrillation. *Circ Arrhythm Electrophysiol* 7: 83-89.
248. Koyama, T., H. Tada, Y. Sekiguchi, T. Arimoto, H. Yamasaki, K. Kuroki, T. Machino, K. Tajiri, X. D. Zhu, M. Kanemoto-Igarashi, A. Sugiyasu, K. Kuga, Y. Nakata, and K. Aonuma. 2010. Prevention of atrial fibrillation recurrence with corticosteroids after radiofrequency catheter ablation: a randomized controlled trial. *J Am Coll Cardiol* 56: 1463-1472.
249. Kim, Y. R., G. B. Nam, S. Han, S. H. Kim, K. H. Kim, S. Lee, J. Kim, K. J. Choi, and Y. H. Kim. 2015. Effect of Short-Term Steroid Therapy on Early Recurrence During the Blanking Period After Catheter Ablation of Atrial Fibrillation. *Circ Arrhythm Electrophysiol* 8: 1366-1372.
250. Iskandar, S., M. Reddy, M. R. Afzal, J. Rajasingh, M. Atoui, M. Lavu, D. Atkins, S. Bommana, L. Umbarger, M. Jaeger, R. Pimentel, R. Dendi, M. Emert, M. Turagam, L. Di Biase, A. Natale, and D. Lakkireddy. 2017. Use of Oral Steroid and its Effects on Atrial Fibrillation Recurrence and Inflammatory Cytokines Post Ablation - The Steroid AF Study. *J Atr Fibrillation* 9: 1604.
251. Deftereos, S., G. Giannopoulos, M. Efremidis, C. Kossyvakis, A. Katsivas, V. Panagopoulou, C. Papadimitriou, S. Karageorgiou, K. Doudoumis, K. Raisakis, A. Kaoukis, D. Alexopoulos, A. S.

- Manolis, C. Stefanadis, and M. W. Cleman. 2014. Colchicine for prevention of atrial fibrillation recurrence after pulmonary vein isolation: mid-term efficacy and effect on quality of life. *Heart Rhythm* 11: 620-628.
252. Semenov, I., S. Xiao, O. N. Pakhomova, and A. G. Pakhomov. 2013. Recruitment of the intracellular Ca^{2+} by ultrashort electric stimuli: the impact of pulse duration. *Cell calcium* 54: 145-150.
253. Man, S. M., and T. D. Kanneganti. 2016. Converging roles of caspases in inflammasome activation, cell death and innate immunity. *Nat Rev Immunol* 16: 7-21.
254. Huang, Y., W. Xu, and R. Zhou. 2021. NLRP3 inflammasome activation and cell death. *Cell Mol Immunol* 18: 2114-2127.
255. Cheung, G. Y. C., J. S. Bae, and M. Otto. 2021. Pathogenicity and virulence of *Staphylococcus aureus*. *Virulence* 12: 547-569.
256. Yang, W., Y. H. Wu, D. Yin, H. P. Koeffler, D. E. Sawcer, P. T. Vernier, and M. A. Gundersen. 2011. Differential sensitivities of malignant and normal skin cells to nanosecond pulsed electric fields. *Technol Cancer Res Treat* 10: 281-286.
257. Ibey, B. L., A. G. Pakhomov, B. W. Gregory, V. A. Khorokhorina, C. C. Roth, M. A. Rassokhin, J. A. Bernhard, G. J. Wilmink, and O. N. Pakhomova. 2010. Selective cytotoxicity of intense nanosecond-duration electric pulses in mammalian cells. *Biochim Biophys Acta* 1800: 1210-1219.
258. Fitzgerald, J. R., D. E. Sturdevant, S. M. Mackie, S. R. Gill, and J. M. Musser. 2001. Evolutionary genomics of *Staphylococcus aureus*: insights into the origin of methicillin-resistant strains and the toxic shock syndrome epidemic. *Proc Natl Acad Sci U S A* 98: 8821-8826.
259. Kaminski, J. J., S. A. Schattgen, T. C. Tzeng, C. Bode, D. M. Klinman, and K. A. Fitzgerald. 2013. Synthetic oligodeoxynucleotides containing suppressive TTAGGG motifs inhibit AIM2 inflammasome activation. *J Immunol* 191: 3876-3883.
260. Liu, X., S. Xia, Z. Zhang, H. Wu, and J. Lieberman. 2021. Channelling inflammation: gasdermins in physiology and disease. *Nat Rev Drug Discov* 20: 384-405.

APPENDICES

Appendix A: Supplementary Figure 1



Supplementary Fig. 1. nsPEF exposure setups. **A.** Representative 200 ns waveforms generated either by the Pulse Biosciences generator used for experiments in cuvette **B.** Setup for the in vivo nsPEF stimulation. **I** shows the mouse skin trapped between the silicon support and the ring through which the electrode array was inserted into the skin. Picture **II** displays the needle electrode array. **III** is the 2D simulation of the electric field in the skin when 15 kV are applied across the electrode array.

VITA

ALEXANDRA ELIZABETH CHITTAMS-MILES

Address

Frank Reidy Research Center for Bioelectrics, ODU, Norfolk, VA, 23508.

Education

Doctor of Philosophy, Biomedical Sciences, Old Dominion University, 2019-2024.

Master of Science, Biology, American University, 2017-2019.

Bachelor of Science, Biology, University of South Alabama, 2014-2016.

Awards

ODU Graduate Student Research Travel Award, 2023, Old Dominion University.

1st Place Best Student Presentation Award, The Frank Reidy Research Center for Bioelectrics Retreat 2023.

2nd Place Best Student Presentation Award in the Basic Sciences Category, 4th World Congress on Electroporation, 2022.

Recipient of the Doreen J Putrah Cancer Foundation Travel Grant for the 4th World Congress on Electroporation, 2022.

Recipient of the Karl Schoenbach Endowed Fellowship in Bioelectrics, 2021.

Publications

Flavia Mazzarda, **Alexandra E. Chittams-Miles**, Julia L Pittaluga, Esin B Sozer, P. Thomas Vernier, Claudia Muratori. Inflammasome activation and IL-1 β release triggered by nanosecond pulsed electric fields in murine primary macrophages and skin, 2023. *Journal of Immunology*.

Alexandra E. Chittams-Miles, Areej Malik, Erin B. Purcell, Claudia Muratori. Nanosecond pulsed electric fields increase antibiotic susceptibility in methicillin-resistant *Staphylococcus aureus*, 2023. *Microbiology Spectrum*.